

MICROBIAL DYNAMICS IN THE ARCTIC CHUKCHI SEA: DIFFERENCES IN  
MICROBIAL ABUNDANCE AND BACTERIAL COMMUNITY COMPOSITION IN  
HIGH AND LOW PRODUCTION REGIMES

by

LISA RENEE HODGES

(Under the direction of Dr. Patricia Yager)

ABSTRACT

This research examines the importance of bottom-up and top-down controls on bacterial abundance and community composition during summertime production in the coastal Arctic Ocean. Bacterial and viral abundance, bacterial community composition, and free-living (3  $\mu\text{m}$ -filtered, FL) and particle-associated (unfiltered, FL+PA) assemblages were examined in the Chukchi Sea during August 2000. Nutrients, chlorophyll a, and particulate organic matter (POM) were also measured. Bacteria were isolated and analyzed by DGGE, 16S rDNA sequence analysis, and for substrate utilization. Increased bacterial and viral abundance, decreased species richness, and decreased similarity (Sorenson's Index) between FL and PA assemblages occurred in high versus low POM regions. Bacterial abundance, species richness, and Sorenson's Index correlated best with POM, while viral abundance correlated best with bacterial abundance. Algal bloom conditions producing high POM concentrations may therefore increase bacterial and viral abundance, reducing species richness, and promote differences between FL and PA assemblages.

INDEX WORDS: Bacterioplankton, Bacterial abundance, Viral abundance, Bacterial community composition, DGGE, Particle-associated bacteria, Free-living bacteria, Psychrophiles, Arctic, Marine.

MICROBIAL DYNAMICS IN THE ARCTIC CHUKCHI SEA: DIFFERENCES IN  
MICROBIAL ABUNDANCE AND BACTERIAL COMMUNITY COMPOSITION IN  
HIGH AND LOW PRODUCTION REGIMES

by

LISA RENEE HODGES

B.S., The University of Washington, 1998

Thesis Submitted to the Graduate Faculty of The University of Georgia in Partial  
Fulfillment of the Requirements for the Degree

MASTER OF SCIENCE

ATHENS, GEORGIA

2002

© 2002

Lisa Renee Hodges

All Rights Reserved.

MICROBIAL DYNAMICS IN THE ARCTIC CHUKCHI SEA: DIFFERENCES IN  
MICROBIAL ABUNDANCE AND BACTERIAL COMMUNITY COMPOSITION IN  
HIGH AND LOW PRODUCTION REGIMES

by

LISA RENEE HODGES

Approved:

Major Professor: Patricia Yager

Committee: J. T. Hollibaugh  
Mary Ann Moran

Electronic Version Approved:

Gordhan L. Patel  
Dean of the Graduate School  
The University of Georgia  
August 2002

## ACKNOWLEDGEMENTS

I especially thank my advisor, Patricia Yager, for her guidance and support during this research project. I also thank my committee members, Tim Hollibaugh and Mary Ann Moran, for their guidance and participation. I especially thank Dr. Hollibaugh for financial support and providing me with access to his lab and equipment. I am especially grateful to his lab members, Nasreen Bano and Erin Biers, for teaching me molecular methods pertinent to this research. I thank Eric Wommack for his help and guidance in viral direct counts, and Bob Hodson and his lab members for providing me access to their lab and equipment to perform those counts. I thank Rosalynn Lee for performing NO<sub>x</sub> analysis, and Samantha Joye for providing me access to her lab to perform nutrient analysis. I thank Josh Baumann for helping me to perform bacterial direct counts. I especially thank Chief Scientist, Glen Cota (Old Dominion University), for providing me with chlorophyll data and for his help and guidance during AWSOO. I also thank Laura Belicka and her advisor, Rodger Harvey (UMCES-CBL), for providing me with POM data and Annelie Skoog (U Connecticut), for providing me with DOC data. A very special thanks must go to Captain Garrett and the crew members of the USCGC Polar Star for their excellent technical support and hospitality, and all scientists on board during AWSOO, for making this research cruise a memorable experience. I also thank those faculty, staff, and graduate students in the Department of Marine Sciences that helped me during my studies at UGA, and friends and family, especially Susan White, for their support.

## TABLE OF CONTENTS

	Page
ACKNOWLEDGEMENTS .....	iv
LIST OF TABLES .....	vii
LIST OF FIGURES .....	viii
CHAPTER 1: INTRODUCTION .....	1
Background .....	1
My Research .....	15
CHAPTER 2: METHODS .....	20
Location .....	20
Seawater Chemistry .....	20
Microbial Abundance and Variables .....	22
Bacterial Community Composition .....	25
Correlation Analysis .....	31
Bacterial Isolates .....	32
CHAPTER 3: RESULTS .....	36
Location .....	36
Seawater Chemistry .....	36
Microbial Abundance and Variables .....	42
Station Bloom Sequence .....	44
Bacterial Community Composition .....	50
Correlation Analysis .....	56

Bacterial Isolates.....	63
CHAPTER 4: DISCUSSION.....	76
Bottom-up versus Top-down Control.....	76
PA and FL Assemblages.....	81
Bacterial Isolates.....	83
Future Work.....	86
CHAPTER 5: CONCLUSION.....	88
REFERENCES.....	90
APPENDIX.....	103

**LIST OF TABLES**

Table	Page
1 Station Data.....	37
2 Microbial Data .....	38
3 Correlation Coefficients.....	57
4 Partial Correlation Coefficients .....	58
5 Correlation Coefficients for $D_{mg}$ and S Indexes .....	64
6 Bacterial Isolate Data.....	66

## LIST OF FIGURES

Figure	Page
1 Location Map with Stations.....	2
2 Station Nutrient Depth Profiles.....	40
3 Station Organic Matter Depth Profiles .....	41
4 Station Microbial Abundance Depth Profiles.....	43
5 Viral versus Bacterial Abundance Graph .....	45
6 Station Sequence Graphs (CHLa and microbial abundance).....	47
7 Station Sequence Graphs (POC and microbial abundance).....	48
8 Station Sequence Graphs (POC and VB).....	49
9 Station 1 DGGE Gel .....	51
10 Station 2 DGGE Gel .....	52
11 Station 3 DGGE Gel .....	53
12 Station 4 DGGE Gel .....	54
13 Station DGGE Dendrogram.....	55
14 Bacterial Abundance Correlation Graphs .....	59
15 Viral Abundance Correlation Graphs .....	61
16 Lytic Threshold (VB) Correlation Graphs.....	62
17 Isolate DGGE Gel 1 .....	67
18 Isolate DGGE Gel 2.....	68
19 Isolate DGGE Gel 3 .....	69

20	Isolate DGGE Dendrogram.....	70
21	Isolate Phylogenetic Tree.....	72
22	BIOLOG Plate Results for Isolates AWSOO3-B1 and AWSOO3-B2.....	74
23	Comparison of Isolates AWSOO1-B1 and AWSOO1-B2 .....	75
24	Schematic Diagram.....	89

# CHAPTER 1

## INTRODUCTION

This research examines the importance of bottom-up and top-down controls on bacterial abundance and community composition during summertime production in the coastal Arctic Ocean. Studies that combine measurements of environmental variables with microbial abundance, activity, and community composition provide insight into the significant factors controlling the microbial loop in the marine environment. While recent studies of this nature have been performed in temperate environments (Riemann et al 2000; Riemann and Winding 2001), few studies have examined polar environments (Yager et al. 2001). This study represents an examination of correlations between bacterial and viral abundance, bacterial community composition, and the differences between free-living (FL) and particle-associated (PA) assemblages in the Arctic Chukchi Sea (Fig. 1).

### **Background**

Bacterioplankton. Bacterioplankton are abundant (Hobbie et al. 1977; Watson et al. 1977; Porter and Feig 1980) and important (Pomeroy 1974; Azam et al. 1983) organisms in the marine food web. Heterotrophic bacterial species comprise the majority of bacterioplankton (Ducklow et al. 1986; although this paradigm may be changing, e.g. Zehr et al., 2001; Karl 2002). These heterotrophic bacteria can have high production rates

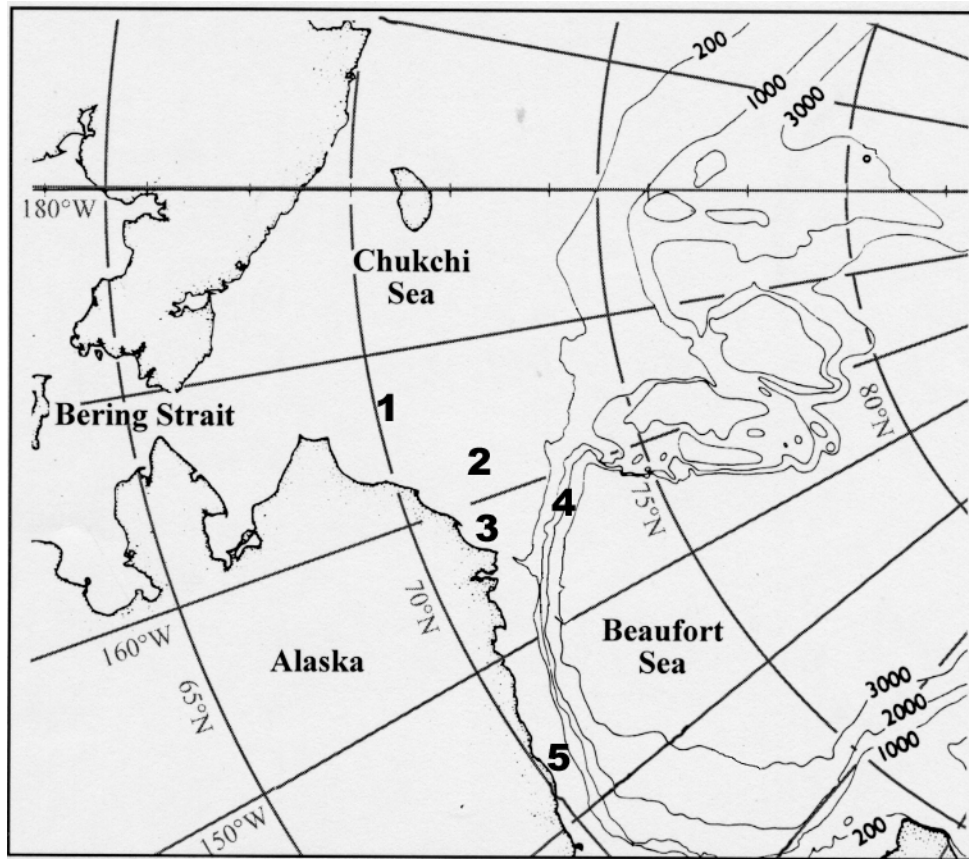


**Figure 1.** Map of research location (modified from Yager et al. 2001). Stations (numbered) were sampled during the Arctic West Cruise of Opportunity (AWSOO) aboard the USCGC Polar Star during August 2000. Temperature ranged from  $-1.3 - 0.1$  °C and ice cover ranged from 3/10 to 9/10 coverage.

(Rich et al. 1997) and may be responsible for more than half of pelagic respiration and consumption of primary production (P. le B. Williams 1981; Azam et al 1983). The “microbial loop” paradigm suggests that microbial communities are important in the cycling of organic matter in the surface layer, regenerating nutrients and energy that otherwise might be unavailable to higher trophic levels (Pomeroy 1974; Azam et al. 1983). The effectiveness of the microbial loop in the polar environment is important to determine the role Arctic summertime production plays in the global carbon cycle (Yager 1996).

Bacterioplankton abundance typically ranges from  $10^5$  cells  $\text{mL}^{-1}$  (Cho and Azam 1990) to  $10^7$  cells  $\text{mL}^{-1}$  (Ducklow and Shiah 1993) in oligotrophic and eutrophic marine systems, respectively. Bacterioplankton abundance varies seasonally in most marine environments (Ducklow et al. 1993; Karl et al. 1993; Yager et al. 2001). Studies of phytoplankton blooms in mesocosms (Castberg et al. 2001; Larsen et al. 2001) and in the environment (Yager et al. 2001) show that bacterial abundance and activity can vary significantly on short time scales. The factors regulating these changes in the polar environment, however, are largely unknown.

Controls on bacterioplankton biomass are theorized to incorporate both bottom-up and top-down mechanisms, depending on system dynamics and trophic status (Metzler et al. 2000; Anderson and Rivkin 2001; Gasol et al. 2002). Bottom-up studies in a number of aquatic environments correlate bacterial abundance to chlorophyll a (CHL<sub>a</sub>) concentrations (Cole et al. 1988; Poremba et al. 1999; Kimura et al. 2001), nutrients such as C, N, or P (Rivkin and Anderson 1997; Vrede et al. 1999; Hagström et al. 2001), and dissolved and/or particulate organic matter (DOM, POM; Kimura et al. 2001). Grazing

by protists (Sherr and Sherr 1994; Sherr et al 1997) and viral lysis (Fuhrman 1999) are significant top-down removal processes that keep bacterial abundance relatively stable. Estimates of bacterivory often fall short of those needed to balance bacterial production, however, suggesting that other removal processes such as viral infection are important (McManus and Fuhrman 1988). Viral enrichment studies show that bacterial mortality increases with the addition of viruses (Proctor and Fuhrman 1992; Noble et al. 1999), suggesting that bacteriophages are important controls on bacterial biomass. Viral infection can cause similar bacterial mortality comparable to grazing by heterotrophic nanoflagellates (HNF; Fuhrman and Noble 1995), and may exert stronger control on bacterial abundance than predation (Weinbauer and Peduzzi 1995; Weinbauer et al. 1995).

*Virioplankton.* Marine viruses are dynamic and important components of marine microbial food webs (Fuhrman 1999). Virioplankton are abundant and typically exceed bacterial abundance by one order of magnitude (Bergh et al. 1989; Proctor and Fuhrman 1993). Viral abundance typically ranges from  $10^4 - 10^8 \text{ mL}^{-1}$  in oligotrophic and eutrophic marine systems, respectively (see review by Wommack and Colwell 2000). Strong seasonal variations (Bergh et al. 1989; Bratbak et al. 1990; Wommack et al. 1992; Jiang and Paul 1994; Weinbauer et al. 1995) and rapid temporal changes (Heldal and Bratbak 1991; Suttle and Feng 1992; Jiang and Paul 1994; Bratbak et al. 1996; Weinbauer et al. 1995) are observed in a variety of aquatic ecosystems. Viral abundance is often strongly correlated to bacterial abundance (Boehme et al. 1993; Cochlan et al. 1993; Jiang and Paul 1994; Weinbauer et al. 1995; Steward et al. 1996; see review by

Wommack and Colwell 2000) and CHLa to a lesser extent (Fuhrman 1980; Boehme et al. 1993; Cochlan et al. 1993; Jiang and Paul 1994; Weinbauer et al. 1995).

Morphological data from viroplankton diversity studies suggest that the majority of viroplankton are bacteriophages (Wommack et al. 1992; Cochlan et al. 1993; Maranger et al. 1994). The strong correlation to bacterial abundance (Cochlan et al. 1993; Maranger and Bird 1995, 1996; Almeida et al. 2001), high bacterial-viral encounter rates (Fuhrman et al. 1989; Boehme et al. 1993; Cochlan et al. 1993), and high viral production rates (Noble and Fuhrman 2000) all support this theory. Marine viruses are estimated to be responsible for 5-50% of total bacterial mortality in the marine environment (Proctor and Fuhrman 1990; Heldal and Bratbak 1991; Proctor et al. 1993, Suttle 1994; Fuhrman and Noble 1995; Maranger and Bird 1995; Maranger and Bird 1996; Noble and Fuhrman 2000). Clearly, viroplankton play an important role in the microbial loop in aquatic ecosystems.

Marine viruses are small (20-200  $\mu\text{m}$ ), non-motile “cells” composed of DNA/RNA surrounded by a protein coat (Fuhrman 1999). Viruses contact their host by passive diffusion and attach to the cell by recognition of an extracellular feature such as a transporter protein or flagellum (Fuhrman 1999). Viruses are highly genus and species specific (Koga et al. 1982; Bigby et al. 1995); <0.5% of marine viruses are found to infect more than one genus (Ackermann and DuBow 1987). Host abundance and recognition of the host are therefore the keys to viral success.

Viroplankton reproduce by injecting their nucleic acids into the bacterial host cell, using host cellular machinery for replication via three mechanisms (Fuhrman 1999):

- 1) Viral genomes are replicated by the host and progeny viruses are produced and

released from the cell by non-lethal mechanisms during chronic infection, 2) Lysogenic infection involves non-lethal incorporation of the viral genome into the host genome to be copied with cell replication; progeny viruses are only produced when an induction event causes lytic infection to occur, 3) Lethal viral replication occurs during lytic infection, where progeny viruses are produced within the cell and released during cell lysis.

Lytic infection is density-dependent, where a minimum host concentration is needed for viral replication (Wiggins and Alexander 1985; Wilcox and Fuhrman 1994). The product of bacterial and viral abundance must reach a threshold for lytic infection to occur. The “lytic infection threshold” is theorized to be the product of bacterial  $\times$  viral abundance (VB) equal to  $10^{12}$  mL<sup>-1</sup> (Wilcox and Fuhrman 1994). This measurement may be a good indicator of whether a marine microbial ecosystem is experiencing viral infection.

The ratio of viral to bacterial abundance (VBR) is another parameter that may be calculated to determine the importance of viruses in marine systems (see review by Wommack and Colwell 2000). The VBR in marine systems will usually be greater than 1 since viruses are typically more abundant (Bergh et al. 1989; Proctor and Fuhrman 1993). Measured VBR values range from  $<1$  to 72, but values between 3 and 10 are usually observed (Wommack and Colwell 2000). Higher VBR values are measured in more nutrient-rich, productive ecosystems where viral infection may be more prevalent (Wommack and Colwell 2000). VBR values often correlate to bacterial abundance (Weinbauer et al. 1995); an inverse relationship between the VBR and bacterial abundance is most often observed (Jiang and Paul 1994; Maranger et al. 1994; Maranger

and Bird 1995; Wommack et al. 1992; Tuomi et al. 1997). VBR can, however, remain constant during changes in bacterial and viral abundance (Tuomi et al. 1997). VBR values may also correlate with bacterial host diversity, with low VBR values demonstrating low bacterial diversity, and vice versa (Bratbak and Heldal 1995; Tuomi et al. 1995).

Both lytic and lysogenic infections occur in marine ecosystems, but lytic infection is the most common mechanism of viral replication in the marine environment (Wilcox and Fuhrman 1994; see review by Wommack and Colwell 2000). Lysogeny may vary seasonally (Cochran and Paul 1998) and be increased in the oligotrophic ocean, but it only accounts for a small percentage (< 4%) of bacterial mortality (Weinbauer and Suttle 1999). The prevalence of lytic infection (Wilcox and Fuhrman 1994; Weinbauer and Suttle 1999) suggests that viruses can strongly affect the microbial loop and the marine food web.

Lysis of bacterial and phytoplankton cells releases DOM that can be readily used by bacteria (Bratbak et al. 1990; Proctor and Fuhrman 1990; Fuhrman 1992; Weinbauer and Peduzzi 1995; Middleboe et al. 1996; Noble and Fuhrman 1998). A theoretical “viral loop” (Fuhrman 1999) is therefore created within the marine food web where bacteria consume bacterial biomass, preventing fixed carbon from passing to higher trophic levels (Fuhrman 1992; Bratbak et al. 1994; Thingstad and Lignell 1997). Models incorporating viral lysis show a 27-33% increase and 20-25% decrease in bacterial and nanozooplankton production, respectively (Fuhrman 1992; Fuhrman and Suttle 1993). Mesocosm experiments show that bacterial growth can be stimulated by the addition of viral lysis products (Middleboe et al. 1996).

This “viral loop” actually aids the ecosystem by promoting the oxidation of organic matter and regeneration of nutrients, therefore increasing overall production in the surface layer (Bratbak et al. 1990; Fuhrman 1992; Fuhrman 1999). Viruses and bacteria are non-sinking fractions of DOM, so the stronger the “viral loop”, the more nutrients are retained in the surface, resulting in a positive feedback mechanism that maintains primary and bacterial production in the euphotic zone (Fuhrman 1992). Conversely, decreased viral activity causes organic matter to be passed onto larger organisms that can sink, stripping nutrients from the surface (Fuhrman 1999). An examination of the “viral loop” is therefore important to resolve marine ecosystem carbon budgets.

Lytic infection can also strongly affect bacterial community composition (Peduzzi and Weinbauer 1993; Tuomi et al 1995). Viruses are density-dependent (Wiggins and Alexander 1985; Wilcox and Fuhrman 1994) and genus/species specific (Ackermann and DuBow 1987), so dominant nonresistant bacterial species are more likely to be infected and lysed (Fuhrman and Suttle 1993). Viral infection of these bacteria may therefore reduce their abundance while resistant bacterial species thrive on the DOM released through lysis (Wommack and Colwell 2000). Clonal diversity shifted from phage-sensitive to phage-resistant clones in a cultured phage-host system (Middleboe et al. 2001).

Shifts in dominant bacterial species can occur over periods of weeks to months (Rehnstam et al. 1993; Pinhassi et al. 1997) and community succession during algal blooms has been observed (Peduzzi and Weinbauer 1993; Fandino et al. 2001; Yager et al. 2001). The cause of these changes in community structure is unknown, however.

Elevated VBR values occurring with changes in bacterial community structure during peaks in primary production indicate that viral infection is likely shaping the community during algal blooms (Yager et al. 2001). One study of viral infection on cyanobacteria correlates bacterial community composition to viruses (Waterbury and Valois 1993) and modeling shows that viruses may control bacterial diversity (Thingstad and Lignell 1997; Wommack and Colwell 2000). Successional changes in virioplankton diversity further support the hypothesis that viruses may control bacterial diversity (Wommack et al. 1999; Steward et al. 2000).

*Bacterial community composition.* Top-down controls other than viral infection may also influence bacterial community composition. Selective predation of bacteria by heterotrophic nanoflagellates is found in some aquatic ecosystems (Lebaron et al. 1999; Suzuki 1999). Experimental removal of predators increases the abundance of bacterial phylotypes that were rare in the original water sample, suggesting that predation can be species-specific (Suzuki 1999). Enhanced nanoflagellate grazing may also stimulate viral activity and combine with viral infection in shaping bacterial community structure (Simek et al. 2001). Top down controls may therefore influence bacterial community composition synergistically.

Bottom-up controls may also influence bacterial community structure. Inorganic nutrients and predation can work together to regulate bacterial community structure (Gasol et al. 2002). Bacteria exhibit ribotype succession during phytoplankton blooms (Peduzzi and Weinbauer 1993; Castberg et al. 2001; Yager et al. 2001). Micro-scale patchiness of bacterial species richness has been attributed to differences in POM; 1-ul

samples from the same area show increased assemblage richness with enriched POM (Long and Azam 2001). Organic particles may therefore be important in shaping bacterial community composition.

Particle-associated and free-living assemblages. Particles produced during times of high production create a specialized niche for marine bacteria. Bacteria residing on particles can contribute more than half of the total bacterial production (Lee et al. 2001). Particle-associated (PA) bacteria have extracellular enzymes that degrade POM (Chróst 1991); therefore, species that thrive on particles may differ from free-living (FL) species. FL and PA assemblages are indeed shown to be different in some aquatic systems (Giovannoni 1990; Fandino et al. 2001; Moeseneder et al. 2001; Riemann and Winding 2001). During a dinoflagellate bloom,  $\alpha$ - and  $\gamma$ - *Proteobacteria* and *Cytophaga*-like bacteria are associated with FL and PA assemblages, respectively, with some overlap of *Cytophaga*-like bacteria in both assemblages (Fandino et al. 2001). Changes in bacterial community structure during that bloom correlated to peaks in extracellular enzyme activity of PA bacteria having higher cell-specific growth rates than FL species (Fandino et al. 2001). FL and PA assemblages may be interacting communities where species overlap may depend on POM (Riemann and Winding 2001). Differences in the response of FL and PA assemblages to algal blooms and POM must therefore be studied in order to understand bacterial succession.

Mortality of FL and PA assemblages may vary (Proctor and Fuhrman 1991; Proctor et al. 1993). Virus-mediated mortality is estimated to cause 6-62% and 6-52% of FL and PA bacterial mortality, respectively (Proctor et al. 1993). Another study in the

North Pacific Ocean estimates that 2-37% of PA bacteria are lysed by viruses (Proctor and Fuhrman 1991). Protists preferentially consume small FL bacterial species (Jurgens and Sala 2000) and size/morphological selectivity is observed (Simek et al. 1999; Jurgens and Sala 2000; Hahn and Hofle 2001). Predation may therefore enhance PA assemblages by encouraging aggregation of bacteria (Jurgens and Sala 2000). Interestingly, preferential predation by heterotrophic nanoflagellates on small virus particles is observed (Gonzalez and Suttle 1993), which may also serve to shape bacterial community structure by influencing viral infection. Examining community structure of FL and PA assemblages and their relation to viral abundance and predation is therefore necessary to determine the relative importance of these assemblages and the factors controlling their composition.

Denaturing gradient gel electrophoresis (DGGE). Bacterioplankton identification is problematic because the most abundant species are often unculturable (Giovannoni et al. 1990). Microscopic counts yield higher bacterial abundance estimates than earlier plate counts, suggesting the existence of bacterioplankton that cannot be identified by standard autecological techniques (Jannasch and Jones 1959). Molecular identification techniques involving sequencing of the 16S (SSU) rRNA subunit (Olsen et al. 1986) are now used to identify bacterioplankton. Initial studies using these molecular techniques in marine systems showed that more than 80% of these unculturable species can be placed into 9 phylogenetic groups (Schmidt et al. 1991).

The molecular methods used initially to investigate bacterial community structure are labor intensive. These methods compare cloned nucleotide sequences of the 16S

rRNA gene using DNA extracted from the environment (Giovannoni et al. 1990; DeLong et al. 1993; Fuhrman et al. 1993). Cloning and sequencing of large populations of 16S rRNA genes can be laborious. Denaturing gradient gel electrophoresis (DGGE; Myers et al. 1985, 1987) coupled with polymerase chain reaction (PCR; Saiki et al. 1988) is now used to analyze bacterial community structure more easily (Murray 1994; Murray et al. 1996; Muyzer et al. 1993, 1996). This technique offers a quick view of the bacterial community without laborious gene cloning and sequencing. Large sample sets can therefore be processed and compared with ease (e.g. Bano and Hollibaugh 2001).

The PCR-DGGE method (Muyzer et al. 1993, 1996) separates PCR products of 16S rDNA fragments from a community sample according to their specific melting points ( $T_d$ ; Abrams and Stanton 1992). Melting points are determined by hydrogen bonding in the nucleotide sequence; therefore, different 16S rDNA sequences have different melting points. A polyacrylamide gel containing a linear gradient of denaturant of urea and formamide is used in DGGE. The 16S rDNA fragments will partially denature and stop migration when they reach the position of their specific melting point (denaturant) in the gel. A GC-clamp, or GC-rich sequence (Myers et al. 1985), is added to the PCR products to prevent the DNA strands from complete separation and rapid migration through the gel. Ethidium bromide or a fluorescently labeled primer can be used to visualize the DNA “fingerprint”. Each band represents a unique phylotype (Murray et al. 1996), or operational taxonomic unit (OTU), within the bacterial assemblage and each lane within the gel represents the phylotype profile of the community sample (Murray et al. 1996). Bands extracted from the gel may also be sequenced for phylogenetic analysis

Bacterial community structure in the Arctic Ocean has been assessed recently with PCR-DGGE (Ferrari and Hollibaugh 1999; Bano and Hollibaugh 2000; Yager et al. 2001; Bano and Hollibaugh 2002). Large spatial (Ferrari and Hollibaugh 1999) and temporal (Yager et al. 2001) variations in bacterial community composition are observed. More studies using this technique must be completed, however, to obtain a mechanistic understanding of bacterial diversity in the Arctic Ocean.

*The Arctic environment.* The Arctic environment is characterized by perennially cold temperatures and strong seasonality of physical conditions (Smith and Sakshaug 1990). Day length varies seasonally from 0 to 24 hours of solar radiation in winter and summer months, respectively (Holm-Hansen et al. 1977). Sea-ice retreats poleward and melts in localized areas such as leads and polynyas in the spring and summer months, creating conditions favorable for primary production (Smith and Nelson 1985; Sullivan et al. 1988). These physical conditions create intense spring/summer algal blooms in open water (Sverdrup 1953; Smith and Nelson; 1985; Sullivan 1988; Yager et al. 2001) and under sea-ice (Grossi et al. 1987). Integrated daily primary production during the summer can reach up to  $4000 \text{ g C m}^{-2} \text{ d}^{-1}$  in the Chukchi Sea (Hameedi 1978).

Microbial communities are found to be active components in cold ecosystems (Friedmann 1993; Steward et al. 1996; Yager et al. 2001). Temperature, substrate availability, predation, and viral infection are regulating factors of bacterial activity in permanently cold seas (Li and Dickie 1987; Pomeroy et al. 1990; Fuhrman 1992). Initial microbial research in the Arctic Ocean underestimated the effectiveness of the microbial loop under the hypothesis that cold temperatures coupled with low substrate conditions

decrease bacterial activity (Pomeroy and Diebel 1986; Pomeroy et al. 1990). More recent studies, however, reveal substantial production and microbial activity in the Arctic Ocean (Maranger et al. 1994; Muller-Niklas and Herndl 1996; Rivkin et al. 1996; Steward et al. 1996; Wheeler et al. 1996; Rich et al. 1997; Børsheim 2000; Yager et al. 2001), with the highest measurements of bacterial production occurring in the Chukchi Sea (Rich et al. 1997).

Episodic pulses of primary production are a major source of DOM/POM used by heterotrophic cold-loving bacteria in the Arctic (Sullivan et al. 1990). Algal “bloom” stages observed in the Chukchi Sea during the Arctic West Section 1998 (AWS98), show that bacterial and viral abundance, bacterial activity, and bacterial community structure change significantly during peak bloom stages (Yager et al. 2001). These observed changes may be the result of viral infection, bacterivory, and/or the availability of DOM/POM during the peak stage. A seasonal study of bacterivory in polar oceans, however, shows that grazing of bacterioplankton by protists is negligible immediately before and after peaks in primary production (Anderson and Rivkin 2001). Alternatively, differences in FL and PA assemblages may be enhanced with the availability of POM during the peak stage and viral infection may be increased, producing significant changes in bacterial community composition.

Despite growing interest in research on the microbial loop in the Arctic, relatively few studies have examined viral abundance (Maranger et al. 1994; Steward et al. 1996; Steward et al. 2000; Yager et al. 2001) or bacterial community composition (Ferrari and Hollibaugh 1999; Bano and Hollibaugh 2000; Yager et al. 2001; Bano and Hollibaugh 2002). Differences between FL and PA assemblages with bacterial and viral abundance

and POM are as yet unexamined in the Arctic Ocean or Chukchi Sea. A study in the Chukchi Sea that incorporates measurements of environmental parameters, bacterial and viral abundance, and bacterial community composition of FL and PA assemblages in different production regimes was therefore needed to determine significant factors controlling the microbial populations of this cold environment.

### **My Research**

Bacterial and viral abundance, bacterial community composition, and a suite of environmental parameters were measured in samples from the Chukchi Sea taken during the Arctic West Science of Opportunity Cruise (AWS00) in August 2000 aboard the USCGC Polar Star WAGB-10. Varying production regimes were sampled in order to examine variations among microbial abundance and bacterial community composition in high versus low production/POM regions. Correlation analyses were used to determine the most significant factors controlling bacterial and viral abundance and FL and PA bacterial community composition. Bacterial isolates were also obtained to determine the culturable bacterial species present, to compare isolate to community DGGE fingerprints, and for characterization by substrate utilization tests.

This study attempts to distinguish between FL and PA assemblages in response to variations in environmental parameters and microbial abundance in different production regimes in the Chukchi Sea. Filtration was used to separate the bacterial community into two size fractions: 3  $\mu\text{m}$ -filtered and unfiltered samples represented the FL and whole community (FL and PA) assemblages, respectively. PA bacteria in this research are defined as those bacteria residing on particles  $\geq 3 \mu\text{m}$ .

Questions. I was interested in how polar microbial communities varied in different production regimes and the parameters that controlled this variation. Do bottom-up or top-down parameters control differences in bacterial abundance and community structure in the polar environment? Are PA or FL communities affected differently? To address these general questions for high and low production regimes in the Chukchi Sea, I asked the following more specific questions:

**A: In high and low production regimes of the Chukchi Sea,**

**Question 1:** do bacterial and viral abundance vary spatially, and what other variables correlate with any variation?

**Question 2:** does bacterial community structure vary spatially, and what other variables correlate with any variation?

**B: FL and PA bacterial communities in the Chukchi Sea:**

**Question 3:** How different are FL and PA bacterial assemblages?

**Question 4:** Do differences between FL and PA assemblages vary between high and low production regimes?

**Question 5:** What variables control these differences?

**C: Bacterial isolates in the Chukchi Sea:**

**Question 6:** Are different isolates obtained in high and low production regimes?

**Question 7:** Does substrate utilization differ between isolates obtained from regions of high and low production?

**Question 8:** Are bands representing isolate phylotypes present in the community DGGE fingerprint?

*Hypotheses.* To answer these specific questions, I addressed the following hypotheses:

**A: Hypothesis 1 (bottom-up control):** The availability of dissolved and particulate organic matter is a significant factor determining bacterial abundance and community structure.

*Justification.* Bacterial abundance is elevated in regions of high production in the Chukchi Sea. Bacterial abundance and CHLa, DOM, and POM are likely to be correlated. Community composition is different in high and low production regimes, therefore different DGGE fingerprints in regions of high and low CHLa, DOM, and/or POM are likely to be obtained. Differences in bacterial community structure (i.e. Margalef's and Sorensen's Indexes) are therefore likely to correlate to CHLa, DOM, and POM.

**Hypothesis 2 (top-down control):** Viral infection is a significant factor determining bacterial abundance and community structure. In cases where viruses are controlling bacterial abundance, a strong correlation between bacterial and viral abundance should be found.

*Justification.* Viral abundance commonly correlates positively with bacterial abundance and the VBR is commonly inversely correlated with bacterial abundance. Viral infection is more likely in high production regimes where bacterial production and abundance is elevated. The VBR and VB values are

likely to be elevated, reaching the hypothetical lytic threshold ( $10^{12}$  VB mL<sup>-1</sup>) in these regions. Variations in community structure indexes of high and low production regions will likely correlate, therefore, to viral abundance.

**B: Hypothesis 3:** FL and PA bacterial assemblages are different and will produce different DGGE fingerprints.

*Justification.* Particles are niches for specialized bacterial species, such as certain members of the *Cytophaga* clade, which may be less abundant in the free-living community. DGGE fingerprints for unfiltered (whole community) and 3 $\mu$ m-filtered (FL community), therefore, will likely be different.

**Hypothesis 4:** Differences between FL and PA assemblages are more prominent in high production regions, where POM and viral abundance are elevated.

*Justification.* Higher production regions produce more particulate organic matter, so PA bacterial species should thrive in these regions. Percent similarity between unfiltered (whole community) and 3  $\mu$ m-filtered (FL community) DGGE fingerprints should therefore be reduced in regions of high production. POM availability and viral infection are significant factors in determining differences in FL and PA bacterial assemblages. A correlation between percent similarity (Sorensen's Index) of unfiltered and filtered samples and POM and viral abundance should therefore be observed.

**C: Hypothesis 5:** Dilution to extinction followed by culturing will yield the sample's numerically dominant culturable bacterial species, which will be different in high and low production regimes.

*Justification.* If bacterial community composition is controlled by DOM, POM, and viral infection, which are elevated in regions of high production, then dominant bacteria in high production regimes will likely be the most effective at incorporating elevated substrate concentrations and will also likely be more resistant to viral lysis. Isolates from the same station or production regime will likely be closely related and use the same substrates in the BIOLOG assay.

**Hypothesis 6:** The most abundant bacteria should be present in the DGGE fingerprint of the community.

*Justification.* PCR-DGGE fingerprints should resolve bands (OTUs) for all members of the bacterial community within a sample. Dilution to extinction should yield the sample's most abundant culturable species, so its phylotype should be present in the community DGGE.

## CHAPTER 2

### METHODS

#### **Location**

Arctic seawater samples were collected from the Chukchi Sea (continental shelf) aboard the United States Coast Guard Cutter Polar Star WAGB-10 during the Arctic West Science of Opportunity Cruise in August 2000 (AWS00). Seawater was collected using a standard CTD/rosette equipped with 12 30-L Niskin bottles. Five stations were chosen in a nearly south to north transect ( $70^{\circ}19'$ - $73^{\circ}14'$  N,  $144^{\circ}37'$ - $167^{\circ}35'$  W; Fig. 1) to sample variable ice-cover and production regimes. Three sampling depths were determined over the photic zone according to light intensity ( $I_0$ ) predetermined by Secchi depth and the CTD: 100%  $I_0$  (surface – 0 m), 30%  $I_0$  (usually chlorophyll maximum), and 1%  $I_0$  (bottom of the photic zone).

#### **Seawater Chemistry**

Seawater samples were analyzed for the following organic and inorganic constituents. Some analyses were performed by other scientists aboard the USGC Polar Star during AWSOO or at other institutions using samples I collected.

Chlorophyll a. Chlorophyll data from AWSOO was analyzed with standard fluorometric protocols (Holm-Hansen et al. 1965) at Old Dominion University (Dr. Glen Cota).

Nutrients. Duplicate seawater samples were collected in acid and base washed amber 32 oz. Nalgene bottles from two separate Niskins at each depth. Samples were then filtered through 47 mm Whatman GF/F filters with a glass tower filtration device and hand vacuum pumps. Filters were frozen and saved for chlorophyll a analysis and 100 mL filtrate was placed into acid and base washed 125 mL HDPE Nalgene bottles. Samples were frozen and stored in a  $-40\text{ }^{\circ}\text{C}$  freezer until shipment in iced coolers to University of Georgia for analysis.

Samples were analyzed for nitrate ( $\text{NO}_3$ ) and nitrite ( $\text{NO}_2$ ) with an OI Analytical Alpkem EnviroFlow 3000 with standard techniques (Strickland and Parsons 1972). The autoanalyzer read the nitrite ( $\text{NO}_2$ ) concentration. Nitrate ( $\text{NO}_3$ ) was reduced to  $\text{NO}_2$  with a cadmium column to get  $\text{NO}_x$  ( $\text{NO}_3 + \text{NO}_2$ ) concentration.  $\text{NO}_2$  was then subtracted from  $\text{NO}_x$  to get  $\text{NO}_3$  concentration.

Ammonium ( $\text{NH}_4$ ) was measured with standard spectrophotometric techniques (Solorzano 1969). Samples were mixed with an alkaline citrate medium with sodium hypochloride and phenol in the presence of sodium nitroprusside acting as a catalyst. Ammonium forms a blue indophenol color with the reagents that was read with a spectrophotometer. Ammonium concentration was then calculated from a standard curve.

Phosphate ( $\text{PO}_4$ ) was analyzed with standard spectrophotometric methods (Strickland and Parsons 1972). A mixed reagent of molybic acid, ascorbic acid, and antimony was reacted with the sample. The phosphate reacted with the reagents to form a blue complex that was read on the spectrophotometer. Phosphate concentrations were then calculated from a standard curve.

Dissolved organic carbon (DOC). Duplicate seawater samples were collected in ashed 500 mL glass bottles from two separate Niskins at each depth. Samples were frozen immediately in a  $-40$  °C freezer until shipment to the University of Connecticut (Dr. Annelie Skoog) for DOC analysis (Skoog et al. 1997).

Particulate organic carbon and nitrogen (POC and PON). Duplicate seawater samples were collected through Tygon tubing into clean plastic bottles and processed shipboard. Seawater was filtered through 25 mm combusted Whatman GF/F filters. Filters were frozen and stored in a  $-40$  °C freezer until analysis at University of Maryland's Chesapeake Biological Laboratories (Dr. H. Rodger Harvey and Laura Belicka: Standard Operating Procedure of CBL).

Total organic carbon (TOC). Measured DOC and POC values were added to obtain the total organic carbon (TOC) for the depth at each station.

### **Microbial Abundance and Variables**

Duplicate seawater samples were collected at each depth from 2 separate Niskin bottles into sterile 50 cc centrifuge tubes (Corning). Two sets of 10 mL were then placed into sterile 15 cc centrifuge tubes (Corning) and fixed with 0.2  $\mu\text{m}$ -filtered formaldehyde to a final concentration of 2%. Samples were then stored aboard in a  $-1$  °C incubator and shipped to University of Georgia on ice for analysis.

Bacterial abundance (AODC). Bacteria were enumerated using epifluorescence microscopy (Hobbie et al. 1977; Porter and Feig 1980). In order to obtain about 20-30

bacteria per field, 3-5 mL of sample was filtered through a 25 mm black polycarbonate membrane filter (0.2  $\mu\text{m}$  pore-size; Poretics) using a multiple filtration device (Hoeffler) with low air pressure (<10 cm Hg) vacuum filtration. The Poretics membrane was placed on top of a 25 mm Whatman GF/F on the filter unit to ensure even filtration. Filters were then stained with 4',6-diamidino-2-phenylindole (DAPI, 20  $\mu\text{g mL}^{-1}$ ; Sigma) for 5 minutes on the filtration tower before the DAPI was filtered through the membrane. Towers were rinsed with 0.2 $\mu\text{m}$ -filtered artificial seawater (ASW; 25 g NaCl, 0.7 g KCl, 5.3 g  $\text{MgCl}_2$  hydrate, 7 g  $\text{MgSO}_4$  hydrate, 1 L MilliQ water, pH adjusted to 7.5), ethanol, and deionized  $\text{H}_2\text{O}$  ( $\text{dH}_2\text{O}$ ) between samples. Control slides were also made with ASW to check for contamination.

Bacterial cells were counted under UV light excitation (360-370 nm) with an Olympus BX-40 microscope at 1000X (UPlanFl 100X oil immersion objective with a 10X ocular). Twenty fields per filter were counted. Bacterial abundance in terms of cells  $\text{mL}^{-1}$  were calculated with equation 1 and duplicates were averaged for each depth.

$$\frac{\text{cells}}{\text{field}} \times \frac{\text{fields}}{\text{filter}} \times \frac{1}{\text{volume}} = \# \text{ cells } \text{mL}^{-1}, \quad (1)$$

where volume equals the volume of seawater filtered.

*Viral abundance (VLP)*. Virus-like particles (VLP) were enumerated using epifluorescence microscopy (Lu et al. 1999). In order to obtain fields that were easily counted, a 1-3 mL sample was stained with SYBR Gold nucleic acid gel stain (Molecular Probes) to a final concentration of 2.5X in the dark for 5 minutes. Samples were then filtered through a 25 mm Whatman Anodisc aluminum oxide filter (0.02  $\mu\text{m}$  pore size) using a glass tower filtration device and low vacuum (<10 cm Hg). The Anodisc filter

was placed on top of two back-up filters (25 mm Whatman GF/F and 25 mm black polycarbonate membrane, 0.2  $\mu\text{m}$  pore-size; Poretics) to ensure even filtration. Filtration towers were flamed with ethanol between samples. Control slides were also made with 0.2  $\mu\text{m}$ -filtered ASW to check for contamination.

Slides were viewed at 1000X using oil immersion and epifluorescent light (narrow band excitation wavelength of 470-490 nm) on an Olympus BX-40 microscope. Pictures were taken of 10 fields per filter using a Photometrics Sensys (Tucson, Arizona) air-cooled charge coupled device (CCD) camera that was mounted onto the microscope and connected to OnCor Image Analysis System Version 2.0.5d software (Gaithersburg, Maryland). Image exposure time was adjusted to gain the “best” picture in terms of clarity and contrast. Bacterial cells were also counted directly on the microscope for each field. Digital images were recorded as TIFF files and processed in Adobe Photoshop 5.0. Image contrast was inverted and adjusted to produce pictures with the best contrast. VLP were counted on printouts by hand.

Derived microbial variables (VBR, VB). Bacterial and viral abundance from the viral abundance slides were calculated in terms of cells  $\text{mL}^{-1}$  (equation 1). These values were used to calculate the virus:bacteria ratio (VBR). VBR duplicate values were then averaged and used to adjust the virus counts in terms of the DAPI bacterial counts. This calculation created new viral counts to account for loss of VLP due to storage (viral counts were completed up to four months later than initial bacterial counts). Mean DAPI bacterial and adjusted viral counts were then used to calculate the product of bacterial  $\times$  viral abundance (VB).

## **Bacterial Community Composition**

Two 10 L seawater samples were collected with Tygon tubing from separate Niskins for each sampling depth into clean 10 L Nalgene cubitainers. One sample from each depth was filtered through a 293 mm Nucleopore polycarbonate membrane (3  $\mu\text{m}$  pore size) with gravity filtration directly from the Niskin for the 3  $\mu\text{m}$ -filtered (free-living community) sample. Samples were stored in a  $-1\text{ }^{\circ}\text{C}$  incubator until pressure filtration using a peristaltic pump through a sterile 0.22  $\mu\text{m}$  Millipore Sterivex GV filter cartridge. Sterivex filtrate was collected in clean 10 L cubitainers and stored in a  $-1\text{ }^{\circ}\text{C}$  incubator for later use in bacterial isolations and grazer experiments shipboard. Excess water was expelled from the cartridge and 1.8 mL lysis buffer (40 mM EDTA, 50 mM Tris-HCl, 0.75 M sucrose) was added to each cartridge. Cartridges were then frozen and stored in the  $-40\text{ }^{\circ}\text{C}$  freezer until shipment to UGA where they were stored in a  $-80\text{ }^{\circ}\text{C}$  freezer until processed.

Whole (particle-associated and free-living bacteria) and free-living (3  $\mu\text{m}$ -filtered) assemblages were analyzed using PCR-DGGE (Muyzer et al. 1993, 1996). DNA was extracted from the Sterivex units and universal 16S bacterial primers were used with the polymerase chain reaction (PCR) to produce products to be analyzed by DGGE.

*DNA extraction.* Frozen Sterivex cartridges were thawed at room temperature. An extraction blank was made by adding 1.8 mL lysis buffer to a sterile Sterivex unit as a control. Lysozyme solution (40  $\mu\text{l}$ ; 50  $\text{mg mL}^{-1}$  in lysis buffer) was added to each cartridge (capped with 3 cc Luer-Lok syringe tips and Parafilm to prevent leakage) and

cartridges were incubated for one hour on a rotator in a 37 °C oven. Proteinase K solution (50 µl; 20 mg mL<sup>-1</sup> in lysis buffer) and 20% SDS (100 µl; sodium dodecyl sulfate, BioRad) were added to each cartridge. Cartridges were incubated for 2 hours on a rotator in a 55 °C oven. Lysate from the cartridge was then transferred to two sterile 2 mL eppendorf centrifuge tubes using a “female” 3 cc syringe.

DNA was purified from 800 µl of lysate by sequential extraction. Lysate was placed into a sterile 2 mL eppendorf tube with 800 µl phenol:chloroform:isoamylalcohol (24:24:1; Ambion) and vortexed. Samples were then centrifuged (Eppendorf Centrifuge) at 4 °C and 12000 RPM for 10 minutes. Supernatant was removed and placed into another 2 mL eppendorf tube with 800 µl chloroform:isoamylalcohol (21:1; Sigma) and centrifuged as described previously. Supernatant was removed, placed into a sterile eppendorf tube, and 800 µl 1-butanol (Sigma) was added. Samples were vortexed and centrifuged as before. Supernatant was removed and discarded and subnatant was placed into a sterile Centricon-100 concentrator (Amicon). Stock 5X TE Buffer (500 µl; 1X TE: 1.58 g Tris-HCl and 0.37 g EDTA in 1 L MilliQ, adjusted to pH 8.0) was added and concentrators were centrifuged (SpeedFuge Savant) at 1000 RPM for 10 minutes on medium heat. Another 500 µl of 5X TE Buffer was added and concentrators were centrifuged again. Samples were removed from the concentrator tip, placed into sterile eppendorf tubes, and frozen at -20 °C until further processing.

Agarose gel procedures. The presence of DNA in the extracts was confirmed by electrophoresing a portion of the extracts on a 1.5% agarose gel. The agarose gel was placed into a Buffer Puffer (Owl B3) electrophoresis tank and covered with 0.5X TBE

Buffer (10X: 108 g Tris base, 55 g boric acid, and 40 mL 0.5 M EDTA in 1 L MilliQ, and adjusted to pH 8.3 with acetic acid). Equal volumes of blue loading dye and sample (3 $\mu$ l:3 $\mu$ l) were placed on parafilm, mixed with a sterile pipette, and loaded into wells in the gel. A 1 kb DNA ladder (100  $\mu$ g mL<sup>-1</sup>; Promega) size marker was loaded into the first well. The gel was run at 200V (BioRad PowerPac3000 power source) for 30 minutes and then stained in ethidium bromide (10 mg mL<sup>-1</sup>) for 5 minutes. Gel images were taken using an UVP GDS 7500 Gel Documentation System.

PCR amplification. Extracted DNA was amplified using PCR with primers 356f (bacterial) and fluorescein-labeled 517r (universal). These primers amplify positions 340 to 533 in *Escherichia coli* where a large fraction of the total variability in 16S rDNA is found (Barry et al. 1990). A 40 bp GC clamp (Myers et al. 1985) and a fluorescein label were added to the 5' end of the primers 356f and 517r, respectively:

356f with a GC-clamp (in bold): **CGC CCG CCG CGC CCC CGC CCC GTC CCG CCG CCC CCG CCC CCC TAC GGG AGG CAG CAG,**

517r tagged with Fluorescein (F): **F ATT ACC GCG GCT GCT GG.**

PCR reaction mixtures containing 4 $\mu$ l DNA extract and 91  $\mu$ l “master mix” (59 $\mu$ l Nuclease-free H<sub>2</sub>O, 10  $\mu$ l Thermophilic DNA 10X Buffer, 10  $\mu$ l 25 mM MgCl<sub>2</sub>, 5  $\mu$ l 356f primer with GC clamp, 5  $\mu$ l F-517r primer, and 2  $\mu$ l dNTP; Promega) were mixed in sterile 1.5 mL thin-walled eppendorf tubes and placed into a DNA Engine thermocycler (MJ Research). Touchdown 1 (Don et al. 1991) and “hot start” protocols (100  $\mu$ l total

volume) were used. The Touchdown 1 program includes an initial 5 minutes of denaturing at 94 °C where 5 µl “hot mix” (4.5 µl Nuclease-free H<sub>2</sub>O and 0.5 µl TAQ DNA Polymerase; Promega) is added prior to 30 cycles of denaturing (94 °C), annealing (beginning with 65 °C and decreasing 1°C with each cycle), and extension (72 °C). The program ends with a 10 minute cool-down to 4 °C. A post-PCR agarose gel (same procedure as above) was made to check for the presence of PCR products. DNA was then precipitated from samples containing PCR product.

*Product DNA precipitation.* DNA from PCR products was precipitated and quantified by adding sodium acetate (10 µl; 3 M sodium acetate adjusted to pH 5.2 with glacial acetic acid) and 2 volumes of ice-cold ethanol (220 µl) to each sample tube containing the PCR product. Tubes were held at -20 °C overnight. Samples were then centrifuged at 12000 RPM and 4 °C for 30 minutes. The supernatant was discarded and the tube containing the pellet DNA was dried in a SpeedVac (Savant) at 1000 RPM on medium heat for 10 minutes (tubes open). The dried DNA pellet was then resuspended in 16 µl 1X TE Buffer in the same tube. DNA concentrations were measured with the Hoescht dye assay (Paul and Myers 1982) on a Hoefer DyNA Quant200 fluorometer.

*Product DNA quantification.* A 2 mL fluorometric cuvette was rinsed with deionized H<sub>2</sub>O (dH<sub>2</sub>O) and 2 mL Hoescht dye solution (9 mL dH<sub>2</sub>O, 1 mL TNE Buffer: 11.69 g NaCl, 1.21 g Tris base, 0.37 g EDTA, 80 mL UV-pure water, adjusted pH 7.4, and 1 µl Hoescht dye) was added and used to zero the fluorometer. The fluorometer was calibrated by adding 1 µl DNA standard (Calf Thymus DNA , 250 ng/µl; Sigma). Samples were

then measured by adding 1  $\mu$ l sample to 2 mL dye solution. DNA product was quantified and the volume needed to load 0.5-0.7  $\mu$ g DNA in the DGGE gel was determined.

DGGE procedures. DGGE was performed on a CBS Scientific DGGE System (Del Mar, CA) on a 6.5% polyacrylamide gel (BioRad) containing a 45-65% gradient of denaturant (formamide and urea). Exactly 11.5 mL of each acrylamide solution (45 and 65%) were mixed with 80  $\mu$ l of APS (10% ammonium persulfate; Sigma) and 10  $\mu$ l of TEMED (N,N,N',N'-Tetramethylethylenediamine; Sigma) before placing into a gradient mixer that injected the gel solution into the gel form. The gel was allowed to polymerize for 2 hours at room temperature before loading DNA. TAE buffer (40 mM Tris Base, 20 mM sodium acetate, 1 mM EDTA, adjusted to pH 7.4) in the DGGE system (CBS Scientific) was allowed to warm to 62 °C for 15 minutes before inserting the gel. Gel wells were rinsed thoroughly with buffer solution and the gel was allowed to acclimate to the buffer temperature for 15 minutes before loading. Wells were loaded with 24  $\mu$ l of sample consisting of 7  $\mu$ g PCR product, 5  $\mu$ l TE Buffer, and 12  $\mu$ l loading dye and run at 75V for 15 hours. PCR/DGGE amplicons from *Clostridium perfringens* and *Bacillus thuringiensis* (Sigma) genomic DNA were combined to create a marker and positive control in DGGE and loaded in three lanes (outside and middle lanes). Gels were read using a FMBIO II Multi-View scanning unit and software (Hitachi).

DGGE analysis. DGGE gels were analyzed with Molecular Analyst-Fingerprint Plus software (BioRad version 1.12, Hercules, CA) according to the specifications found in

Hollibaugh et al. 2000. Gel images were converted to TIFF files and then downloaded into the Molecular Analyst program. First, the program converted the image by rescaling band intensities over 8 pixels against the highest and lowest values for each lane. Band position and intensity values were then stored as densitometric curves. Second, all gel lanes from the study were normalized to one reference standard lane chosen from one DGGE gel. Reference standard lanes on gels were then used to reformat the gel lanes by lining up reference points to match the chosen standard for normalization. Third, normalized densitometric curves were used in regression-based similarity analysis and cluster analysis (UPGMA) to create similarity dendrograms that gave the percent similarity between samples. This analysis used the overall shape of the densitometric curve without placing significance on band intensity. Finally, bands (operational taxonomic units: OTU) were counted for each sample lane. Bands that were not identified by the program, but were visible on the densitometric curve and by eye, were added manually.

Species richness was determined using the number of DGGE bands (OTU) in the calculation of Margalef's Diversity Index (Magurran 1988). Richness is represented by the number of OTUs resolved by DGGE from the unfiltered sample divided by bacterial abundance for that depth:

$$\text{Margalef's Diversity Index, } D_{mg} = \frac{(S-1)}{\ln N}, \quad (2)$$

where S and N represent the OTU number and bacterial abundance in cells mL<sup>-1</sup>, respectively. Richness was not calculated for filtered (free-living) samples since bacterial abundance was determined on unfiltered water samples only.

Differences between unfiltered (whole community) and 3 µm-filtered (free-living) DGGE samples were assessed by determining the percent similarity of their DGGE fingerprints using the Molecular Analyst software and through calculation of Sorenson's Index (Magurran 1988). Dendrograms provided the percent similarity between densitometric curves of sample lanes. Sorenson's Index (Magurran 1988), a pairwise similarity coefficient, was calculated using the number of common phylotypes (OTU) between unfiltered and filtered DGGE fingerprints:

$$\text{Sorenson's Index, } S = \frac{2j}{(a + b)}, \quad (3)$$

where a and b represent the number of phylotypes (OTU) in the unfiltered and filtered DGGE fingerprints, respectively, and j represents the number of phylotypes common to both samples.

### **Correlation Analysis**

Pearson product-moment correlation coefficients ( $r_{xy}$ ; Sokal and Rohlf 1995) were calculated between all measured variables. Partial product-moment correlation analysis (Sokal and Rohlf 1995) that removed the effect of one ( $r_{xy.z}$ ) variable was conducted to determine if variables correlated to bacterial abundance, viral abundance, and VB remained significant. The same correlation analysis was performed between species richness ( $D_{mg}$ ), Sorenson's Index of similarity (S), and measured microbial and environmental variables.

## **Bacterial Isolates**

Seawater samples for bacterial isolation were collected at Stations 1-4 from the 30% I<sub>0</sub> sampling depth only. Seawater was collected in sterile 50 cc centrifuge tubes from the Niskin. Three sets (named A, B, and C) of ten serial 1:10 dilutions were performed with seawater from the 0.2 µm Sterivex filtrate (from DGGE processing) from the same depth. Dilutions were stored in the shipboard -1 °C incubator until shipment home on ice.

Isolation. Dilutions were analyzed for bacterial presence using epifluorescence microscopy with DAPI. The last serial dilution showing bacterial presence was used for isolation. In all cases, the 10<sup>th</sup> dilution contained bacteria and was used, so dilution to extinction did not occur. Then 1 mL of the 10<sup>th</sup> dilution series was inoculated in 30 mL filtered (Whatman GF/F) autoclaved liquid medium (Marine Broth 2216, pH adjusted to 7.5; Difco) for growth at 3 °C for 2 weeks. Nutrient plates (made by boiling 1000 mL MilliQ, 15 g Agar, and 37.4 g Marine Broth 2216, pH adjusted to 7.6) were then inoculated with 10 µl of the liquid culture and incubated at 3 °C for 1 week. Two colonies (named 1 and 2) were picked from each plate and transferred to new liquid medium for growth. Liquid medium was added over the period of 2 weeks at 3 °C until a 400 mL culture was obtained for each isolate (24 isolates total).

Isolate cultures were analyzed for Gram Stain (Fisher), growth at room temperature, substrate utilization (BIOLOG GN2 Microplate), DGGE, and sequenced (16S rDNA). Isolates were also preserved for future studies.

Growth at room temperature. Isolates were checked for room temperature growth by placing 10 µl culture into 10 mL sterile liquid media (Marine Broth 2216; Difco) in a sterile 15 cc centrifuge tube. Tubes were capped and left to stand in the laboratory. Cultures were checked by eye at 48 h, 120 h, and 1 week for turbidity. A tube containing only liquid media was made as a control.

Substrate utilization (BIOLOG). BIOLOG plates (GN2 BIOLOG MicroPlate; Hayward, CA) were inoculated with rinsed isolate cells. First, 30 mL of the culture was centrifuged at 6000 RPM and 4 °C for 10 minutes. Second, the supernatant was poured off and cells were suspended in 10 mL autoclaved artificial seawater (ASW, cooled to 3 °C). This process was repeated until media was removed. Third, the absorbance of the final cell suspension was measured with a spectrophotometer and cultures were diluted or concentrated with ASW as needed to obtain a 30 mL inoculum with an absorbance of 0.1. The inoculum was stored at 3 °C for a maximum period of 2 hours before BIOLOG plates were inoculated using an Eppendorf multipipettor with sterile pipettes and troughs. One hundred twenty five µl of inoculum was placed in each well on the BIOLOG plate and duplicate plates were made for each isolate. The plates were then wrapped and stored at 3 °C until analysis. Wells were scored by eye in order of color intensity (1-3 grading system). Plates were scored every two weeks until no change was recorded (final reading taken at 8 weeks).

Culture concentration. Cultures were concentrated into a 1-2 mL pellet by centrifuging cultures at 4 °C and 6000 RPM in 15 cc centrifuge tubes. The supernatant was removed

after each 10 mL addition and the process repeated until a 1-2 mL pellet of cells was obtained. The pellet was then resuspended in lysis buffer at a ratio of 3:1 (lysis buffer:pellet) and stored in the -80 °C freezer until DNA extraction.

DNA extraction. DNA was extracted from the cultures for use in DGGE analysis and 16S rDNA sequencing using a modified method of the Sterivex (community) extraction. Lysozyme solution (40 µl) was added to 750 µl culture concentrate in a sterile 2 mL Eppendorf tube and tubes were incubated for one hour on a rotator in an oven at 37 °C. Proteinase K solution (25 µl) and 20% SDS (50 µl) were then added to the tubes and they were incubated on a rotator in an oven at 55 °C for 2 hours. Serial extraction then proceeded in steps identical to the community extraction protocol.

PCR-DGGE of isolates. Extracted isolate DNA was amplified with PCR in methods identical to community analysis using the 356f (bacterial) with a GC-clamp (Myers et al. 1985) and Fluorescein-labeled 517r primer sets. PCR products were then analyzed on agarose and DGGE gels in the same manner as community samples to create isolate DGGE gels for comparison to community DGGE gels with Molecular Analyst-Fingerprint Plus software (BioRad version 1.12, Hercules, CA).

16S rDNA sequencing. Extracted isolate DNA was also amplified by PCR using the 9f and 1492r primer sets. These products were used for 16S rDNA sequence analysis. These primer sets (written 5'-3' below) were used in sequences with primer 356f serving as an internal primer:

**9f** (EUB1): GAG TTT GAT CCT GGC TCA G (with degeneracy: GAG TTT GAT CMT GGC TCA G),

**1492r**: GGT TAC CTT GTT ACG ACT T.

PCR reactions were run through an agarose gel (procedures above) to check for the presence of PCR product. Isolate PCR products were then purified using a Wizard PCR Preps DNA Purification System (Promega). Purified isolate DNA was sequenced on an automated sequencer at the University of Georgia Molecular Genetics Instrument Facility (MGIF). Sequences obtained from the 9f, 341f, and 1492r primers were aligned and combined with the Genetics Computer Group Package (Madison, Wis.; RCR). Isolate 16S rDNA sequences were aligned to database sequences from the National Center for Biotechnology Information (NCBI: <http://www.ncbi.nlm.nih.gov/BLAST>) using a basic local alignment search tool (Altschul et al. 1990; BLAST) to search for similarity to other sequences. Database sequences from bacteria with the highest BLAST similarity values (NCBI) were used for phylogenetic analysis. A phylogenetic tree was created using Jukes-Cantor distances and the neighbor-joining method (PHYLIP package; Felsenstein 1993).

## CHAPTER 3

### RESULTS

#### Location

Stations lie within the Chukchi Sea between 70-74° N and 144-168° W, except for Station 5, which lies in the Beaufort Sea (Fig. 1; Table 1). All stations lie on the continental shelf except for Station 4, which lies on the continental slope leading into the Arctic Basin (Fig. 1). Surface water temperature was fairly constant at -1 °C for all stations and ice cover generally increased northward from 3/10 (Station 2) to 9/10 (Stations 3 and 4; Table 1).

#### Seawater Chemistry

Chlorophyll a (Table 1 and Fig. 2). Chlorophyll a (CHLa) concentrations ranged from 0.1-18.5 mg CHLa m<sup>-3</sup> with a mean value of  $3.9 \pm 5.8$  mg CHLa m<sup>-3</sup> ( $\pm$  SD). Highest CHLa concentrations were measured at Stations 2 and 3 and were nearly 10 and 4 times higher than other stations, respectively. A distinct chlorophyll maximum (18.5 mg CHLa m<sup>-3</sup>) was observed at 4 m at Station 2. Less pronounced chlorophyll maxima (2.2-7.7 mg CHLa m<sup>-3</sup>) were observed at Stations 1 and 3 at deeper depths (25 and 20 m, respectively). Chlorophyll a concentrations were low (0.1-0.2 mg CHLa m<sup>-3</sup>) and constant with depth at Stations 4 and 5.

**Table 1.** AWS00 Station data including location, station information, and seawater chemistry. Depth is indicated by “Z” for Secchi and bottom depth data. DIN is the sum of nitrate, nitrite, and ammonia concentrations. TOC is the sum of DOC and POC concentrations. The asterisk (\*) indicates mean values (n=2).

Station	Date	Lat/Long	Time	Ice Cover	Secchi Z (m)	Water Temp (°C)	Bottom Z (m)	Depth (m)	CHLa (mg m <sup>-3</sup> )	DIN* uM	PO <sub>4</sub> * uM	TOC uM	DOC uM	POC uM	PON uM	POC:PON
1	8/7/2000	70.19.00.8 N 167.35.42.6 W	12:45	7/10	10	-1.15	45	0	0.54	0.1	0.2	63	48	14.8	2.1	7
								5	0.85	0.1	0.6	87	72	15.2	2.5	6
								20	2.24	2.1	0.9	154	138	16.2	2.7	6
2	8/9/2000	72.03.57.5 N 162.50.32.1 W	9:30	1-5/10	5.5	-0.77	42	0	15.56	0.2	1.0	153	82	70.5	10.9	6
								3.9	18.51	2.3	1.1	140	74	66.3	10.9	6
								14.9	6.79	18.6	1.8	94	59	34.9	6.6	5
3	8/12/2000	71.32.54.3 N 158.06.32.2 W	9:40	9/10	6.2	-1.3	72	0	3.06	1.0	0.7	117	79	37.5	6.4	6
								14.2	3.32	1.3	1.1	119	86	33.3	5.8	6
								16.3	7.25	7.4	3.5	108	78	29.6	5.1	6
4	8/14/2000	73.14.37.3 N 158.03.49.2 W	9:00	9/10	29	-1.16	2189	0	0.07	0.6	0.6	60	58	1.8	0.3	6
								21.2	0.13	0.4	0.7	60	58	2.4	0.3	7
								81.3	0.07	14.1	1.6	57	56	1.4	0.2	9
5	8/18/2000	70.39.00.1 N 144.37.47.1 W	10:15	8/10	14.2	0.06	145	0	0.22	0.7	0.6	89	84	5.5	1.0	6
								10.6	0.17	1.1	0.7	76	71	5.1	0.8	6
								40.6	0.15	4.4	1.6	73	57	16.2	1.8	9

**Table 2.** AWS00 microbial data for Stations 1-5. Mean bacterial (AODC) and viral (VLP) abundance, the mean virus:bacteria ratio (VBR), and the product of mean AODC and mean VLP (VB) were calculated using samples from two separate Niskins at each sampling depth (n=2). The number of phylotype bands (#OTUs) in DGGE fingerprints is shown for unfiltered (U; whole community) and 3 $\mu$ m-filtered (F; free-living) samples. The number of common bands to unfiltered and filtered DGGE samples are shown. Margalef's index ( $D_{mg}$ ; whole community only) and Sorenson's index (S) show species richness and the similarity of DGGE fingerprints between unfiltered and filtered samples, respectively. Percent similarity of unfiltered and filtered DGGE fingerprints was obtained using cluster analysis from the Molecular Analyst program. The asterisk (\*) indicates mean values (n=2).

Station	Depth (m)	AODC* (ml <sup>-1</sup> )	VLP* (ml <sup>-1</sup> )	VBR*	VB*	# OTUs (U)	#OTUs (F)	# common OTUs	$D_{mg}$ (U)	%Similarity U vs. F	S Index
1	0	4.5E+05	1.7E+06	3.8	7.8E+11	23	18	14	1.6	87.6	0.68
	5	8.7E+05	8.3E+05	0.96	7.2E+11	16	17	12	1.1	88.9	0.73
	20	7.8E+05	1.3E+06	1.7	1.0E+12	30	28	25	2.2	96.2	0.86
2	0	6.9E+05	1.7E+06	2.5	1.2E+12	17	19	13	1.2	72.6	0.72
	3.9	7.5E+05	1.2E+06	1.6	9.0E+11	nd	14	nd	nd	nd	nd
	14.9	5.4E+05	1.2E+06	2.2	6.3E+11	14	17	9	1.0	69.1	0.58
3	0	7.5E+05	1.4E+06	1.8	1.0E+12	10	13	5	0.7	74.8	0.43
	14.2	7.8E+05	1.6E+06	2.1	1.3E+12	nd	8	nd	nd	nd	nd
	16.3	8.5E+05	1.4E+06	1.6	1.1E+12	8	10	6	0.5	74.1	0.67
4	0	9.0E+04	1.2E+05	1.3	1.1E+10	23	26	19	1.9	92.7	0.78
	21.2	1.4E+05	1.9E+05	1.4	2.5E+10	22	21	18	1.8	93.1	0.84
	81.3	7.7E+04	2.2E+05	2.8	1.7E+10	21	29	20	1.8	90.9	0.80
5	0	1.9E+05	1.5E+05	0.79	2.8E+10	nd	nd	nd	nd	nd	nd
	10.6	1.8E+05	2.0E+05	1.1	3.6E+10	nd	nd	nd	nd	nd	nd
	40.6	1.8E+05	3.7E+05	2.1	6.6E+10	nd	nd	nd	nd	nd	nd

Nutrients (Table 1 and Fig. 2). Dissolved inorganic nitrogen (DIN) concentrations ranged from 0.1-18.6  $\mu\text{M}$  with a mean value of  $3.7 \pm 5.6 \mu\text{M}$  ( $\pm$  SD). Phosphate ( $\text{PO}_4$ ) concentrations ranged from 0.2-3.5  $\mu\text{M}$  with a mean value of  $1.1 \pm 0.8 \mu\text{M}$  ( $\pm$  SD). Highest and lowest surface DIN values were measured at and Station 3 (0.7  $\mu\text{M}$ ) and Station 1 (0.1  $\mu\text{M}$ ), respectively. Surface  $\text{PO}_4$  concentrations were highest at Stations 2 (1.0  $\mu\text{M}$ ) and 3 (0.7  $\mu\text{M}$ ) and lowest at Station 1 (0.2  $\mu\text{M}$ ). DIN and  $\text{PO}_4$  concentrations increased with depth at all stations.

Carbon: TOC and DOC (Table 1 and Fig. 3). Total organic carbon (TOC) concentrations ranged from 57-154  $\mu\text{M}$  with a mean value of  $97 \pm 34 \mu\text{M}$  ( $\pm$  SD). Dissolved organic carbon (DOC) concentrations ranged from 48-138  $\mu\text{M}$  with a mean value of  $73 \pm 21 \mu\text{M}$  ( $\pm$  SD). Station 2 contained the highest surface (100 and 30%  $I_0$ ) TOC values (140-153  $\mu\text{M}$ ). Station 1 had the highest TOC value (154  $\mu\text{M}$ ) and the highest DOC concentration (138  $\mu\text{M}$ ) at the 1%  $I_0$ , but contained the lowest surface value (48  $\mu\text{M}$ ). The highest surface DOC was measured at Station 5 (84  $\mu\text{M}$ ). Depth- averaged DOC at Stations 1, 2, and 3 was slightly higher than Stations 4 and 5. TOC and DOC increased with depth at Station 1, decreased with depth at Station 2, and remained fairly constant with depth at Stations 3, 4 and 5.

Particulate organic matter (POM): POC and PON (Table 1 and Fig. 3). Particulate organic carbon (POC) concentrations ranged from 1.4-70.5  $\mu\text{M}$  with a mean value of  $23.4 \pm 22.1 \mu\text{M}$  ( $\pm$  SD). Particulate organic nitrogen (PON) concentrations ranged from 0.1-10.9  $\mu\text{M}$  with a mean value of  $3.8 \pm 3.6 \mu\text{M}$  ( $\pm$  SD). POC:PON ratio ranged from

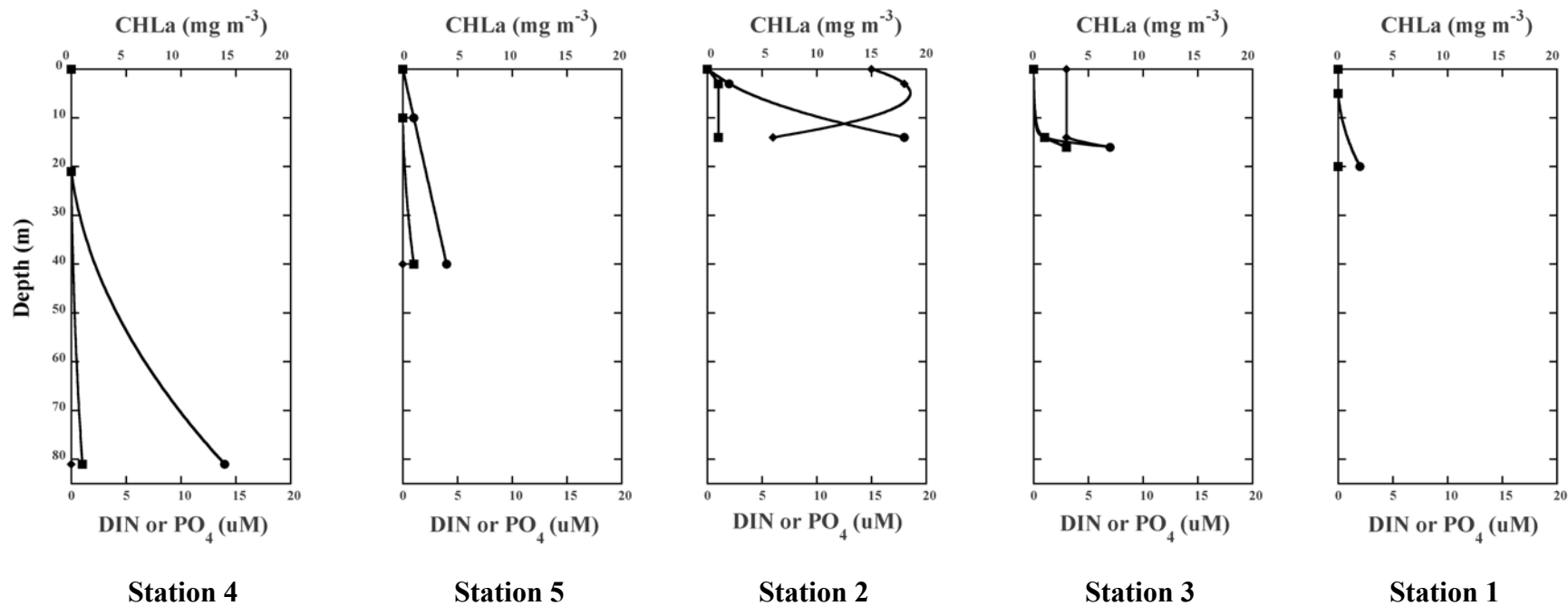


**Figure 2.** AWSOO depth profiles of chlorophyll a ( $\blacklozenge$ ), DIN ( $\bullet$ ), and  $\text{PO}_4$  ( $\blacksquare$ ) over the photic zone of Stations 1-5. Stations are arranged in order of a hypothetical bloom sequence with Stations 4 and 5, Station 2 and 3, and Station 1 representing pre-, peak, and post bloom stages, respectively. Data points represent samples from 100, 30, and 1%  $I_0$ .

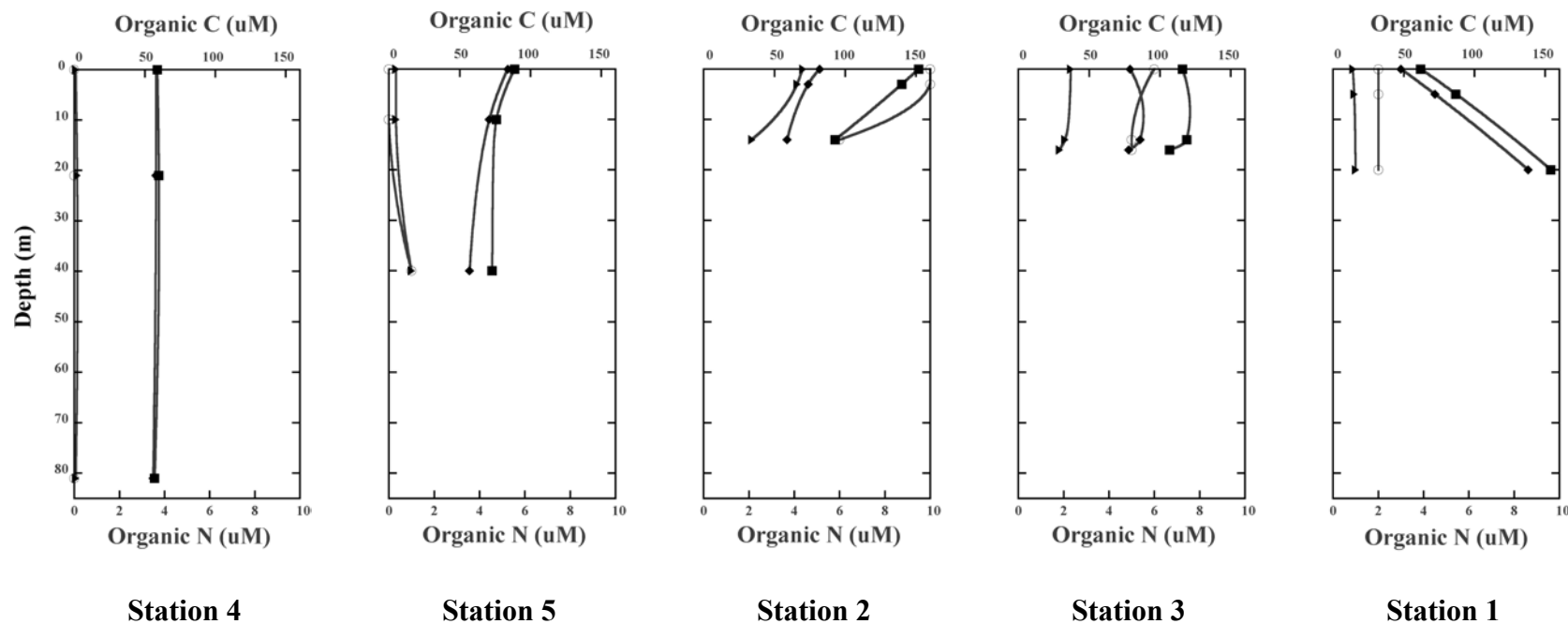


**Figure 3.** AWSOO depth profiles of organic matter over the photic zones of Stations 1-5: TOC (■), DOC (◆), POC (▲), and PON (○). Stations are arranged in order of a hypothetical bloom sequence with Stations 4 and 5, Station 2 and 3, and Station 1 representing pre-, peak, and post bloom stages, respectively. Data points represent samples from 100, 30, and 1%  $I_0$ .

5.3-9.3 with a mean value of  $6.5 \pm 1.1$  ( $\pm$  SD). Stations 2 and 3 contained higher POM concentrations than Stations 1, 4, and 5. The POC:PON ratio averaged  $\sim 6$  (“fresh” organic matter) for Stations 1, 2, and 3, but was slightly higher at  $\sim 7$  at Stations 4 and 5.

### **Microbial Abundance and Variables**

Bacterial abundance (AODC) (Table 2 and Fig. 4). Bacterial abundance (AODC) ranged from  $7.7 \times 10^4$ - $8.7 \times 10^5$   $\text{mL}^{-1}$  with a mean value of  $5.2 \times 10^5 \pm 3.6 \times 10^5$   $\text{mL}^{-1}$  ( $\pm$  SD).

Surface (100%  $I_0$ ) bacterial abundance was highest at Station 3 ( $7.5 \times 10^5$   $\text{mL}^{-1}$ ) and lowest at Station 4 ( $9.0 \times 10^4$   $\text{mL}^{-1}$ ). Station 1, 2, and 3 bacterial abundance was nearly 7 times higher than Stations 4 and 5. Bacterial abundance increased slightly with depth at Stations 1 and 3, but remained fairly constant with depth at other stations.

Viral abundance (VLP) (Table 2 and Fig. 4). Viral abundance was an order of a magnitude higher than bacterial abundance at most stations. Viral abundance ranged from  $1.2 \times 10^5$ - $1.7 \times 10^6$   $\text{mL}^{-1}$  with a mean value of  $9.0 \times 10^5 \pm 6.3 \times 10^5$   $\text{mL}^{-1}$  ( $\pm$  SD). Station variation in viral abundance matched that of bacterial abundance. Overall viral abundance was about 1 order of magnitude higher at Stations 1, 2, and 3 ( $\sim 10^6$   $\text{mL}^{-1}$ ) than Stations 4 and 5 ( $\sim 10^5$   $\text{mL}^{-1}$ ). Highest and lowest surface values of viral abundance were measured at Station 2 ( $1.7 \times 10^6$   $\text{mL}^{-1}$ ) and Station 4 ( $1.2 \times 10^5$   $\text{mL}^{-1}$ ), respectively. Viral abundance increased slightly with depth at Stations 4 and 5, and remained fairly constant with depth at Stations 1, 2, and 3.

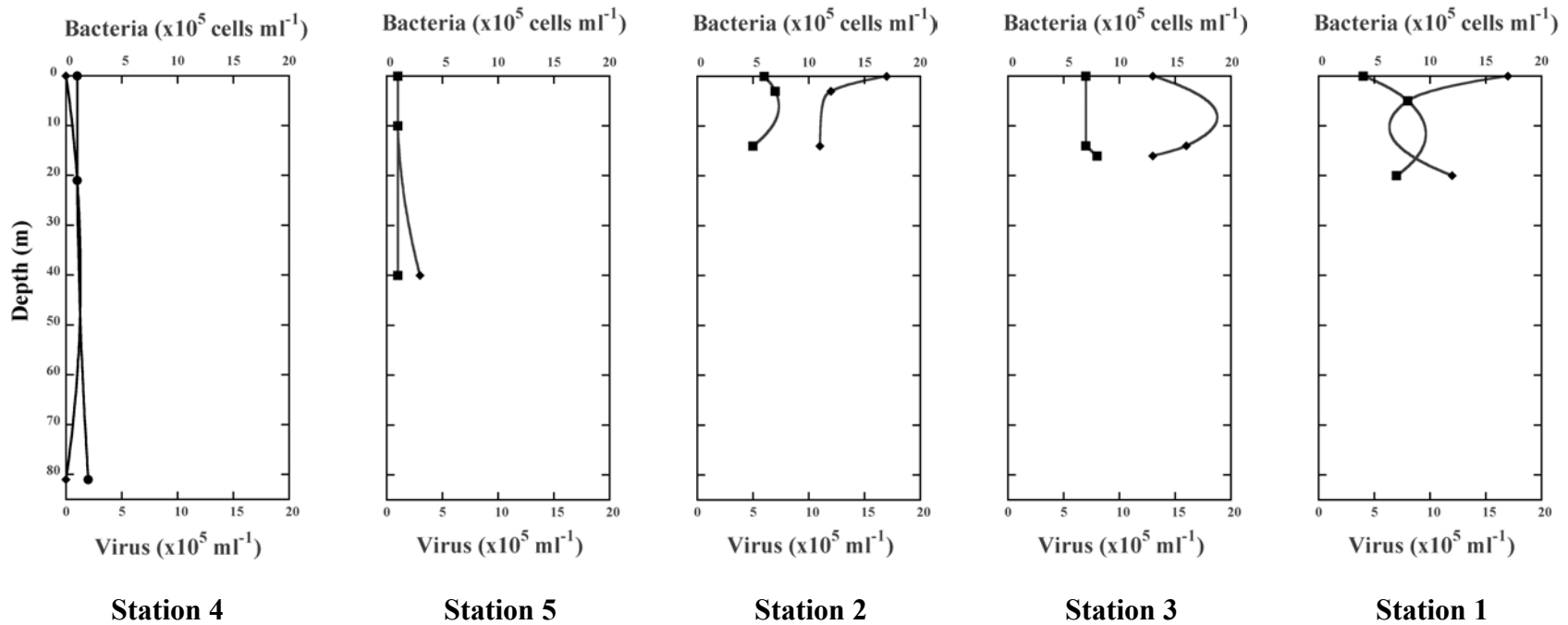


**Figure 4.** AWSOO depth profiles of bacterial (■) and viral (◆) over the photic zone of Stations 1-5. Stations are arranged in order of a hypothetical bloom sequence with Stations 4 and 5, Station 2 and 3, and Station 1 representing pre-, peak, and post bloom stages, respectively. Data points represent samples from 100, 30, and 1%  $I_0$ .

Microbial variables: VBR and VB (Table 2). The ratio of viral to bacterial abundance (VBR) ranged from 0.75-3.8 with a mean value of  $1.9 \pm 0.90$  ( $\pm$  SD). The depth-averaged VBR was about 2 for all stations. Stations 1 and 2 contained the highest surface (100%  $I_0$ ) VBR values at 3.8 and 2.5, respectively. The lowest surface VBR value was measured at Station 5 (0.79). Slight increases in VBR with depth were observed at Stations 1, 4, and 5.

The product of bacterial  $\times$  viral abundance (VB) ranged over 2 orders of magnitude from  $1.0 \times 10^{10}$ - $1.0 \times 10^{12}$   $\text{mL}^{-1}$ . The theoretical lytic threshold ( $10^{12}$   $\text{mL}^{-1}$ ; Wilcox and Fuhrman 1994) was reached at all depths at Station 3, the surface of Station 2, and at 1%  $I_0$  at Station 1 (Table 2; Fig. 5). VB values at other depths at Stations 1 and 2 were close to the lytic threshold value. VB values at Stations 1, 2, and 3 were about an order of magnitude higher than Stations 4 and 5. VB values increased and decreased with depth at Stations 1 and 2, respectively (Fig. 5).

### **Station Bloom Sequence**

Stations 1-5 were arranged in a hypothetical bloom sequence according to their CHLa, DIN, and  $\text{PO}_4$  depth profiles (Fig. 2, 3, and 4). Stations 4 and 5 were determined to represent pre-bloom stages due to their location (Fig. 1) and their low CHLa (Fig. 2) and POC (Fig. 3) concentrations that were constant with depth. Peak bloom stages are represented by Stations 2 and 3 due to their CHLa maxima (Fig. 2), low DIN (Fig. 2), and high OM (Fig. 3) concentrations. Station 3 was placed after Station 2 because it had a deeper CHLa maximum (Fig. 2) and lower POM concentration (Fig. 3). Station 1 was

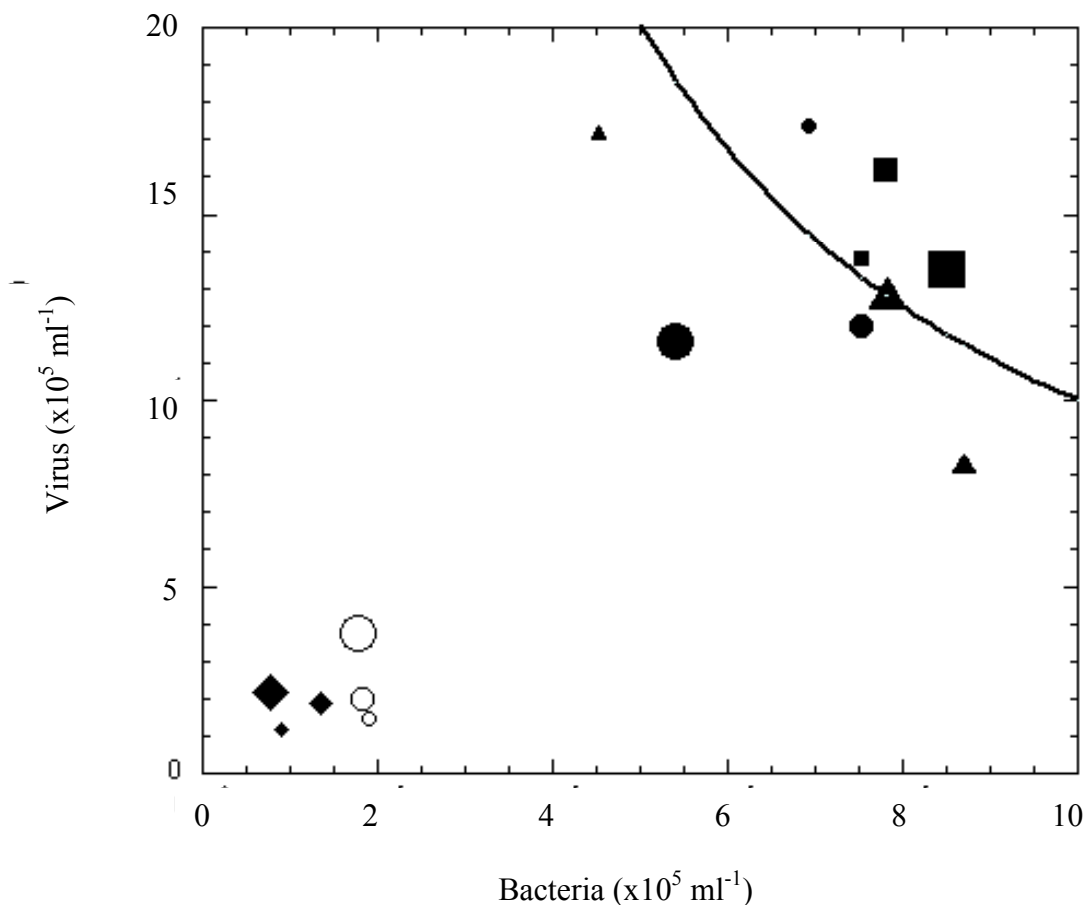


**Figure 5.** Graph of AWS00 Station microbial data showing viral vs. bacterial abundance in cells mL<sup>-1</sup>. The line represents the theoretical lytic threshold ( $VB = 10^{12} \text{ mL}^{-1}$ ; Wilcox and Fuhrman 1994). Data points above this line (Stations 1, 2, and 3) represent samples that exceed the lytic threshold, i.e. viral infection may be widespread. The graph depicts samples by Station (Sta 1: ▲, Sta 2: ●, Sta 3: ■, Sta 4: ◆, and Sta 5: ○) and depth: surface (100%  $I_0$ ), mid-depth (30%  $I_0$ ), and deep (1%  $I_0$ ) samples are represented by the smallest, mid-sized, and biggest icons, respectively. A relationship between viral and bacterial abundance is also observed ( $r=0.82$ ,  $n=15$ ).

chosen to represent a post-bloom stage due to its low CHLa and DIN concentrations (Fig. 2) and its decreased surface POM concentration (Fig. 3).

Sequence graphs of station microbial abundance and CHLa (Fig. 6), POC (Fig. 7), and PON (not shown) showed concomitant increases in CHLa, POM, and bacterial and viral abundance at the peak-bloom stations (Stations 2 and 3). Bacterial and viral abundance remained elevated during the post-bloom stage (Station 1) while CHLa, POC, and PON concentrations decreased to pre-bloom (Stations 4 and 5) values. Changes in CHLa, POC, PON, and microbial abundance during the bloom were more dramatic in the surface (100% I<sub>0</sub>) samples.

Sequence graphs of station VB (Fig. 8) and VBR (not shown, but can be seen in Fig. 4) showed that these parameters also changed during the bloom. Concomitant increases in VB with POC (Fig. 8), PON (not shown), and CHLa (not shown) were observed at peak-bloom Station 2. VB decreased slightly in the surface (100% I<sub>0</sub>), but continued to increase at 30% and 1% I<sub>0</sub> during peak Station 3. VB then decreased at all depths during the post-bloom stage (Station 1). Surface (100% I<sub>0</sub>) VB values rose above the theoretical lytic threshold value of 10<sup>12</sup> mL<sup>-1</sup> during peak-bloom Stations 2 and 3 (Fig. 5 and 8). Mid-depth (30% I<sub>0</sub>) VB values reached this threshold at peak-bloom Station 3 only (Fig. 5 and 8). Deep (1% I<sub>0</sub>) VB values reached the threshold at peak-bloom Station 3 and remained above the threshold during the post-bloom stage (Station 1; Fig. 5 and 8). VBR was increased during the peak (Stations 2 and 3) and post-bloom (Station 1) stages (Fig. 4).

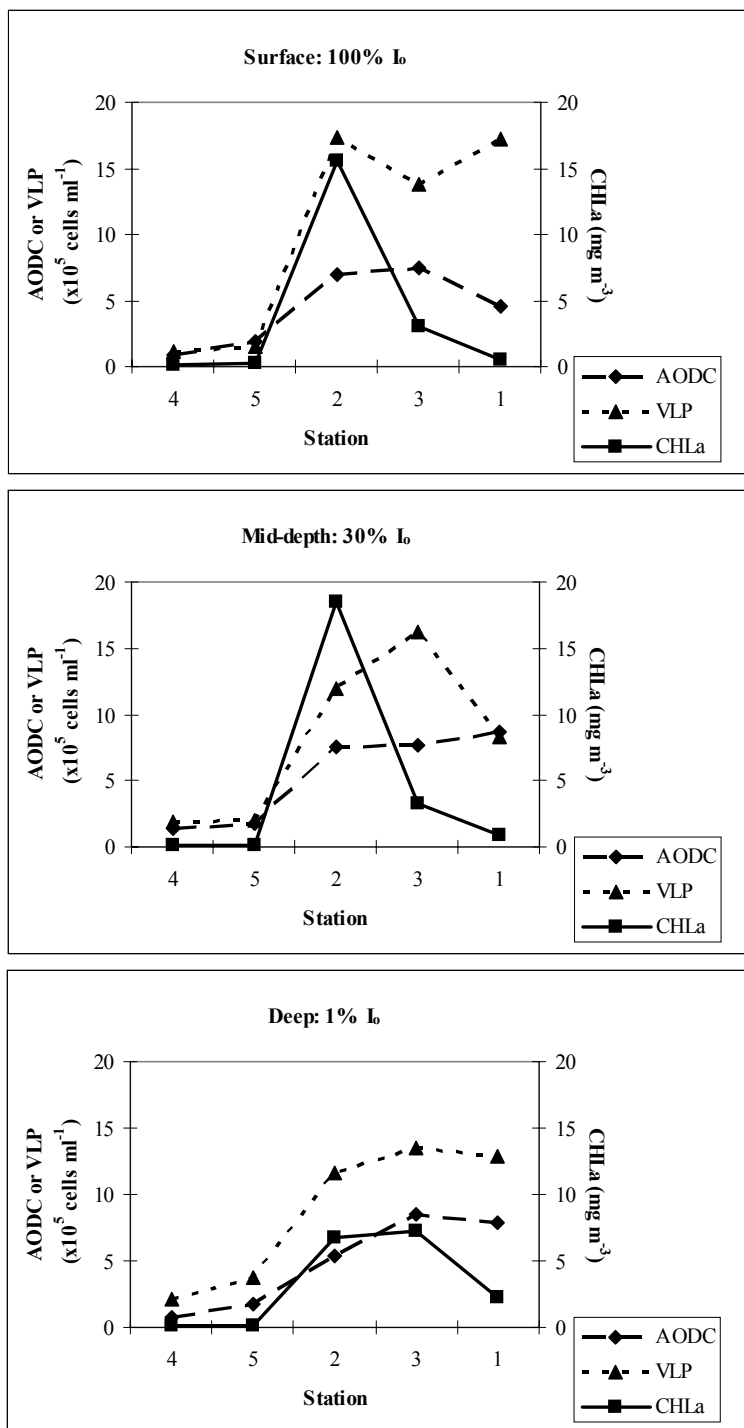


**Figure 6.** AWS00 Station sequence graphs showing CHLa (■) and bacterial (AODC; ◆) and viral abundance (VLP; ▲) for a) surface (100% I<sub>0</sub>), b) mid-depth (30% I<sub>0</sub>) and c) deep (1% I<sub>0</sub>) data. Stations 1-5 are arranged in a hypothetical bloom sequence: 4 and 5 are pre-bloom, 2 and 3 are peak-bloom, and 1 is post-bloom.

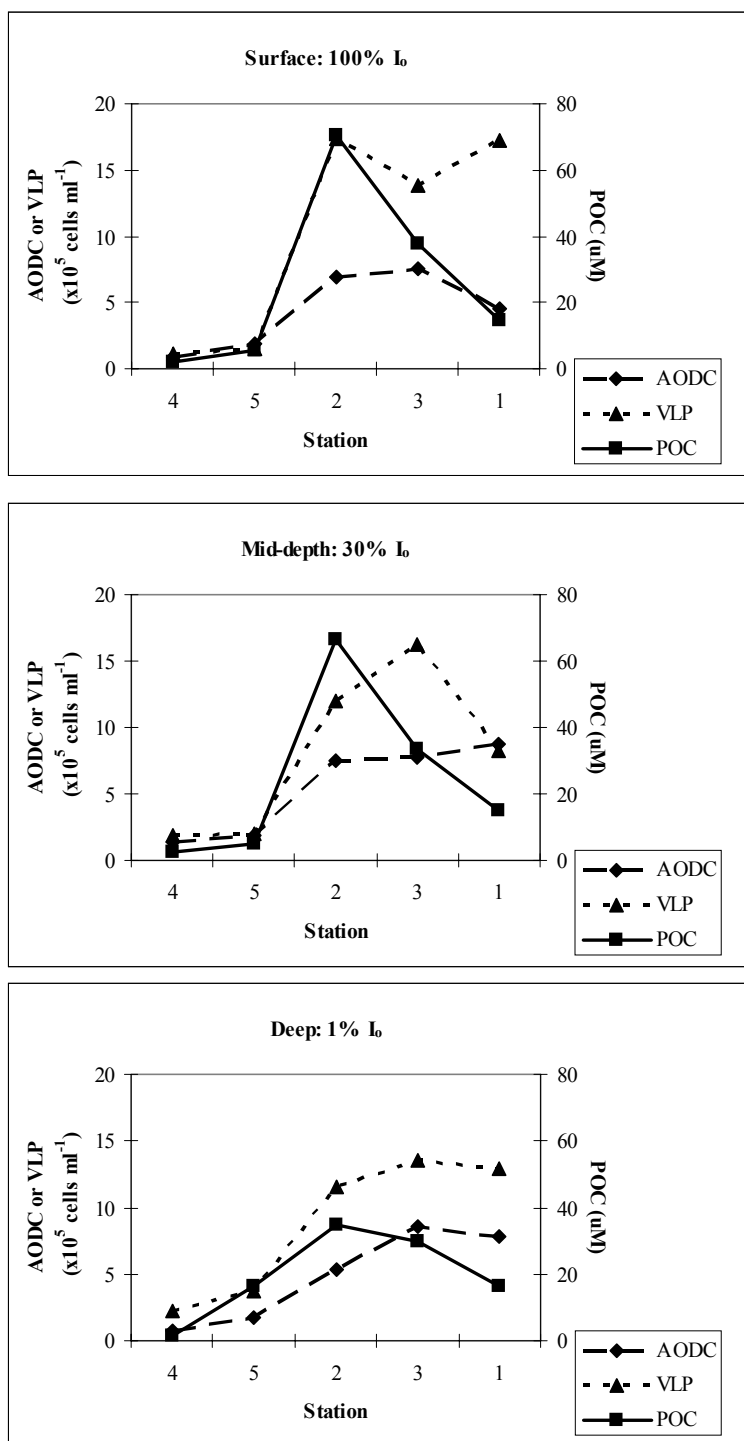


**Figure 7.** AWS00 Station sequence graphs showing POC (■) and bacterial (AODC; ◆) and viral abundance (VLP; ▲) for a) surface (100% I<sub>0</sub>), b) mid-depth (30% I<sub>0</sub>) and c) deep (1% I<sub>0</sub>) data. Stations 1-5 are arranged in a hypothetical bloom sequence: 4 and 5 are pre-bloom, 2 and 3 are peak-bloom, and 1 is post-bloom.

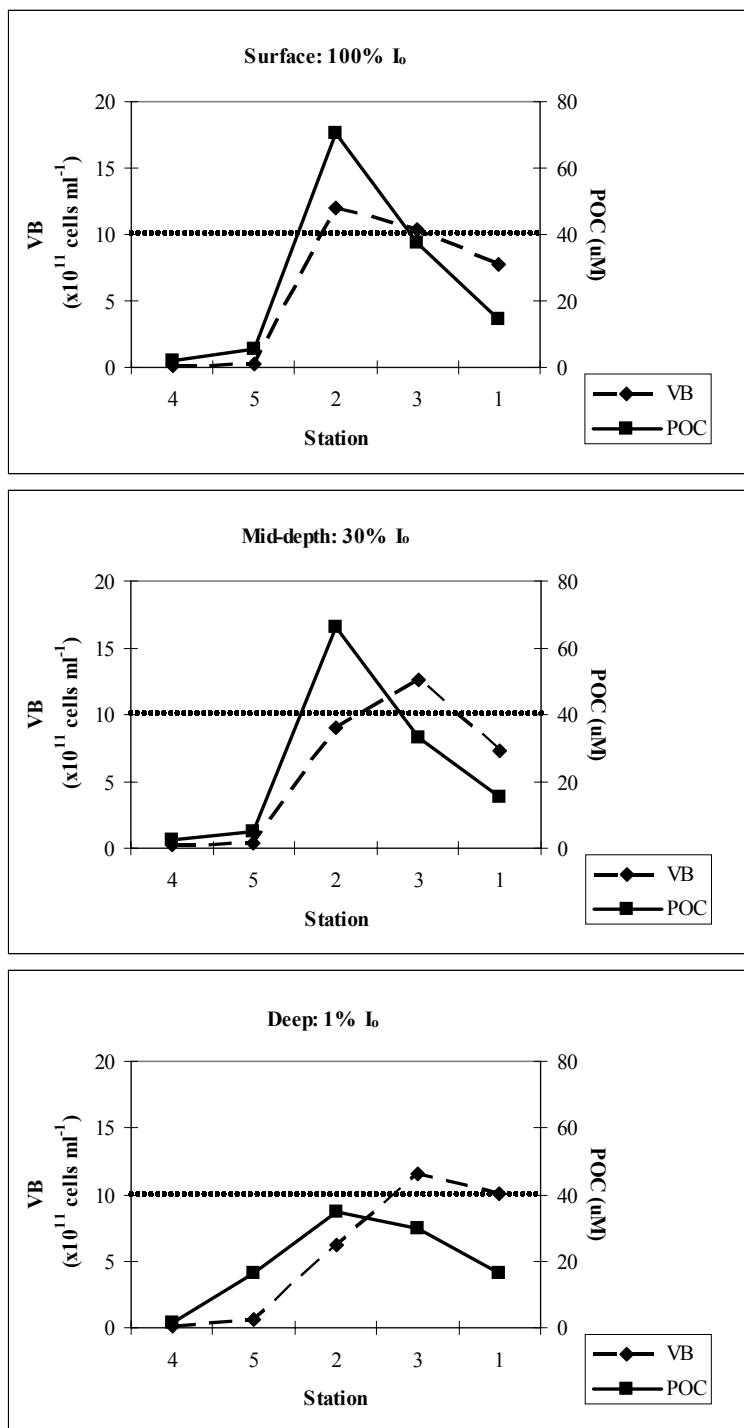


**Figure 8.** AWS00 Station sequence graphs showing POC (■) and bacterial  $\times$  viral abundance (VB; ◆) for a) surface (100%  $I_0$ ), b) mid-depth (30%  $I_0$ ) and c) deep (1%  $I_0$ ) data. Stations 1-5 are arranged in a hypothetical bloom sequence: 4 and 5 are pre-bloom, 2 and 3 are peak-bloom, and 1 is post-bloom. Sequence graphs for PON look identical (not shown).

## Bacterial Community Composition

DGGE was performed only on samples from Stations 1-4 (Fig. 9-12). The number of Operational Taxonomic Units (OTU), or bacterial phylotype bands, ranged from 8-30 and 8-29 for unfiltered and filtered samples, respectively (Table 2). DGGE fingerprints varied between station and depth (Fig. 9-12). Noteworthy differences included: 1) the appearance of unique phylotypes at the surface (relative to other depths at the same station) in Station 1 (bands a and b; Figure 9) and Station 4 (band c; Fig. 12); 2) Station 4 contained phylotypes not found in other stations (i.e. band d in Fig. 12; can be seen on the right in Fig. 13); 3) the disappearance of a phylotype from Station 2 (band e; Fig. 9 and 13). Cluster analysis showed that DGGE fingerprints clustered by station except for samples from 81 m (1% I<sub>o</sub>) from Station 4 (Fig. 13).

Species richness and OTU count differed between stations. Stations 1 and 4 OTU count and species richness ( $D_{mg}$ ) was about 1.5-2 times higher than Stations 2 and 3, respectively (Table 2). Species richness ( $D_{mg}$ ) decreased with depth except at Station 1 where it increased (Table 2).

The number and position of phylotypes (OTU) differed between unfiltered (whole community) and 3- $\mu$ m filtered (free-living assemblage) samples (Table 2). Noteworthy OTU that were exclusive to one or the other sample type included; the filtered sample from 15 m at Station 2 (band f; Figure 13) and the unfiltered sample from 0 m at Station 3 (band g; Figure 14). Filtered samples generally produced more OTU in Stations 2, 3, and 4, and less OTU in Station 1 (Table 2, Fig. 13). Filtered and unfiltered DGGE fingerprints from the same depth had a higher percentage of common bands and banding patterns at Stations 1 and 4 (87.6-96.2% similarity) than Stations 2 and 3 (69.1-74.8%

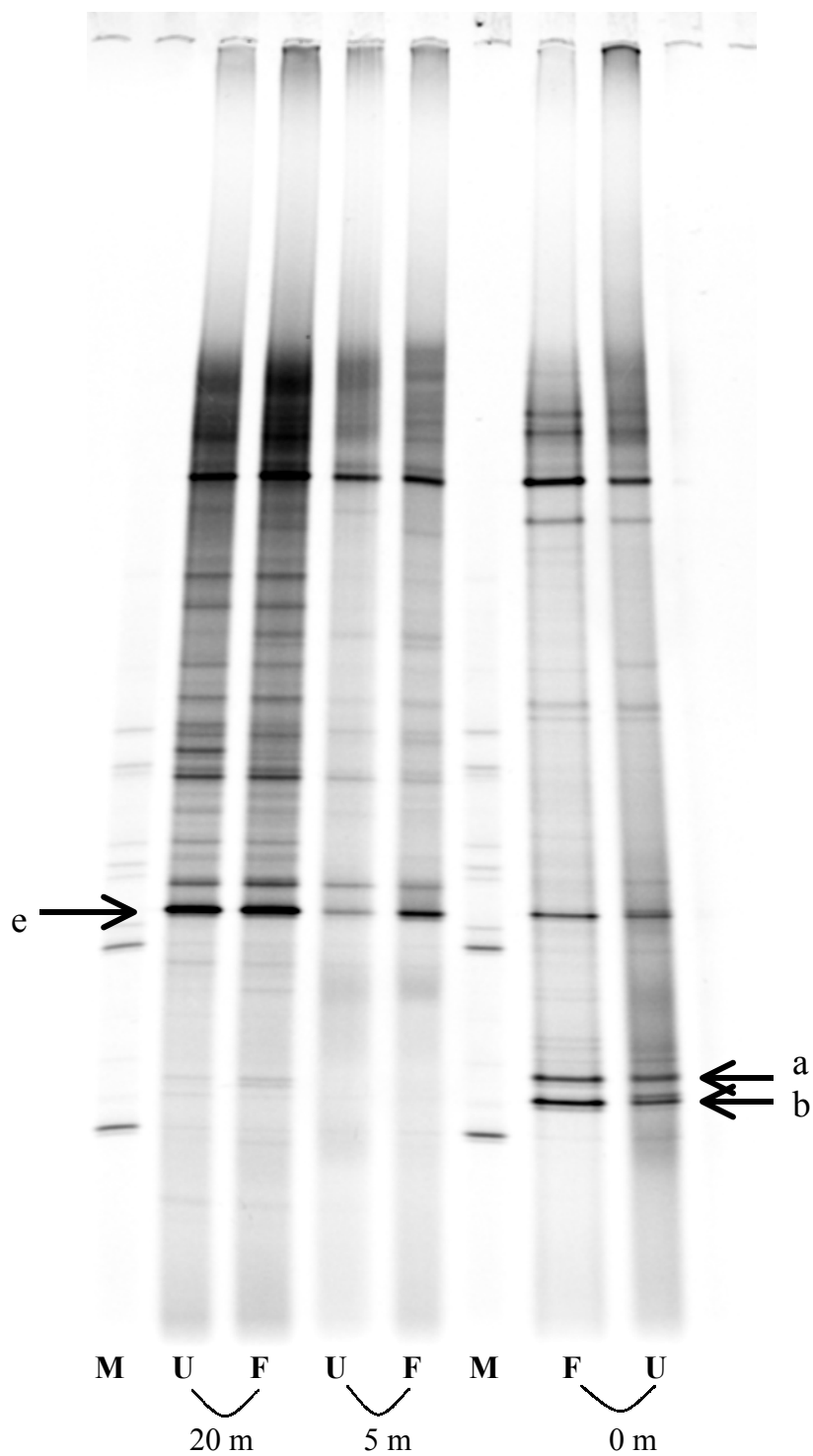


**Figure 9.** DGGE gel of AWS00 Station 1 unfiltered (U) and 3µm-filtered (F) samples with standard marker lanes (M). Bands a and b are only present in the surface (0 m) sample, and band e is present at all depths and stations except for Station 2 (see Fig. 10-12).

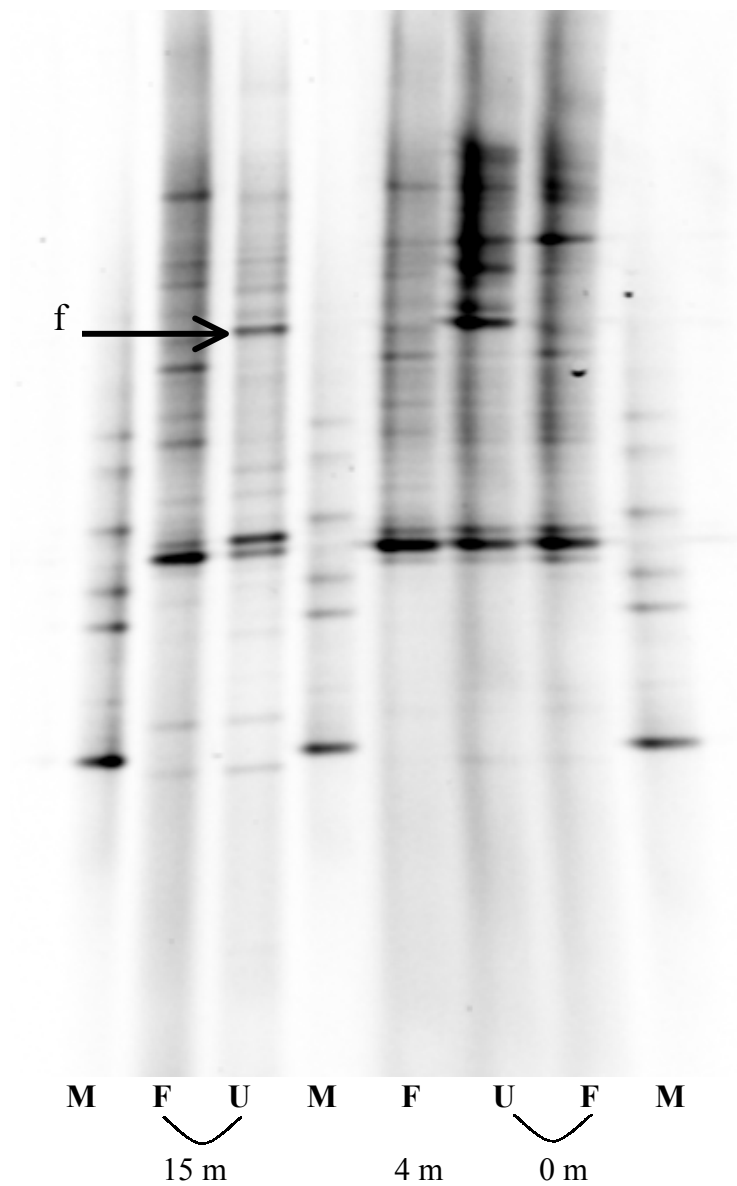


**Figure 10.** DGGE gel of AWS00 Station 2 unfiltered (U) and 3µm-filtered (F) samples with standard marker lanes (M). Band f is present in the unfiltered sample but not the 3µm-filtered sample from 15 m.

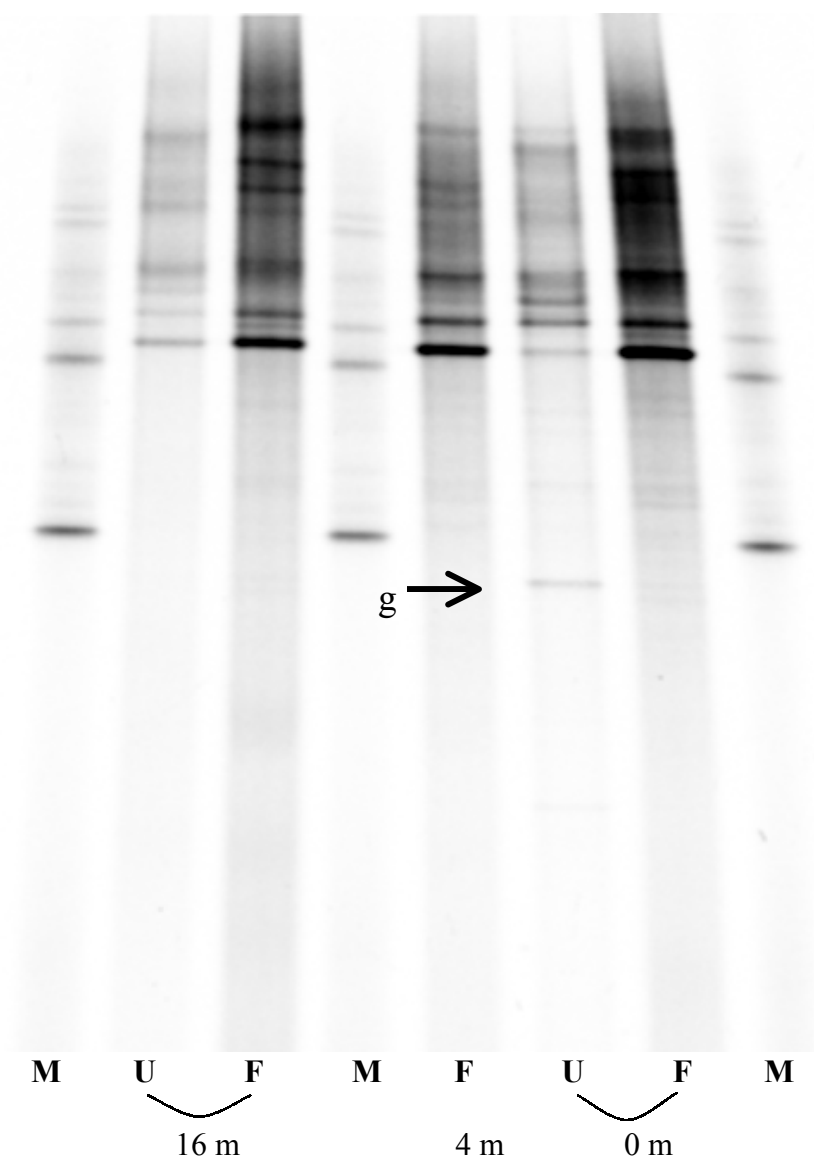


**Figure 11.** DGGE gel of AWS00 Station 3 unfiltered (U) and 3 $\mu$ m-filtered (F) samples with standard marker lanes (M). Band g is present in the unfiltered sample but not the 3 $\mu$ m-filtered sample from 0 m.

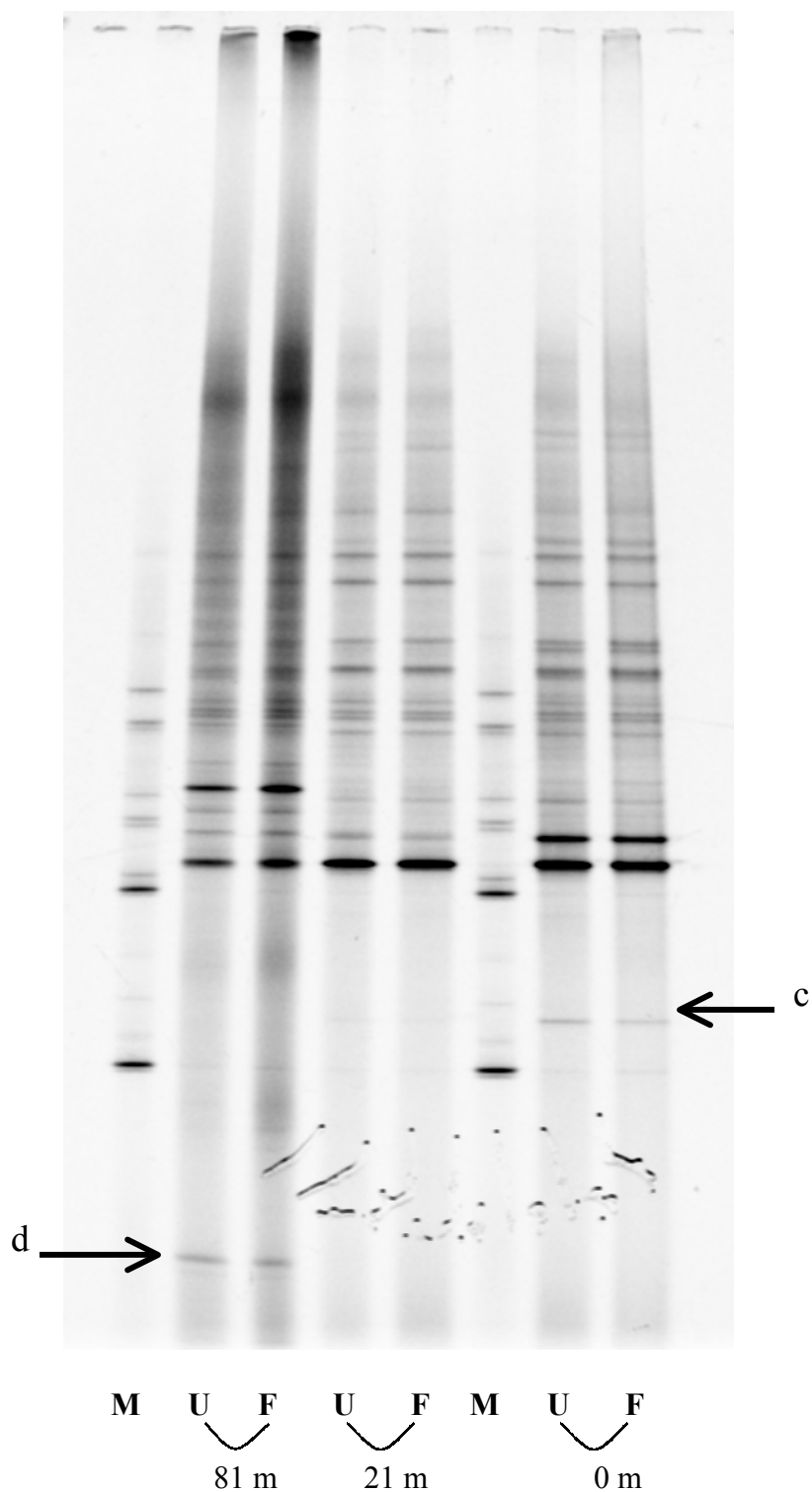


**Figure 12.** DGGE gel of AWS00 Station 4 unfiltered (U) and 3 $\mu$ m-filtered (F) samples with standard marker lanes (M). Bands c and d are only present at Station 4 and at 0 and 81 m, respectively.

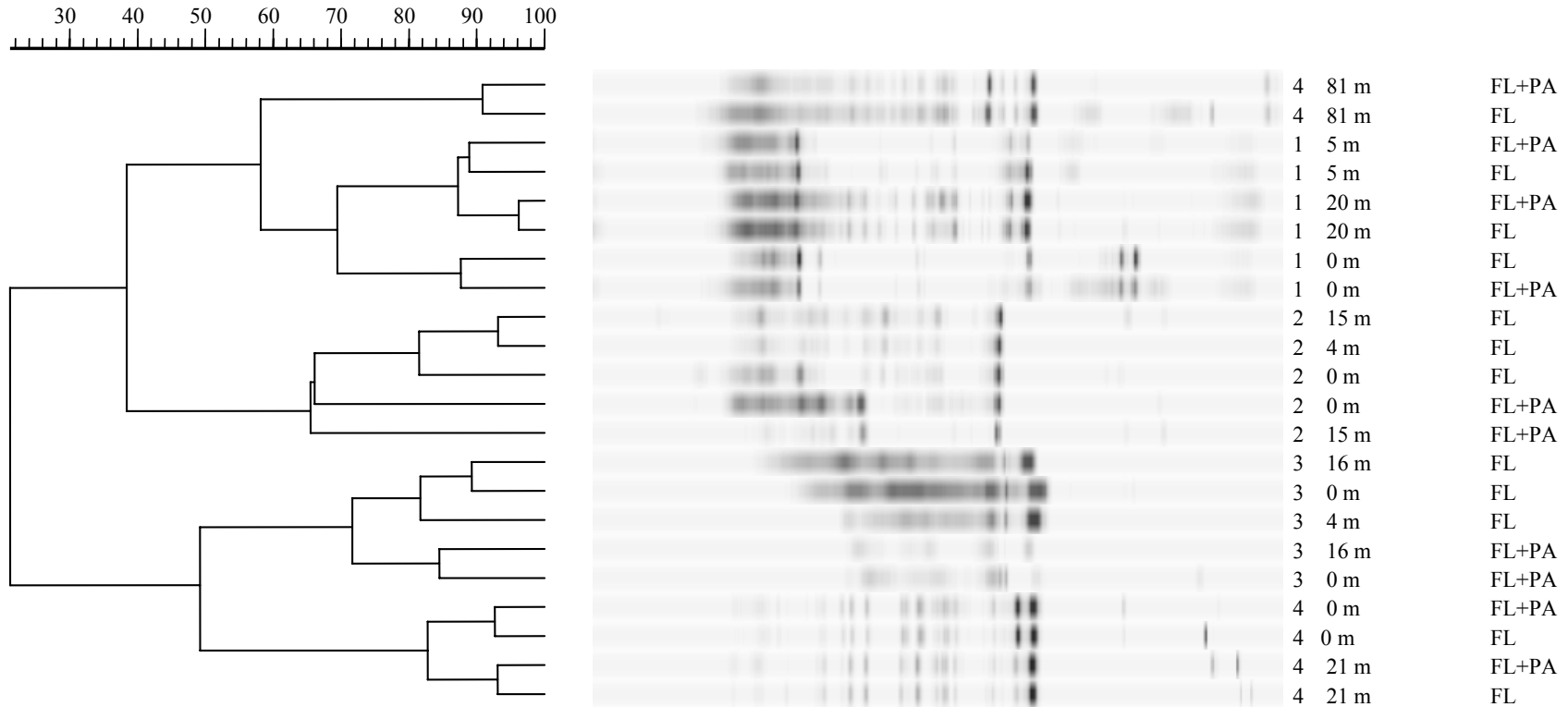


**Figure 13.** AWSOO Station dendrogram showing processed DGGE fingerprints for Stations 1-4. The scale shows percent similarity of banding patterns derived from cluster analysis in the Molecular Analyst program. Samples are labeled for Station (1-4), depth, and unfiltered (FL+PA; whole community) or filtered (FL; free-living assemblage).

similarity) (Table 2; Fig.13). Sorensen's Index showed similar results between stations (Table 2). Sorensen's Index increased except at Station 2 where it decreased slightly (Table 2).

### **Correlation Analysis**

Pearson product-moment correlation coefficients ( $r_{xy}$ ; Sokal and Rohlf 1995) were calculated between all measured variables (Table 3). POC and PON were strongly correlated ( $r_{xy}=0.99$ ). TOC correlated best with POC and PON ( $r_{xy}=0.78$ ). DIN,  $PO_4$ , and the VBR did not correlate significantly with any other measured variables. Partial product-moment correlation analysis was then conducted to determine if variables correlated to AODC, viral abundance, and VB remained significant (Table 4).

*Bacterial abundance (AODC) correlation analysis* (Table 4a and Fig. 14). Bacterial abundance (AODC) correlated best to viral abundance ( $r_{xy}=0.82$ ). AODC then correlated to POC and PON ( $r_{xy}>0.66$ ) and CHLa and DOC ( $r_{xy}>0.52$ ) at the 1% and 5% level, respectively. Partial correlation analysis ( $r_{xy.z}$ ) revealed that PON and POC were more significantly correlated with AODC than CHLa and DOC. POC and PON remained significantly correlated with AODC after the removal of all other variables ( $r_{xy.z}>0.55$ ). The CHLa correlation with AODC lost significance after the removal of POC and PON ( $r_{xy}<0.47$ ) but remained significant after the removal of DOC and DIN ( $r_{xy.z}>0.53$ ). DOC remained significant after the removal of POC, PON, and CHLa ( $r_{xy.z}>0.52$ ), but lost significance after the removal of DIN and depth ( $r_{xy.z}<0.51$ ). Depth and inorganic nutrients did not correlate with AODC in partial correlation analysis.

**Table 3.** Pearson product-moment correlation coefficients ( $r_{xy}$ ) between measured variables from Stations 1-5 in the Chukchi Sea (AWS00). Critical r values for significance at the 5% and 1% levels are 0.51 and 0.64, respectively (n=15). R values significant at the 5% and 1% (\*) levels are marked in bold-face.

r	AODC	VLP	PON	POC	DOC	TOC	CHLa	Depth
AODC	----	<b>0.82*</b>	<b>0.69*</b>	<b>0.66*</b>	<b>0.52</b>	<b>0.77*</b>	<b>0.53</b>	-0.43
VLP	<b>0.82*</b>	----	<b>0.73*</b>	<b>0.72*</b>	0.31	<b>0.67*</b>	<b>0.54</b>	-0.40
VB	----	----	<b>0.75*</b>	<b>0.74*</b>	0.48	<b>0.79*</b>	<b>0.58</b>	-0.42
VBR	----	----	0.17	0.20	-0.31	-0.07	0.01	0.27
PON	<b>0.69*</b>	<b>0.73*</b>	----	<b>0.99*</b>	0.20	<b>0.78*</b>	<b>0.93*</b>	-0.38
POC	<b>0.66*</b>	<b>0.72*</b>	<b>0.99*</b>	----	0.19	----	<b>0.93*</b>	-0.36
DOC	<b>0.52</b>	0.31	0.20	0.19	----	----	0.15	-0.19
TOC	<b>0.77*</b>	<b>0.67*</b>	<b>0.78*</b>	----	----	----	<b>0.71*</b>	-0.36
DIN	-0.10	-0.05	0.04	-0.01	-0.24	-0.16	0.06	<b>0.59</b>
PO <sub>4</sub>	0.23	0.13	0.22	0.19	-0.01	0.12	0.27	0.38

**Table 4.** Product-moment ( $r_{xy}$ ) and partial ( $r_{xy.z}$ ) correlation coefficients between a) bacterial abundance (AODC), b) viral abundance (VLP), and c) bacterial  $\times$  viral abundance (VB) and environmental variables. The critical  $r$  value at the 5% and 1% level is 0.51 and 0.64, respectively ( $n=15$ ).  $R$  values significant at the 5% and 1% (\*) levels are marked in bold-face.

$r_{xy.z} \rightarrow$

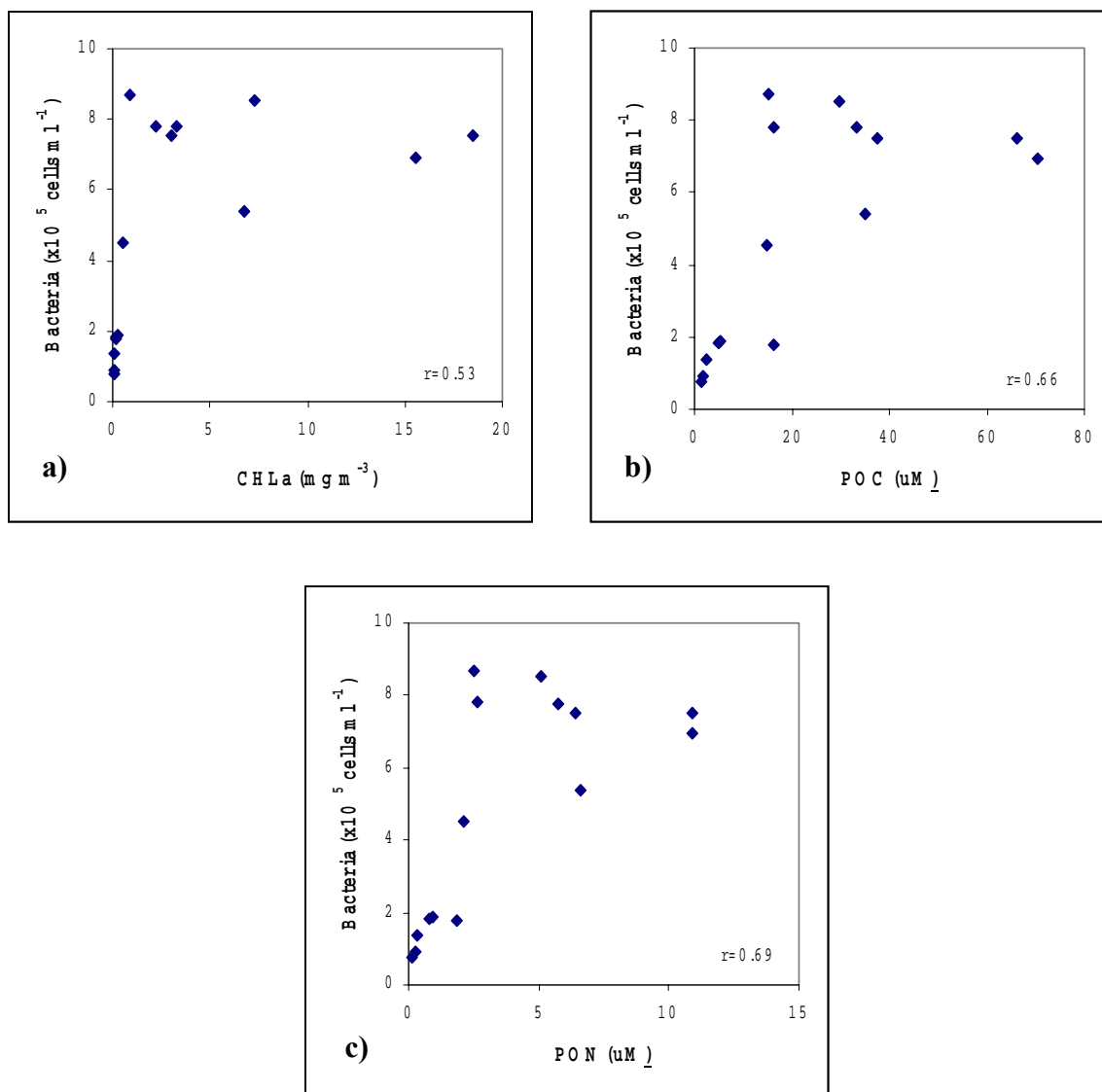
a) AODC	$r$	w/o PON	w/o POC	w/o CHLa	w/o DOC	w/o Depth	w/o DIN	w/o PO <sub>4</sub>
PON	<b>0.69*</b>	-----	0.38	<b>0.62</b>	<b>0.70*</b>	<b>0.63</b>	<b>0.70*</b>	<b>0.67*</b>
POC	<b>0.66*</b>	-0.29	-----	<b>0.55</b>	<b>0.67*</b>	<b>0.60</b>	<b>0.66*</b>	<b>0.65*</b>
CHLa	<b>0.53</b>	-0.41	-0.32	-----	<b>0.53</b>	0.47	<b>0.54</b>	0.50
DOC	<b>0.52</b>	<b>0.53</b>	<b>0.53</b>	<b>0.52</b>	-----	0.49	0.51	<b>0.53</b>
Depth	-0.43	-0.25	-0.27	-0.34	-0.39	-----	-0.45	<b>-0.56</b>
DIN	-0.10	0.02	0.03	-0.16	-0.18	0.21	-----	-0.31
PO <sub>4</sub>	0.23	0.27	-0.31	0.10	0.11	0.46	0.37	-----

b) VLP	$r$	w/o AODC	w/o PON	w/o POC	w/o CHLa	w/o Depth	w/o DOC
AODC	<b>0.82*</b>	-----	<b>0.65*</b>	<b>0.67*</b>	<b>0.75*</b>	<b>0.79*</b>	<b>0.82*</b>
PON	<b>0.73*</b>	0.39	-----	0.17	<b>0.71*</b>	<b>0.68*</b>	<b>0.71*</b>
POC	<b>0.72*</b>	0.41	-0.06	-----	<b>0.70*</b>	<b>0.67*</b>	<b>0.75*</b>
CHLa	<b>0.54</b>	0.22	<b>-0.52</b>	-0.50	-----	0.49	<b>0.53</b>
Depth	-0.40	-0.11	-0.20	-0.22	-0.32	-----	-0.37
DOC	0.31	-0.24	0.25	0.26	0.28	0.26	-----

c) VB	$r$	w/o PON	w/o POC	w/o CHLa	w/o DOC	w/o Depth
PON	<b>0.75*</b>	-----	0.29	<b>0.71*</b>	<b>0.76*</b>	<b>0.71*</b>
POC	<b>0.74*</b>	-0.17	-----	<b>0.66*</b>	<b>0.75*</b>	<b>0.69*</b>
CHLa	<b>0.58</b>	-0.49	-0.44	-----	<b>0.58</b>	<b>0.53</b>
DOC	0.48	0.50	0.50	0.48	-----	0.45
Depth	-0.42	-0.22	-0.24	-0.33	-0.38	-----



**Figure 14.** AWS00 mean bacterial abundance ( $n=2$ ) versus a) chlorophyll a, b) POC, and c) PON. Data points are from Stations 1-5. Product-moment correlation coefficients ( $r_{xy}$ ) are shown ( $n=15$ ).

Viral abundance (VLP) correlation analysis (Table 4b and Fig. 15). Viral abundance (VLP) correlated best with AODC ( $r_{xy}=0.82$ ) then with particulate organic matter (POC and PON;  $r_{xy}>0.72$ ) and CHLa ( $r_{xy}=0.54$ ). The AODC remained significantly correlated with VLP ( $r_{xy,z}>0.65$ ) at the 1% level after the removal of all variables in partial correlation analysis. The PON and POC correlations with VLP lost significance after the removal of AODC ( $r_{xy,z}<0.41$ ), but remained significant after the removal of CHLa, DOC, and depth ( $r_{xy,z}>0.68$ ). The CHLa correlation with VLP lost significance after the removal of AODC, POC, and depth ( $r_{xy,z}<0.50$ ), but remained significant after the removal of PON and DOC ( $r_{xy,z}>0.52$ ). The correlation between VLP and CHLa changed from a positive to negative relationship after the removal of POC and PON because CHLa was strongly correlated with POC and PON. DIN,  $PO_4$ , and depth remained insignificant using partial correlation analysis (some data not shown).

VB and VBR correlation analysis (Table 4c and Fig. 16). The product of bacterial  $\times$  viral abundance (VB) correlated best with POC and PON ( $r_{xy}>0.74$ ) then CHLa ( $r_{xy}=0.58$ ). The POC and PON correlations remained significant at the 1% level after the removal of CHLa, DOC, and depth ( $r_{xy,z}>0.66$ ). DOC, inorganic nutrients, and depth remained insignificant with partial correlation analysis.

Correlation analysis was also conducted on environmental variables and the virus:bacteria ratio (VBR, data not shown). No environmental factor correlated significantly with VBR in product-moment (Table 3) or partial correlation analyses (data not shown).

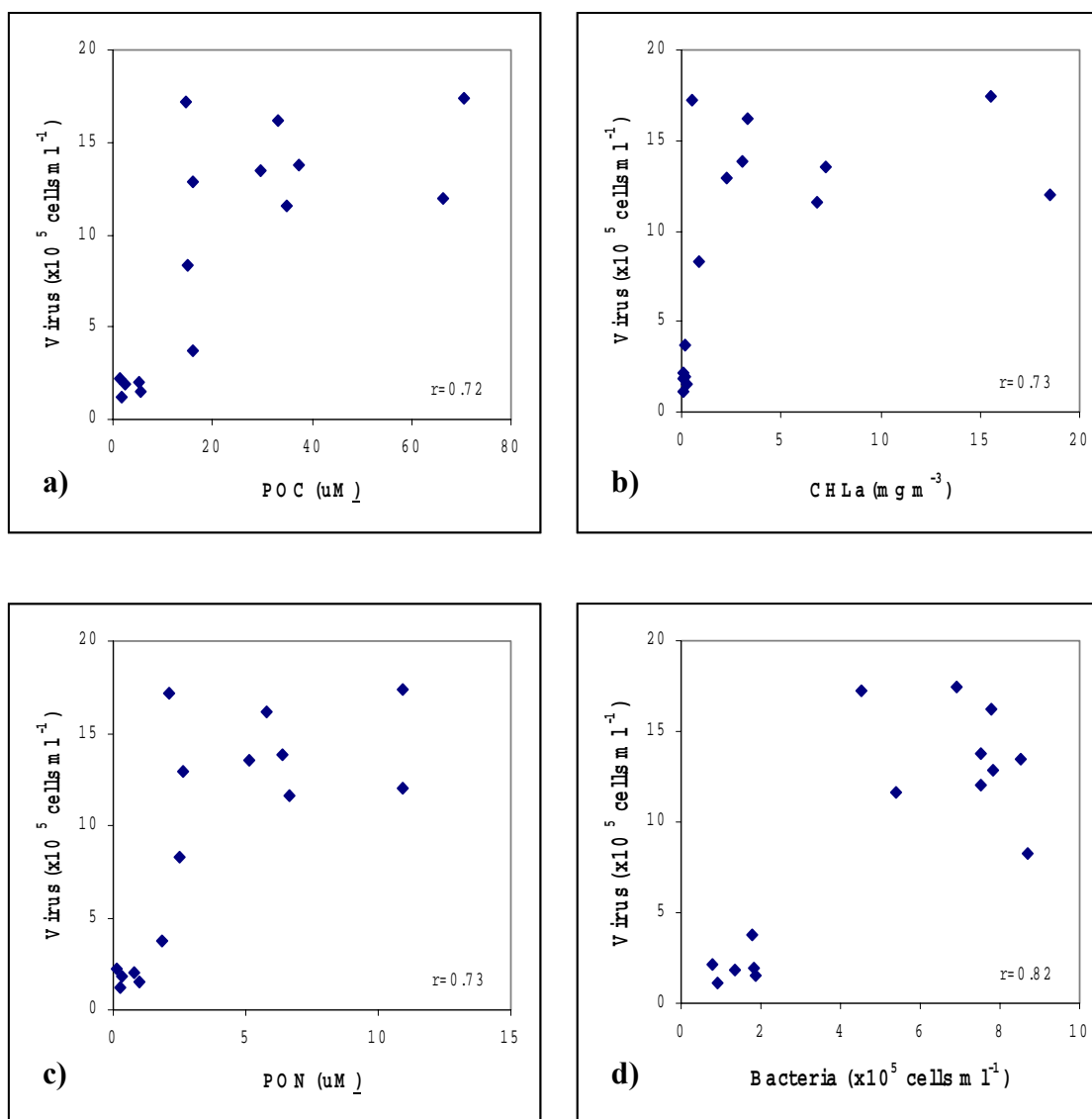


**Figure 15.** AWS00 mean viral abundance ( $n=2$ ) versus a) POC, b) CHLa, c) PON, and d) mean bacterial abundance ( $n=2$ ). Data points are from Stations 1-5. Product-moment correlation coefficients ( $r_{xy}$ ) are shown ( $n=15$ ).

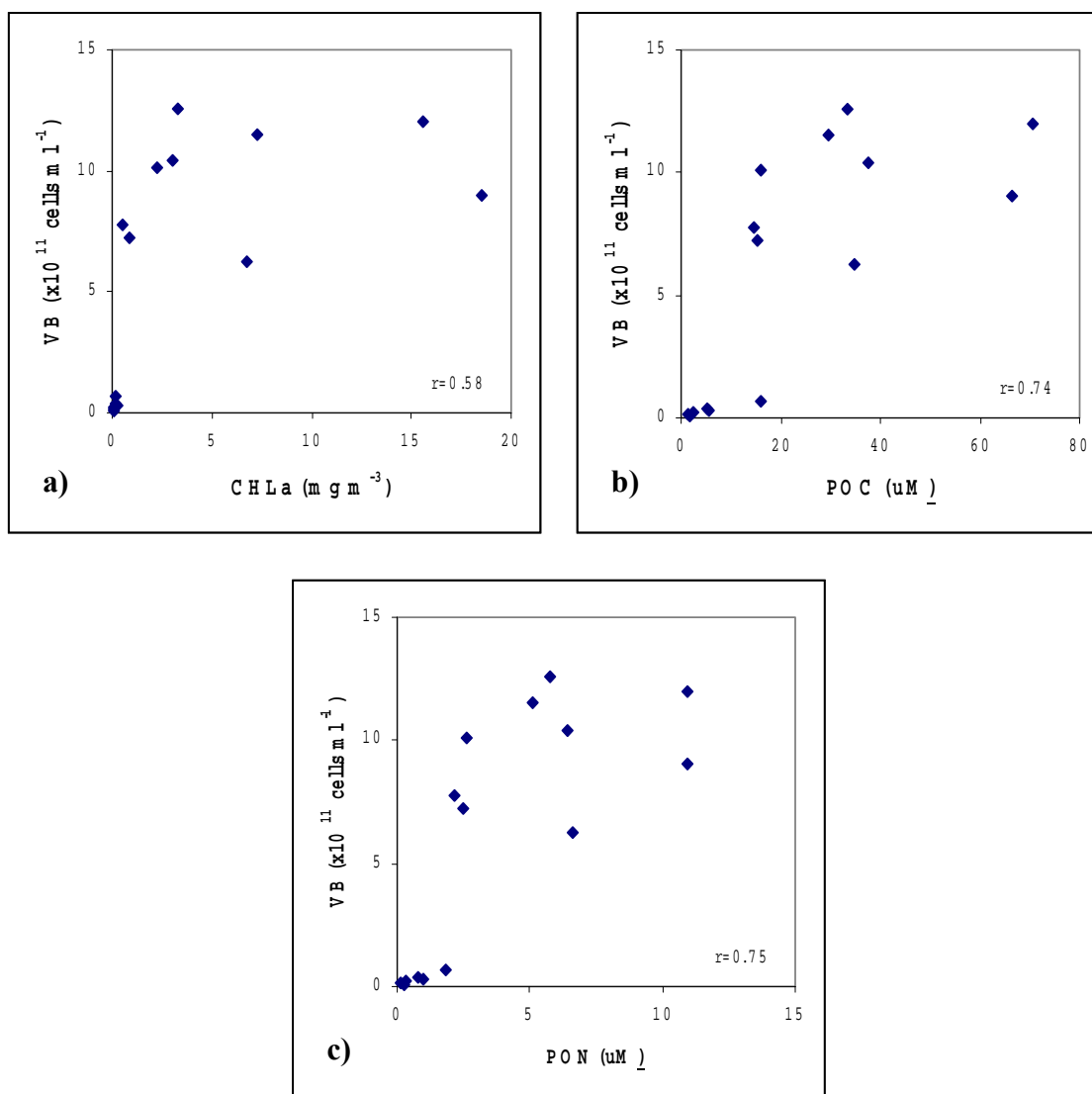


**Figure 16.** AWS00 mean bacterial  $\times$  viral abundance (VB;  $n=2$ ) versus a) chlorophyll a, b) POC, and c) PON. Data points are from Stations 1-5. Product-moment correlation coefficients ( $r_{xy}$ ) are shown ( $n=15$ ).

Species richness ( $D_{mg}$ ) and Sorensen Index ( $S$ ) correlation analysis (Table 5). Species richness ( $D_{mg}$ ) correlated best to PON ( $r_{xy} = -0.62$ ), then next to POC and bacterial abundance ( $r_{xy} = -0.58$ ). Sorensen's index, a measure of similarity between filtered and unfiltered DGGE fingerprints, correlated best to PON ( $r_{xy} = -0.55$ ). The AODC correlation with  $D_{mg}$  lost significance after the removal of POC, PON, and viral abundance ( $r_{xy,z} < -0.42$ ). The PON and POC correlations with  $D_{mg}$  lost significance after the removal of AODC and VLP ( $r_{xy,z} < -0.49$ ). DOC, CHLa, and inorganic nutrients were not significantly correlated with  $D_{mg}$  or  $S$ .

### **Bacterial Isolates**

Isolate Gram Stain and morphology (Table 6). Twenty-four bacterial isolates were obtained (six from each Station 1-4). Bacterial isolates from all stations tested Gram negative. The morphology was determined to be either coccus (spherical) or bacillus (rod-shaped). No connection between morphology, the ability to grow at room temperature, or number of positive BIOLOG wells was found. Isolates that grew at room temperature were both coccus and bacillus shaped. All Station 4 isolates, however, appeared to be bacillus-shaped and grew at room temperature.

Isolate growth at room temperature (Table 6). Isolates from Stations 1 and 2 did not exhibit growth (determined by turbidity of the culture) at room temperature after 48h. Isolates AWS001-A2 and AWS002-C2, however, showed slight growth (turbidity) after 120h and positive growth after 1 week. Other Station 1 isolates remained inactive.

**Table 5.** Product-moment ( $r_{xy}$ ) and partial ( $r_{xy.z}$ ) correlation coefficients between environmental variables and a) species richness ( $D_{mg}$ ) and b) Sorensen's index (S). Critical r values at the 5% and 1% level are 0.55 and 0.68, respectively (n=10). R values significant at the 5% and 1% (\*) levels are marked in bold-face.

		$r_{xy.z} \rightarrow$							
a) $D_{mg}$	r	w/o PON	w/o POC	w/o AODC	w/o $PO_4$	w/o VLP	w/o DIN	w/o DOC	
PON	<b>-0.62</b>	-----	<b>-0.55</b>	-0.38	<b>-0.61</b>	-0.49	<b>-0.63</b>	<b>-0.69*</b>	
POC	<b>-0.58</b>	0.49	-----	-0.32	<b>-0.57</b>	-0.41	<b>-0.59</b>	<b>-0.63</b>	
AODC	<b>-0.58</b>	-0.27	-0.32	-----	<b>-0.56</b>	-0.42	<b>-0.61</b>	<b>-0.80*</b>	
$PO_4$	-0.52	-0.51	-0.51	-0.49	-----	-0.52	-0.52	-0.53	
VLP	-0.45	0.01	-0.06	0.07	-0.45	-----	-0.44	-0.54	
DIN	-0.19	-0.21	-0.24	-0.31	0.19	-0.24	-----	-0.15	
DOC	0.18	0.40	0.36	<b>0.69*</b>	0.21	0.38	0.14	-----	

b) S	r	w/o PON	w/o POC	w/o VLP	w/o AODC	w/o DOC	w/o DIN	w/o $PO_4$
PON	<b>-0.55</b>	-----	<b>-0.60</b>	-0.33	-0.40	<b>-0.61</b>	<b>-0.55</b>	-0.53
POC	-0.49	<b>0.55</b>	-----	-0.25	-0.33	<b>-0.55</b>	-0.50	-0.48
VLP	-0.47	-0.14	-0.20	-----	-0.28	<b>-0.58</b>	-0.49	-0.47
AODC	-0.40	-0.05	-0.12	-0.02	-----	<b>-0.61</b>	-0.43	-0.39
DOC	0.21	0.37	0.36	0.43	0.53	-----	0.18	0.21
DIN	-0.17	-0.17	-0.19	-0.22	-0.23	-0.12	-----	-0.10
$PO_4$	-0.14	-0.02	-0.05	-0.09	-0.05	-0.14	-0.05	-----

Station 2 isolates AWS002-A1, AWS002-A2, and AWS002-B2 showed no growth after 120h, but slight turbidity/growth after 1 week. No increase in turbidity, however, was observed after 2 weeks. Station 3 isolates varied. Isolates AWS003-A1, AWS003-A2, and AWS003-B2 showed slight signs of growth after 48h but did not increase in turbidity after 120h or 1 week. Other Station 3 isolates did not show signs of growth after 1 week. All isolates from Station 4 showed positive growth after 48h and grew more turbid during the incubation period.

Isolates collected during AWS00 were most likely psychrophilic or psychrotolerant heterotrophs. Isolates that did not grow at room temperature were psychrophilic because they grew only at 3 °C in rich media. Isolates that showed signs of slight turbidity/growth after 1 week were likely psychrotolerant because they grew rapidly at 3 °C, but grew slowly at room temperature. Isolates from Station 4 were psychrotolerant because they are both at 3 °C and room temperature.

Isolate DGGE (Fig. 17-20). Bacterial isolates produced more than one band in the DGGE fingerprints. One or two “dark” bands, however, were produced by most isolates. The dominant bands were used to compare isolate DGGE patterns and to search for isolates in community gels. Isolates that had similar DGGE fingerprints (Fig. 20) include: 1) 1B1, 1B2, 1C1, and 1C2 (Figures 17 and 18); 2) 2C1 and 3B2 (Fig. 18 and 19); 3) 3A1, 3C1, and 3C2 (Figure 19); and 4) 4A1, 4A2, 4B1, and 4B2 (Fig. 17 and 19). Similarities can be seen in the isolate dendrogram as well (Fig. 20).

The search for the isolate band in community DGGE fingerprints was difficult. The rescaled isolate fingerprints were lined up against rescaled community fingerprints.

**Table 6.** AWS00 bacterial isolate data showing morphology, Gram stain, growth at room temperature (Yes or No), and the number of positive wells produced in the BIOLOG assay. All isolates were obtained from Stations 1-4 at the 30% light level. Isolates were named by cruise/year (AWS00), station number (1-4), dilution series (A, B, or C) and colony picked during plating (1 or 2). BIOLOG results are mean values for duplicates for each isolate. \* Indicates slight growth with no increase in turbidity during incubation.

STATION	ISOLATE	Morphology	Gram Stain	RT Growth	# Positive wells (n=2)
1	AWS001-A1	cocci	-	N	46.5
	AWS001-A2	cocci	-	Y	47
	AWS001-B1	rod	-	N	18
	AWS001-B2	rod	-	N	47
	AWS001-C1	rod	-	N	26.5
	AWS001-C2	rod	-	N	24
2	AWS002-A1	rod	-	Y*	41
	AWS002-A2	rod	-	Y*	32.5
	AWS002-B1	rod	-	Y*	19
	AWS002-B2	rod	-	N	35
	AWS002-C1	cocci/ovid	-	N	38
	AWS002-C2	cocci/ovid	-	Y	53.5
3	AWS003-A1	rod/ovid	-	Y*	33
	AWS003-A2	cocci	-	Y*	27.5
	AWS003-B1	cocci	-	N	11
	AWS003-B2	rod	-	Y	34.5
	AWS003-C1	cocci	-	N	45
	AWS003-C2	cocci	-	N	39.5
4	AWS004-A1	rod	-	Y	39.5
	AWS004-A2	rod/ovid	-	Y	35
	AWS004-B1	rod	-	Y	36
	AWS004-B2	rod/ovid	-	Y	35
	AWS004-C1	rod/ovid	-	Y	37.5
	AWS004-C2	cocci/rod	-	Y	37.5

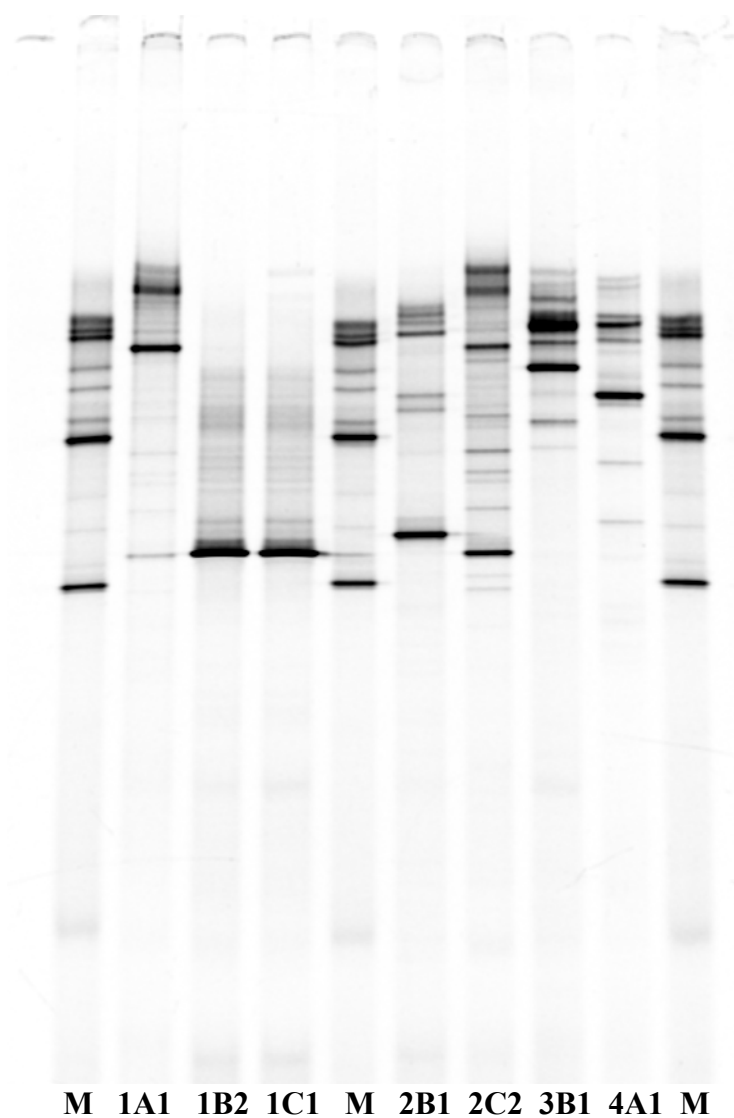


**Figure 17.** DGGE gel containing AWS00 isolates labeled without prefix containing cruise/year (AWS00) and standard marker lanes. Isolates labeled with station number (1-4), dilution series (A, B, or C), and colony picked (1 or 2).

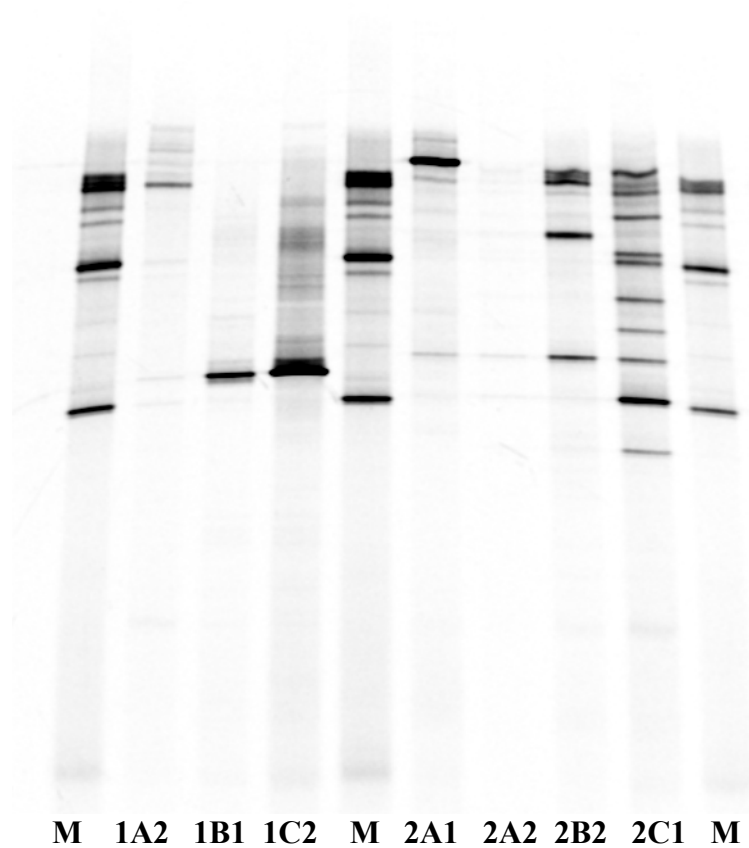


**Figure 18.** DGGE gel containing AWS00 isolates labeled without prefix containing cruise/year (AWS00) and standard marker lanes (M). Isolates labeled with station number (1-4), dilution series (A, B, or C), and colony picked (1 or 2).

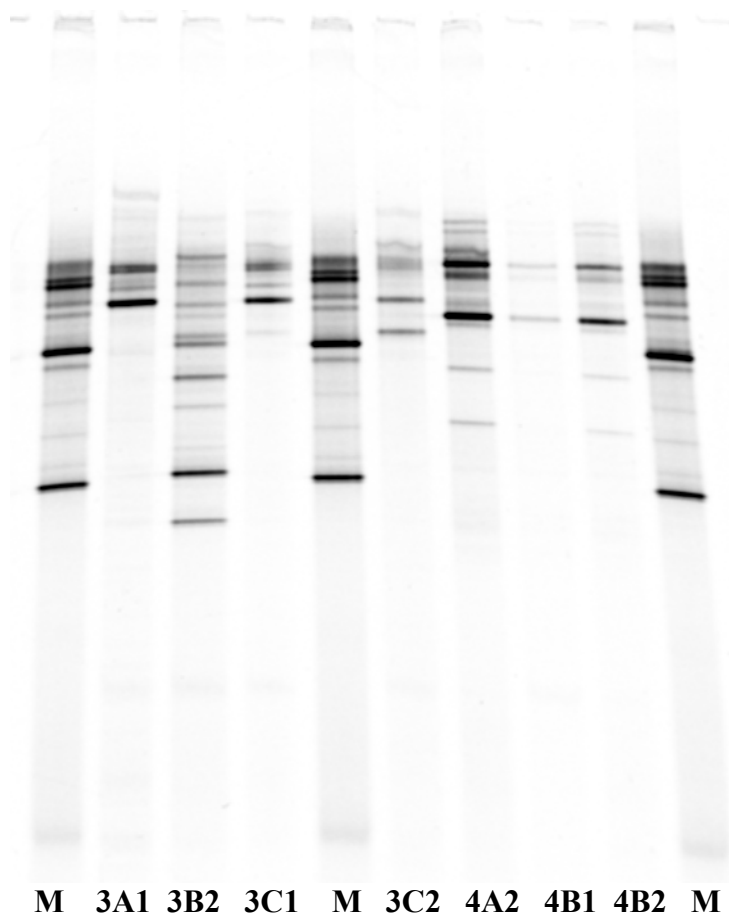


**Figure 19.** DGGE gel containing AWS00 isolates labeled without prefix containing cruise/year (AWS00) and standard marker lanes (M). Isolates labeled with station number (1-4), dilution series (A, B, or C), and colony picked (1 or 2).

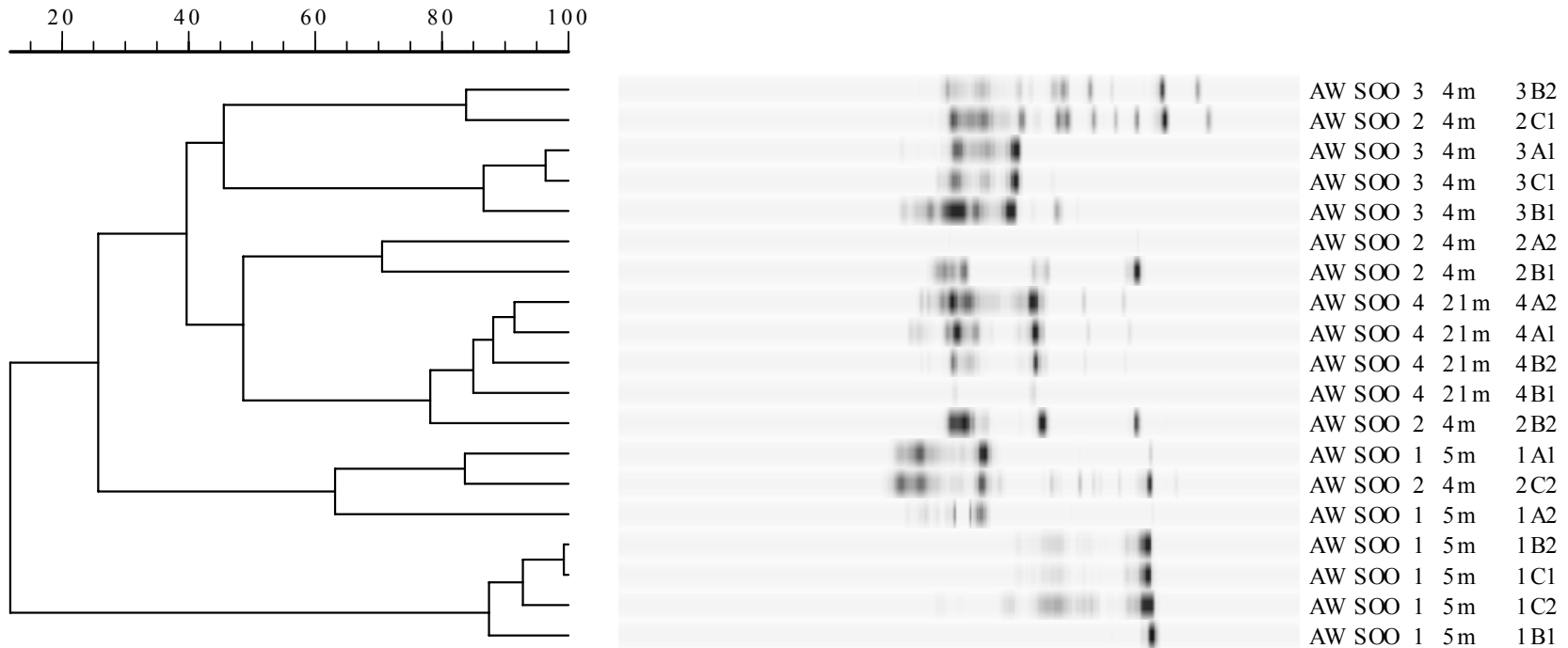


**Figure 20.** AWSOO isolate dendrogram showing percent similarity and each isolate's rescaled fingerprint. Isolates are labeled for cruise (AWSOO), Station (1-4), depth, and name (includes station, dilution series, and colony picked).

Isolates whose dominant bands could be found in community fingerprints from the same depth include: 3A1, 3B1, 3C1, 3C2, 4A1, 4A2, 4B1, and 4B2. The accuracy of these results, however, is uncertain.

Isolate phylogeny (Fig. 21). Partial 16S rDNA sequences (~1400 bp) revealed that all bacterial isolates were closely related to members of the  $\gamma$ -*Proteobacteria* phylogenetic group with BLAST (NCBI). Adequate (1400 bp) 16S rDNA sequences were not obtained for all isolates, so only those isolates (10 total) for which a at least a 1400 bp of 16S rDNA sequence was obtained were used in creating the phylogenetic tree with closely-related members in the NCBI database. AWS00 isolates were named according to cruise/year (AWS/2000), station number (1-4), dilution series (A, B, or C), and colony number (1 or 2). Bacterial isolates clustered by station in the phylogenetic tree except for AWS001-A2 and AWS003-B2. The “dominant” cultivable bacterium therefore differs from station to station with the exception of Station 1 and Station 3. Station 1 bacteria were closely-related to *Shewanella gelidimarina*, except AWS001-A2, which was closely related to *Moritella* species. AWS002-B1 and AWS003-B2 sequences were closely related to *Shewanella* species. Other Station 3 isolates were most closely-related to *Colwellia* psychrophiles. Station 4 isolates were most closely-related to *Pseudoalteromonas* and *Alteromonas* species.

Isolate AWS003-A2, AWS003-B1, and AWS003-C1 sequences from three different dilution series at the same station were >99% similar and therefore appear to be identical (Fig. 21). Station 1 isolates AWS001-B1 and AWS001-B2 sequences were identical (Figure 21), therefore showing that 2 different colonies picked during plating

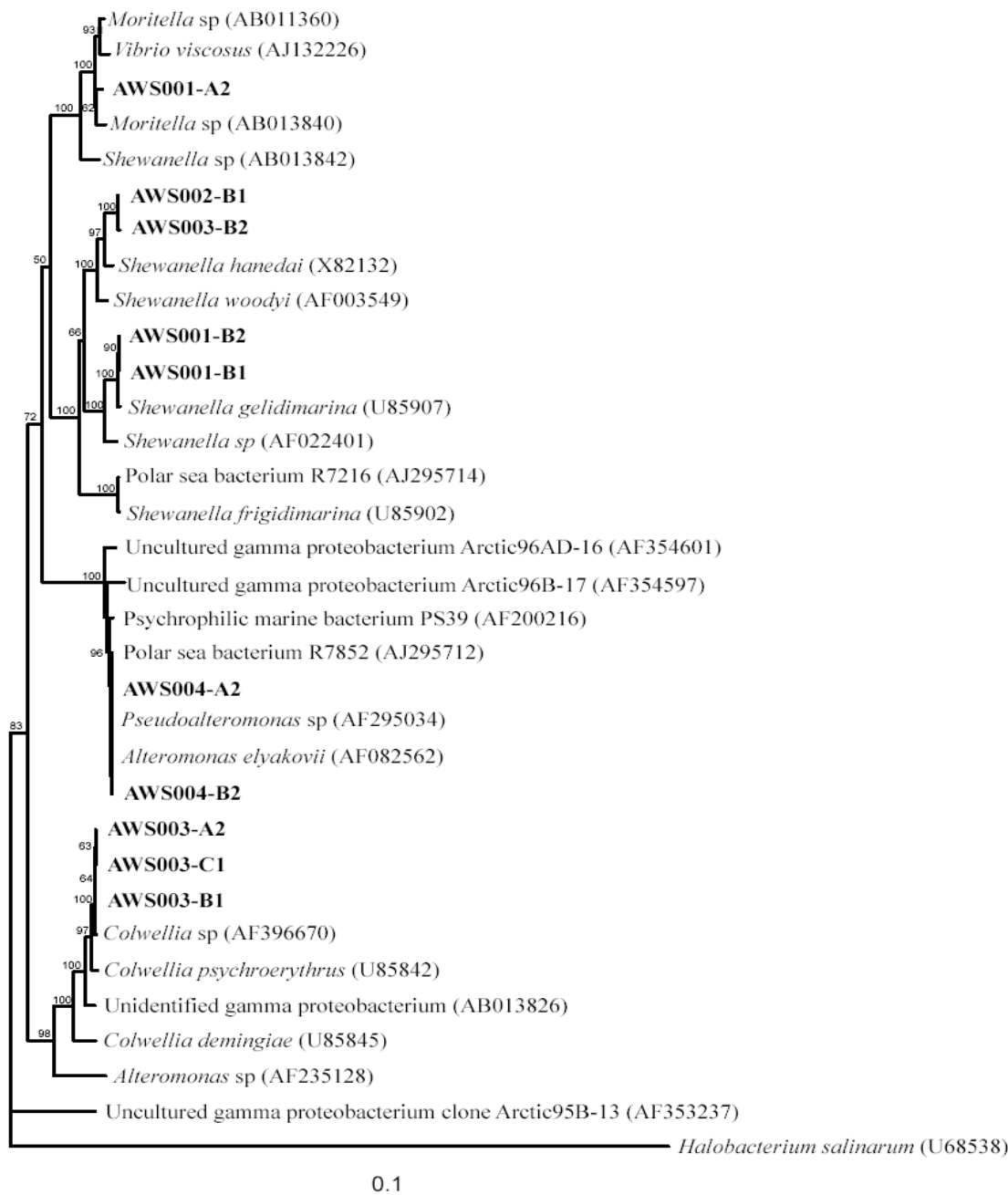


**Figure 21.** Neighbor-joining tree showing the phylogenetic relationships between AWSOO bacterial isolates and closely-related  $\gamma$ -Proteobacteria. Names of isolates indicate cruise/year (AWS00), followed by station number (1-4), dilution series (A, B, or C), and colony picked from that series (1 or 2). Trees were constructed with partial (1400 bp) 16S rDNA sequences. The trees are unrooted, with *Halobacterium salinarum* as the out group. The bar indicates a Jukes-Cantor distance of 0.1. Bootstrap values  $>50$  are shown (n=100).

resulted in cultivation of the same species. The isolation method (Button et al. 1993) was therefore shown to be repeatable. AWS003-B2, cultivated from a separate colony from the Station 3 “B” dilution series, however, was not closely-related to AWS003-B1. In this case, the same dilution series resulted in cultivation of two different bacteria. DGGE fingerprints were also different for these bacteria (Fig. 20).

Isolate BIOLOG assay (Appendix). All BIOLOG results are presented in the Appendix. The number of positive wells for each isolate was determined (Table 6). Selected isolates were chosen for specific comparison of BIOLOG data based on their DGGE fingerprints and 16S rDNA sequences.

Substrate utilization on duplicate BIOLOG plates for each bacterial isolate was nearly identical (Fig. 22 and Appendix). The BIOLOG assay was therefore repeatable. Two cultures picked from the same station and dilution series (AWS003-B1 and AWS003-B2) were different according to substrate utilization with BIOLOG (Fig. 22). DGGE fingerprinting (Fig. 17 and 19) and 16S rDNA sequencing (Fig. 21) confirmed that these isolates were different species. Alternatively, a different pair of isolates from the same station and dilution series (AWS001-B1 and AWS001-B2) gave conflicting results: they were different species according to substrate utilization with BIOLOG, but DGGE fingerprinting and 16S rDNA sequencing revealed that they were the same bacterium (Fig. 23).

## ISOLATE: AWSOO3-B1

	1	2	3	4	5	6	7	8	9	10	11	12
A												
B		1				2						
C								2*				
D												
E						2						
F						3	3					
G									2	2		
H			2									

## ISOLATE: AWSOO3-B1'

	1	2	3	4	5	6	7	8	9	10	11	12
A					3*							
B		1		1		2				1*		
C												
D												
E						3		2*				
F						3	3					
G									3	1		
H			2						3*			

## ISOLATE: AWSOO3-B2

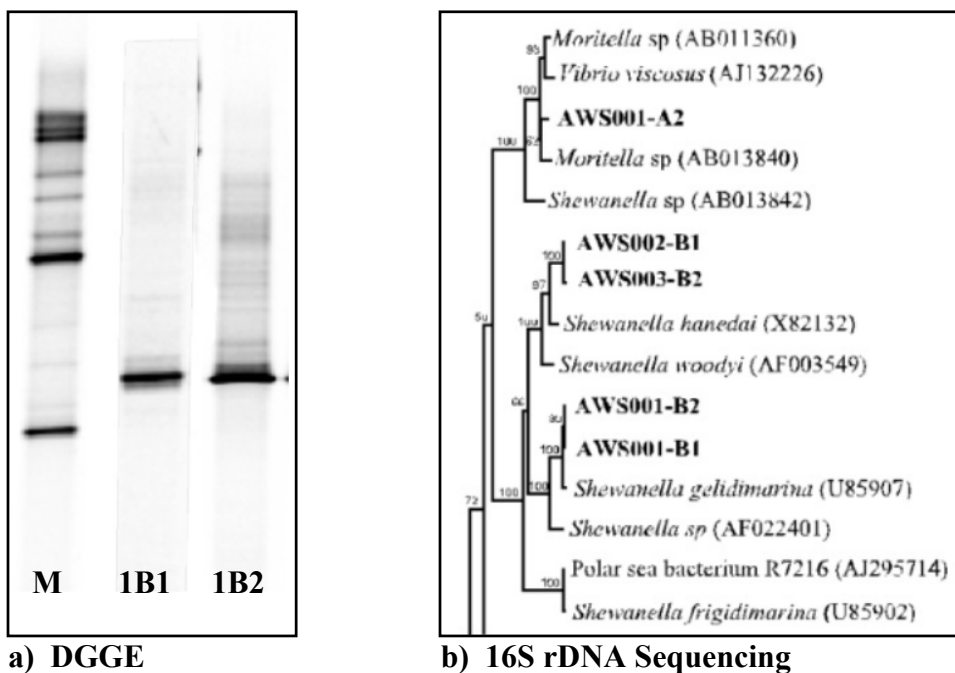
	1	2	3	4	5	6	7	8	9	10	11	12
A		3	3	2	1			2				3
B		3		3	3	3		3	3	3	3	3
C	3			3			3	3			1	
D			2				3					
E								1				2
F						3	3			3		2
G					2	3			2	3		
H									3			

## ISOLATE: AWSOO3-B2'

	1	2	3	4	5	6	7	8	9	10	11	12
A		3	3	3	1	1*	2*	2				3
B		3		3	3	3		3	3	3	3	2
C	3			3			3	3			2	
D			2				3					
E								1				2
F						3	3			3		3
G					3	3			3	3		
H							2*		3			

\*Indicates wells that do not test positive in the duplicate plate.

**Figure 22.** AWSOO BIOLOG results for isolates AWSOO3-B1, AWSOO3-B2, and their duplicates. Both isolates are from the same dilution series (B) from Station 3, but were two different colonies picked during plating. Wells are labeled A1-A12, B1-B12, etc., and correspond to substrates listed in sequential order in the Appendix.



## ISOLATE: AWSOO1-B1

	1	2	3	4	5	6	7	8	9	10	11	12
<b>A</b>		1	2		1	1		2				
<b>B</b>						3				3		
<b>C</b>												
<b>D</b>							3					
<b>E</b>				2		3		2				
<b>F</b>						3	2				2	1
<b>G</b>			2						2			
<b>H</b>		1										

## ISOLATE: AWSOO1-B2

	1	2	3	4	5	6	7	8	9	10	11	12
<b>A</b>		3	3	3	2	3		3	3		3	3
<b>B</b>	3	3	3	3		3	3	3		3	3	3
<b>C</b>						3		3			3	
<b>D</b>			2				3				2	
<b>E</b>				2		3		2	2			1
<b>F</b>					2	3	3			3	2	2
<b>G</b>	3	3	3	3		3	3		3	3		2
<b>H</b>		3				2	2		3			1

## c) BIOLOG

**Figure 23.** Comparison of AWSOO isolates AWSOO1-B1 and AWSOO1-B2 using a) DGGE, b) placement on the phylogenetic tree according to partial 16S rDNA sequence, and c) BIOLOG results. BIOLOG wells are labeled A1-A12, B1-B12, etc., and correspond to substrates listed in sequential order in the Appendix.

## CHAPTER 4

### DISCUSSION

#### **Bottom-up versus Top-down Control**

*Bacterial and viral abundance.* Bottom-up control, primarily by POM, on bacterial abundance was observed in the Chukchi Sea. Bacterial abundance was elevated in high production regimes where the highest CHLa, POC, and PON values were observed (Tables 1 and 2; Fig. 2-4). Bacterial abundance often correlates to CHLa (Cole et al. 1988; Poremba et al. 1999; Kimura et al. 2001) and POM (Kimura et al. 2001). In contrast to other studies (Rivkin and Anderson 1997; Vrede et al. 1999; Hagström et al. 2001), no significant correlation between bacterial abundance and inorganic nutrients was observed. Bottom-up control therefore resulted from the availability of organic nutrients, primarily in the form of POM. The hypothesis (H1) that POM availability may determine bacterial abundance was therefore supported.

Top-down control of bacterial abundance by viral infection was not observed because an increase in viral abundance did not decrease overall bacterial abundance. Determining viral infection rate was beyond the scope of this study. Bacterial abundance correlated best to viral abundance with a strong positive correlation (Table 3) as found in other studies (Boehme et al. 1993; Cochlan et al. 1993; Jiang and Paul 1994; Weinbauer et al. 1995; Steward et al. 1996; see review by Wommack and Colwell 2000), suggesting that the VLPs were bacteriophages. The positive correlation observed between bacterial and viral abundance may be due to the density-dependent nature of viruses (Wiggins and

Alexander 1985; Wilcox and Fuhrman 1994) and may therefore be the result of a bottom-up control of viral abundance by bacterial abundance, rather than vice versa. Viruses also correlated with variables that correlated to bacterial abundance, such as PON and POC (Table 4; Fig. 15), suggesting that POM may indirectly influence viral abundance by increasing the abundance of bacterial hosts. The virioplankton observed in this system were likely bacteriophages replicating faster with increased bacterial production.

The VBR did not correlate, however, to bacterial abundance (Table 3) as seen in other studies where an inverse relationship is often observed (Wommack et al. 1992; Jiang and Paul 1994; Maranger et al. 1994; Maranger and Bird 1995; Tuomi et al. 1997). VBR did not vary significantly between stations in this study (Table 2), so changes in bacterial abundance were matched by changes in viral abundance. VBR values can remain constant during changes in bacterial and viral abundance (Tuomi et al. 1997), if viral production increases in regions of increased bacterial production. Increases of viral abundance were likely due to the lysis of bacterial hosts, so viruses were controlling bacterial abundance to a certain degree. Bacterial and viral production must be measured to adequately test this hypothesis (H2).

The positive correlation between bacterial and viral abundance may also be the result of DOM release from lysis of nonresistant bacterial hosts. Viral lysis of bacterial hosts releases DOM that can be readily used by bacteria (Bratbak et al. 1990; Proctor and Fuhrman 1990; Fuhrman 1992; Weinbauer and Peduzzi 1995; Middleboe et al. 1996; Noble and Fuhrman 1998). Experiments show that the addition of viral lysis products can stimulate bacterial growth (Middleboe et al. 1996; Noble and Fuhrman 1999). In this

study, bacterial and viral abundance increased at the peak stage during the hypothetical bloom sequence, reaching the hypothetical threshold for lytic infection (Fig. 8). Growth of resistant bacterial strains on lysis products of nonresistant hosts may therefore be responsible for the observed increase in bacterial abundance. In this case, viruses would facilitate bottom-up control on bacterial abundance. Viruses may therefore reduce the abundance of nonresistant bacteria (top-down control) while increasing the abundance of resistant bacteria (bottom-up control). More research determining the species specificity of viruses in this system is therefore needed.

*Bacterial community composition.* DGGE fingerprints between high and low production stations were different (Fig. 9-13) and species richness ( $D_{mg}$ ) was decreased at high POM production stations (Table 2). Species richness ( $D_{mg}$ ) correlated best with POC and PON and partial correlation analysis confirmed this correlation (Table 5). POM may therefore be responsible for the observed differences in bacterial community composition in the Chukchi Sea.

Top-down control via viral infection of bacterial community composition may also reduce species richness in high production regions of this study. Elevated VBR values occurring with changes in bacterial community composition during peaks in primary production indicate that viral infection may shape the community during algal blooms in the Chukchi Sea (Yager et al. 2001). While VBR values were not necessarily elevated during times of high production in this study, the product of bacterial  $\times$  viral abundance (VB) reached the theoretical lytic threshold ( $10^{12}$  VB mL<sup>-1</sup>; Wilcox and Fuhrman 1994) at high production stations where decreased bacterial species richness

( $D_{mg}$ ) was observed (Table 2; Fig. 4 and 5). VLP did not significantly correlate with  $D_{mg}$ , but the removal of VLP in partial correlation analysis made the correlations between POC and PON with  $D_{mg}$  insignificant (Table 5).

Both POM and viral infection may therefore reduce species richness in high production regimes in support of the hypothesis (H4). High concentrations of POM may indirectly increase viral infection by increasing the density of bacterial hosts. More studies incorporating viral and POM enrichment assays should be performed to further address this hypothesis.

Decreased species richness in areas of high POM, however, conflicts with another study of micro-scale patchiness that shows increased assemblage richness in 1  $\mu$ l samples enriched with POM (Long and Azam 2001). Micro-scale patchiness was overlooked in the present study since 10 L samples were collected from the Chukchi Sea. Smaller sampling volumes may have changed the results. The decreased  $D_{mg}$  in high production stations may be due to the free-living assemblage since particles represent a smaller portion of the 10 L sample. Viral abundance, however, was not determined in the prior study, and the bacterial-viral dynamics may be different in that study area. More research is clearly needed on the effects of viruses and POM on bacterial species diversity.

With these results, I propose a new hypothesis that a positive correlation between bacterial and viral abundance will be observed until the product of their abundance (VB) exceeds the hypothetical lytic threshold of  $10^{12}$   $\text{mL}^{-1}$  (Wilcox and Fuhrman 1994), after which a negative correlation will be observed. Bacterial and viral abundance appeared to correlate negatively in depth profiles of Stations 1-3 where the lytic threshold was exceeded (Fig. 4). I propose that viruses may shift from bottom-up to top-down control

on total bacterial abundance during times of high production or they may exert both bottom-up and top-down control on bacterial abundance by affecting resistant and nonresistant bacterial species differently. When bacterial production increases in response to increased primary and OM production, viruses should produce more DOM through lysis of nonresistant hosts, increasing bacterial abundance of resistant bacterial strains, and changing bacterial community composition by decreasing diversity. At some threshold of VB, viral community composition should change in response to the lack of available hosts to a new viral community that is able to infect the previously resistant bacterial strains. Resistance to viruses may therefore be a transient state. Successional changes in virioplankton diversity have been observed (Wommack et al. 1999; Steward et al. 2000).

Virioplankton were not identified in this study. Some virus-like particles (VLP) counted by epifluorescence microscopy may not have been bacteriophages. Morphological data from virioplankton diversity studies suggest, however, that the majority of virioplankton are bacteriophages (Wommack et al. 1992; Cochlan et al. 1993; Maranger et al. 1994). Strong positive correlation to bacterial abundance (Cochlan et al. 1993; Maranger and Bird 1995; Maranger and Bird 1996; Almeida et al. 2001), high bacterial-viral encounter rates (Fuhrman et al. 1989; Boehme et al. 1993; Cochlan et al. 1993), and high viral production rates (Noble and Fuhrman 1995) all support this theory. The positive correlation between bacterial and viral abundance (Table 3) found in this study suggests that the majority of VLP were bacteriophages. Virioplankton diversity measurements should be incorporated into future studies in the Chukchi Sea.

Bacterivory was not examined in this study and may be important (Sherr and Sherr 1994; Steward et al. 1996; Sherr et al. 1997). Predation on bacteria by protists may exert control on bacterial abundance and community composition in different production regimes. Estimates of bacterivory often fall short of those needed to balance bacterial production, however, suggesting that other removal processes such as viral infection are important (McManus and Fuhrman 1988). Viral infection can cause similar bacterial mortality as grazing by heterotrophic nanoflagellates (Fuhrman and Noble 1995), and may exert stronger control on bacterial abundance than predation (Weinbauer and Peduzzi 1995, Weinbauer et al. 1995). Selective predation of bacteria by heterotrophic nanoflagellates occurs in some aquatic ecosystems (Lebaron et al. 1999, Suzuki 1999). Experimental removal of predators increases the abundance of bacterial phylotypes that were rare in the original water sample, suggesting that predation can be species-specific (Suzuki 1999). Enhanced nanoflagellate grazing may also stimulate viral activity and work with viral infection in shaping bacterial community structure (Simek et al. 2001). Top down controls such as predation by protists and viral infection may therefore influence bacterial community composition synergistically. Future studies incorporating predation measurements are therefore needed to assess the relative importance of predation and viral infection in the Chukchi Sea.

### **PA and FL Assemblages**

Differences between particle-associated (PA) and free-living (FL) bacterial assemblages in high and low production/POM regimes were found in the Chukchi Sea, as in other aquatic environments (Giovannoni 1990; Fandino et al. 2001; Moeseneder et al.

2001; Riemann and Winding 2001). Unfiltered (whole community) and filtered (free-living) DGGE fingerprints were different at all stations (Fig. 9-13), but the percent similarity and the Sorensen's Index (S) of patterns were decreased in high production stations (Table 2). FL and PA assemblages were therefore more different in regions of high particle production supporting the hypothesis (H4).

The marked increase in differences between unfiltered and filtered DGGE fingerprints at high production stations may be attributed to the availability of POM (bottom-up) and viral infection of nonresistant species (top-down). Particle-associated (PA) bacteria have extracellular enzymes that degrade POM (Chróst 1991). High production regions, rich in POM, may therefore select for specialized particle-associated bacterial species. FL and PA assemblages may be interacting communities where species overlap may depend on POM (Riemann and Winding 2001). VB reached the hypothetical lytic threshold in regions where differences between FL and PA assemblages were increased (Table 2). Viral lysis of nonresistant PA species may therefore facilitate this difference by producing DOM in close proximity to resistant PA bacteria.

Both viral infection and POM were likely shaping the bacterial community during this study in the Chukchi Sea. Sorensen's index values correlated best to PON, but the removal of VLP in partial correlation analysis made this correlation insignificant (Table 5). PA bacterial production and, therefore, viral infection are likely increased in regions enriched with POM. PA bacteria have higher cell-specific growth rates that can correlate to changes in bacterial community structure during an algal bloom (Fandino et al. 2001). The presence of POM may select for fast-growing PA bacteria with extracellular enzymes (Chróst 1991) that are susceptible to viral recognition. Viruses are closer to their

hosts on particles than in the water column; the hypothetical lytic threshold may therefore be reached on the micro-scale level, which may be overlooked if size fractionation and small sample sizes are not used.

### **Bacterial Isolates**

Isolate DGGE fingerprints clustered by station (Fig. 20). Different isolates were therefore obtained in high and low production regimes. Analysis of partial 16S rDNA sequences revealed, however, that all isolates belonged to the  $\gamma$ -*Proteobacteria* clade and differed only at the species level between stations (Fig. 21). Isolates AWS001-A1 and AWS002-C2 were most likely the same bacterium (Figure 20), but were found in different production regimes (Fig. 2). No *Cytophaga*-like, particle-associated, bacteria were isolated in high POM stations as would be expected from Yager et al. (2000) or Fandino et al. (2001).

The isolation method did not therefore produce the key differences originally hypothesized (H5). Dilution to extinction was not achieved in this study because the 10<sup>th</sup> dilution contained bacteria in all samples. Particles containing bacteria may have been transferred in the dilution process, allowing for bacterial growth in the 10<sup>th</sup> dilution. More dilutions are therefore needed to achieve extinction. The rich medium used in culturing may have selected for  $\gamma$ -*Proteobacteria*. The use of a medium that more closely matches that of the oligotrophic ocean may result in the isolation of different members of the bacterial community.

BIOLOG assays produced conflicting results with DGGE fingerprinting and 16S rDNA sequencing. Different bacteria should use a different array of substrates according

to the BIOLOG test. Isolates AWS003-B1 and AWS003-B2, for example, appeared to be different in DGGE fingerprinting (Fig. 20) and 16S rDNA analysis (Fig. 21), produced a different number of positive wells (Table 6), and used different substrates in the BIOLOG assay (Fig. 22; Appendix). Other BIOLOG results, however, did not agree with DGGE and 16S rDNA sequencing. DGGE and partial 16S rDNA analysis revealed that AWS001-B1 and AWS001-B2 were the same bacterium (Fig. 23), but these isolates produced a different number of positive wells (Table 6) and the BIOLOG substrate utilization pattern was different (Fig. 23). AWS001-B2 utilized 29 more substrates than AWS001-B1 (Fig. 23). Isolates AWS003-A2, AWS003-B1, and AWS003-C1 appeared to be the same bacterium with DGGE (Fig. 20) and 16S rDNA sequencing (Fig. 21) but produced different numbers of positive wells in the BIOLOG assay (Table 6). Isolates AWS003-A2, AWS003-B1, and AWS003-C1 used a total of 34, 13, and 45 substrates, respectively, of which only 13 were the same between all three (Appendix). The same inconsistency was observed between isolates AWS002-B1 and AWS003-B2, which used 19 and 33 substrates, respectively, of which 15 were the same (Appendix). In these cases, it appeared that the same bacterium produced different BIOLOG results.

Although cultures were started on the same day and harvested at the same optical density, they may have been in different stages of growth when the BIOLOG plates were inoculated, possibly, utilizing different substrates. All cultures were treated the same according to media addition, plating, handling, and temperature, but the stage of growth before BIOLOG inoculation was not determined. A future experiment involving inoculation of BIOLOG plates when the bacteria are at the same stage of growth should be performed to see if any changes occur. Evidently, the BIOLOG assay may not be an

accurate method of identification of bacterial species and 16S rDNA sequencing is preferred. Conversely, partial (~1400 bp) 16S rDNA sequence analysis may not be adequate for bacterial identification. The bacteria may differ in DNA sequence outside the amplified region and therefore whole genome sequencing may be needed to see differences at the species level.

The hypothesis (H6) that the most abundant bacteria should be present in the DGGE fingerprint of the community was not easily addressed. Unexpectedly, the DGGE of isolates produced more than one phylotype band (Fig. 17-20), so searching community DGGE fingerprints for the presence of an isolate was difficult. Only 8 out of 24 isolate bands appeared to be present in the community DGGE fingerprints. The concentration of any given isolate was likely too low in the community sample to be either copied in the PCR process or seen on the community DGGE gel (Nasreen Bano, personal communication). The isolation method did not therefore produce the most abundant bacterial species because dilution to extinction was not achieved. The most abundant species was most likely present in the community DGGE fingerprint, but was unculturable (Schut et al. 1993, 1997; Eilers et al. 2000). I therefore refuted the hypothesis (H6) that the most abundant species would be isolated and be present in the community DGGE fingerprint.

Identification of the most abundant bacterial species in a community is problematic because the most abundant species are often unculturable (Giovannoni et al. 1990). Cultured microbes often represent a minor fraction of the bacterial community (Schut et al. 1993, 1997; Eilers et al. 2000), so molecular methods like PCR-DGGE were

developed to overcome this obstacle. This study confirmed the conundrum but showed that PCR-DGGE may not capture all members of the bacterial community.

Bacterial species representing less than 1% of total bacterial abundance may be missed by PCR-DGGE (Muyzer et al. 1993). Filtered samples generally produced more bands in DGGE than unfiltered ones (Table 2; Fig. 9-13). Filtration most likely altered the relative abundance of bacterial species and may have reduced the concentration of dominant bacterial strains, allowing DNA from less abundant species to be copied in PCR. Chloroplasts may also be present in the unfiltered DGGE samples (Murray 1994), and some bacteria produce more than one band in the DGGE fingerprint (Ferrari and Hollibaugh 1999). Filtration of different size-fractions before DNA extraction and PCR may be needed to resolve all members of the community in DGGE analysis. New molecular methods like fluorescent in situ hybridization (FISH; as used in Eilers et al. 2000) may create a more accurate view of bacterial community composition of an ecosystem. Clearly, more research in new molecular and culturing techniques is needed in the field of marine microbial ecology in order to fully understand the role marine microbes play in shaping the marine ecosystem.

### **Future Work**

More research is needed to assess the controls at work on the polar microbial community. Studies that include surveys of microbial and environmental variables should contain more detailed DGGE analysis that includes division of the community into smaller sized fractions and the sequencing of all bands (OTU) in the DGGE fingerprint. Viral infection should also be more closely examined by determining the

percent of infected bacterial cells, performing viral enrichment studies, and determining changes in viral community structure. Bacterial and viral production and predation should also be measured. A polar study that measures all of these variables may lead to a better understanding of the processes that shape polar microbial communities and their importance in the polar ecosystem.

## **CHAPTER 5**

### **CONCLUSION**

Both bottom-up and top-down controls were likely shaping the microbial community in the Chukchi Sea during this study (Fig. 24). The availability of POM (bottom-up), however, was more strongly correlated to bacterial abundance and bacterial community composition than viral infection (top-down). POM, particularly PON, could be the driving variable that increased bacterial abundance, decreased species richness, and increased differences between FL and PA assemblages. POM might have influenced viral infection (top-down) indirectly by increasing the number of bacterial hosts that led to increased viral abundance and infection. Viral infection of nonresistant species in regions of high POM concentration may therefore have decreased species richness even further by allowing resistant species to thrive off products of host lysis.

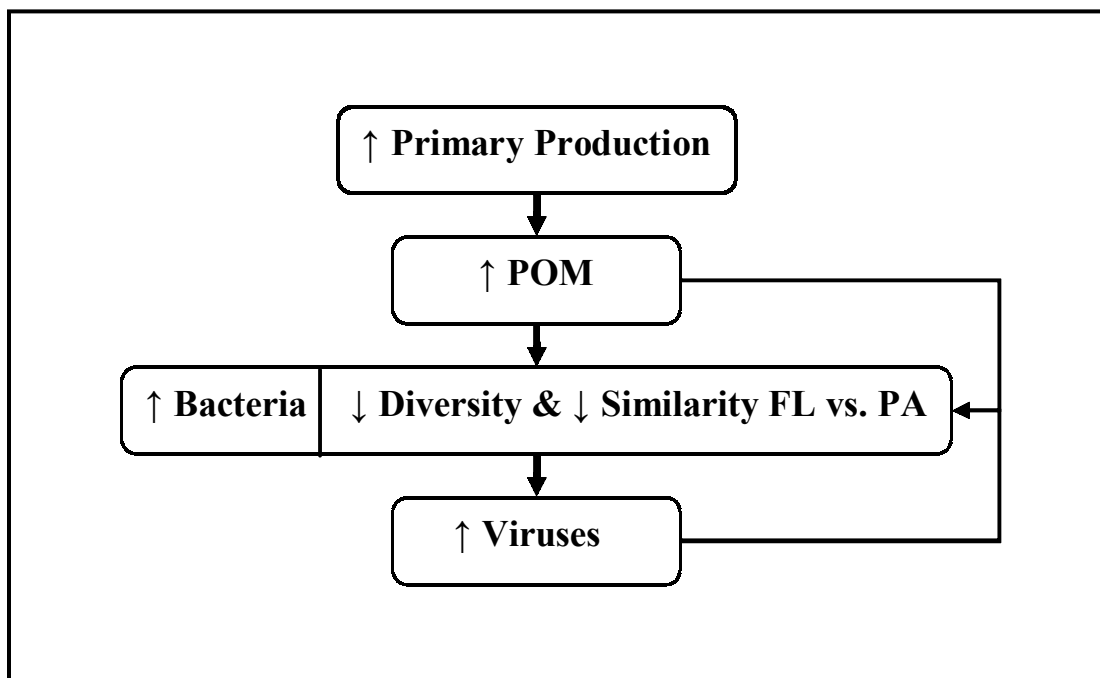


**Figure 24.** Schematic diagram showing the hypothesized cause-effect relationships at work during late summertime production in the Chukchi Sea. Pulses of primary production can lead to increases in POM that may increase bacterial abundance. An increase in host density then leads to an increase in viruses. Both POM and viruses may work together to decrease bacterial species diversity and the similarity between free-living (FL) and particle-associated (PA) assemblages.

## REFERENCES

- Abrams, E. and J. V. Stanton (1992) Use of denaturing gradient gel electrophoresis to study conformational transitions in nucleic acids. *Meth. Enz.* 212: 71-104.
- Ackermann, H. W. and M. S. DuBow (1987) *Viruses of prokaryotes, Vol. 1: general properties of bacteriophages*. CRC Press, Inc., Boca Raton, FL.
- Almeida, M. A., Ma. A. Cunha, and F. Alcantara (2001) Loss of estuarine bacteria by viral infection and predation in microcosm conditions. *Microbiol. Ecol.* 42(4): 562-571.
- Altschul, S.F., W. Gish, W. Miller, E.W. Myers, and D.J. Lipman (1990) Basic local alignment search tool. *J. Mol. Biol.* 215: 403-410.
- Anderson, M. R., and R. B. Rivkin (2001) Seasonal patterns in grazing mortality of bacterioplankton in polar oceans: a bipolar comparison. *Aquat. Microb. Ecol.* 25(2): 195-206.
- Azam, F., T. Fenchel, J. G. Field, J. S. Gray, L. A. Meyer-Reil, and F. Thingstad (1983) The ecological role of water-column microbes in the sea. *Mar. Ecol. Prog. Ser.* 10: 257-263.
- Bano, N. and J. T. Hollibaugh (2000) Diversity and distribution of DNA sequences with affinity to ammonia-oxidizing bacteria of the  $\beta$  subdivision of the class *Proteobacteria* in the Arctic Ocean. *Appl. Environ. Microbiol.* 66(5): 1960-1969.
- Bano, N. and J. T. Hollibaugh (2002) Phylogenetic composition of bacterioplankton assemblages from the Arctic Ocean. *Appl. Environ. Microbiol.* 68(2): 505-518.
- Barry, T., R. Powell, and R. Gannon (1990) A general method to generate DNA probes for microorganisms. *Bio/Technology* 8: 233-236.
- Bergh, O., K. Y. Børsheim, G. Bratbak, and M. Heldal (1989) High abundance of viruses found in aquatic environments. *Nature* 340: 467-468.
- Boehme, J. M., M E. Frischer, S. C. Jiang, C. A. Kellogg, S. Pichard, J. B. Rose, C. Steinway, and J. H. Paul (1993) Viruses, bacterioplankton, and phytoplankton in the southeastern Gulf of Mexico: distribution and contribution to oceanic DNA pools. *Mar. Ecol. Prog. Ser.* 97: 1-10.

- Børsheim, K. Y. (2000) Bacterial production and concentrations of organic carbon at the end of the growing season in the Greenland Sea. *Aquat. Microb. Ecol.* 21(2): 15-123.
- Bratbak, G., M. Heldal, S. Norland, and T. F. Thingstad (1990) Viruses as partners in spring bloom microbial trophodynamics. *Appl. Environ. Microbiol.* 56: 1400-1405.
- Bratbak, G., F. Thingstad, and M. Heldal (1994) Viruses and the microbial loop. *Microb. Ecol.* 28:209-221.
- Bratbak, G., and M. Heldal (1995) Viruses-the new players in the game: their ecological role and could they mediate genetic exchange by transduction? In I. Joint (ed.), *Molecular ecology of aquatic microbes*, vol. 38. Springer-Verlag KG, Berlin, Germany.
- Bratbak, G., M. Heldal, T. F. Thingstad, and P. Tuomi (1996) Dynamics of virus abundance in coastal seawater. *FEMS Microbiol. Ecol.* 19: 263-269.
- Button, D. K., F. Schut, P. Quang, R. Martin, and B. R. Robertson (1993) Viability and isolation of marine bacteria by dilution culture: Theory, procedures, and initial results. *Appl. Environ. Microbiol.* 59: 1707-1713.
- Castberg, T., A. Larsen, R. A. Sandaa, C. P. D. Brussaard, J. K. Egge, M. Heldal, R. Thyraug, E. J. van Hannen, and G. Bratbak (2001) Microbial population dynamics and diversity during a bloom of the marine coccolithophorid *Emiliana huxleyi* (Haptophyta). *Mar. Ecol. Prog. Ser.* 221: 39-46.
- Cho, B. C. and F. Azam (1990) Biogeochemical significance of bacterial biomass in the ocean's euphotic zone. *Mar. Ecol. Prog. Ser.* 63: 253-259.
- Chróst, R. J. (1991) Environmental control of the synthesis and activity of aquatic microbial ectoenzymes. In R.J. Chróst, ed., *Microbial Enzymes in Aquatic Environments*. Springer-Verlag, New York, pp. 22-59.
- Cochlan, W. P., J. Wikner, G. F. Steward, D. C. Smith, and F. Azam (1993) Spatial distribution of viruses, bacteria, and chlorophyll a in neritic, oceanic, and estuarine environments. *Mar. Ecol. Prog. Ser.* 92: 77-87.
- Cochran, P. K., and J. H. Paul (1998) Seasonal abundance of lysogenic bacteria in a subtropical estuary. *Appl. Environ. Microbiol.* 64: 2308.
- Cole, J. J., M. L. Pace, and S. Findlay (1988) Bacterial production in fresh and saltwater ecosystems: A cross-system overview. *Mar. Ecol. Prog. Ser.* 43: 1-10.

- Delong, E. F., D. G. Franks, and A. L. Alldredge (1993) Phylogenetic diversity of aggregate-attached vs. free-living marine bacterial assemblages. *Limnol. Oceanogr.* 38: 924-934.
- Don, R. H., P. T. Cox, B. J. Wainwright, K. Baker and J. S. Mattick (1991) 'Touchdown' PCR to circumvent spurious priming during gene amplification. *Nucleic Acids Res.* 19: 4008.
- Ducklow, H. W., D. A. Purdie, P. J. LeB. Williams, and J. M. Davies (1986) Bacterioplankton: a sink for carbon in a coastal marine plankton community. *Science* 232: 863-867.
- Ducklow, H. W. and F. K. Shiah (1993) Estuarine bacterial production. In Ford, T., ed., *Aquatic Microbiology: An Ecological Approach*. Blackwell, London, pp. 261-284.
- Fandino, L. B., L. Riemann, G. F. Steward, R. A. Long, and F. Azam (2001) Variations in bacterial community structure during a dinoflagellate bloom analyzed by DGGE and 16S rDNA sequencing. *Aquat. Microb. Ecol.* 23(2): 119-130.
- Felsenstein, J. (1993) PHYLIP: Phylogeny Inference Package (version 3.5). University of Washington, Seattle.
- Ferrari, V. C. and J. T. Hollibaugh (1999) Distribution of microbial assemblages in the Central Arctic Ocean Basin studied by PCR/DGGE: analysis of a large data set. *Hydrobiologia* 401: 55-68.
- Friedmann, E. I., ed. (1993) *Antarctic Microbiology*, Wiley-Liss, New York.
- Fuhrman, J. A. and F. Azam (1980) Bacterioplankton secondary production estimates for coastal waters of British Columbia, Antarctica, and California. *Appl. Environ. Microbiol.* 39: 1085-1096.
- Fuhrman, J. A. T. D. Sleeter, C. A. Carlson, and L. M. Proctor (1989) Dominance of bacterial biomass in the Sargasso Sea and its ecological implications. *Mar. Ecol. Prog. Ser.* 57: 207-271.
- Fuhrman, J. A. (1992) Bacterioplankton roles in cycling of organic matter: the microbial food web. In P. G. Falkowski and A. D. Woodhead, eds., *Primary Productivity and biogeochemical cycles in the sea*. Plenum Press, New York.
- Fuhrman, J. A. (1999) Marine viruses and their biogeochemical and ecological effects. *Nature* 399: 541-548.

- Fuhrman, J. A., and C. A. Suttle (1993) Viruses in marine planktonic systems. *Oceanography* 6: 50-62.
- Fuhrman, J. A., K. McCallum, and A. A. Davis (1993) Phylogenetic diversity of subsurface marine microbial communities from the Atlantic and Pacific oceans. *Appl. Environ. Microbiol.* 59: 1294-1302.
- Fuhrman, J. A., and R. T. Noble (1995) Viruses and protists cause similar bacterial mortality in coastal seawater. *Limnol. Oceanogr.* 40(7): 1236-1242.
- Gasol, J. M., M. Coserma, J. C. Garcia, J. Armengol, E. O. Casmayor, P. Kojecka, and K. Simek (2002) A transplant experiment to identify the factors controlling bacterial abundance, activity, production, and community composition in a eutrophic canyon-shaped reservoir. *Limnol. Oceanogr.* 47(1): 62-77.
- Giovannoni, S. J., T. B. Britschgi, C. L. Moyer, and K. G. Field (1990) Genetic diversity in Sargasso Sea bacterioplankton. *Nature* 345: 60-63.
- Gonzalez, J. M., and C. A. Suttle (1993) Grazing by marine nanoflagellates on viruses and viruses-sized particles – ingestion and digestion. *Mar. Ecol. Prog. Ser.* 94(1): 1-10.
- Grossi, S. M., Kottmeier, S. T., Moe, R. L. and Taylor, G. T. (1987) Sea-ice microbial communities. IV. Growth and primary production in bottom ice under graded snow cover. *Mar. Ecol. Prog. Ser.* 35: 153-164.
- Hagström, A., J. Pinhassi, and U. L. Zweifel (2001) Marine bacterioplankton show bursts of rapid growth induced by substrate shifts. *Aquat. Microb. Ecol.* 24(2): 109-115.
- Hahn, M. W., and M. G. Hofle (2001) Grazing of protozoa and its effect on populations of aquatic bacteria. *FEMS Microbiol. Ecol.* 35 (2): 113-121.
- Hameedi, M. J. (1978) Aspects of water column primary productivity in the Chukchi Sea during summer. *Marine Biology* 48: 37-46.
- Heldal, M. and G. Bratbak (1991) Production and decay of viruses in aquatic environments. *Mar. Ecol. Prog. Ser.* 72(3): 205-212.
- Hobbie, J. E., R. J. Daley, and S. Jasper (1977) Use of Nucleopore filters for counting bacteria by fluorescence microscopy. *Appl. Environ. Microbiol.* 33: 1225-1228.
- Hollibaugh, J.T., P. S. Wong, and M. C. Murrell (2000) Similarity of particle-associated and free-living bacterial communities in northern San Francisco Bay, California. *Aquat. Microb. Ecol.* 21: 103-114.

- Holm-Hansen, O., C. J. Lorenzen, R. W. Holmes, and J. D. H. Strickland (1965) Fluorometric determination of chlorophyll. *J. Cons. Int. Explor. Mer.* 30: 3-15.
- Holm-Hansen, O., El-Sayed, S. Z., Franceschini, G. A., and R. L. Cuhel (1977) Primary production and the factors controlling phytoplankton growth in the Southern Ocean. In *Adaptations within Antarctic Ecosystems*, ed. G. A. Llano. Gulf Publishing Company, Houston, TX.
- Jannasch, H. W., and G. E. Jones (1959) Bacterial populations in seawater as determined by different methods of enumeration. *Limnol. Oceanogr.* 4: 128-139.
- Jiang, S. C., and J. H. Paul (1994) Seasonal and diel abundance of viruses and occurrence of lysogeny/bacteriocinogeny in the marine environment. *Mar. Ecol. Prog. Ser.* 104: 163-172.
- Jurgens K, and M. M. Sala (2000) Predation-mediated shifts in size distribution of microbial biomass and activity during detritus decomposition. *OIKOS* 91(1): 29-40.
- Karl, D. M. (1993) Microbial processes in the Southern Ocean. In *Antarctic Microbiology*, ed. E. I. Friedmann, Wiley-Liss, New York.
- Karl, D. M. (2002) Microbiological oceanography- hidden in the sea of microbes. *Nature* 415(6872): 590-591.
- Kimura, H., M. Sato, C. Sugiyama, and T. Naganuma (2001) Coupling of thraustochytrids and POM, and of bacterio- and phytoplankton in a semi-enclosed coastal area: implication for different substrate preferences by the planktonic decomposers. *Aquat. Microb. Ecol.* 25(3): 293-300.
- Larsen, A., T. Castberg, R. A. Sandaa, C. P. D. Brussaard, J. Egge, M. Heldal, A. Paulino, R. Thyrhaug, E. J. van Hannen, and G. Bratbak (2001) Population dynamics and diversity of phytoplankton, bacteria, and viruses in a seawater enclosure. *Mar. Ecol. Prog. Ser.* 221: 47-57.
- Lebaron, P., P. Servais, M. Troussellier, C. Courties, J. Vives-Rego, G. Muyzer, L. Bernard, T. Guindulain, H. Schafer, and E. Stackebrandt (1999) Changes in bacterial community structure in seawater mesocosms differing in their nutrient status. *Aquat. Microb. Ecol.* 19(3): 255-267.
- Lee, C. W., I. Kudo, M. Yanada, and Y. Maita (2001) Bacterial abundance and production and heterotrophic nanoflagellate abundance in subarctic coastal waters (Western North Pacific Ocean). *Aquat. Microb. Ecol.* 23(3): 263-271.

- Li, W. K. W. and P. M. Dickie (1987) Temperature characteristics of photosynthetic and heterotrophic activities: seasonal variations in temperate microbial plankton. *Appl. Environ. Microbiol.* 53: 2282-2295.
- Long, R. A. and F. Azam (2001) Antagonistic interactions among marine pelagic bacteria. *Appl. Environ. Microbiol.* 67(11): 4975-4983.
- Lu, J. R., F. Chen, B. J. Binder, and R. E. Hodson (1999) Enumeration of marine viruses stained with SYBR Gold: Application of digital image analysis and flow cytometry. In: Abstracts 99<sup>th</sup> General Meeting of American Society of Microbiology. Chicago.
- Maranger, R., D. F. Bird, and S. K. Juniper (1994) Viral and bacterial dynamics in Arctic sea-ice during the spring algal bloom near Resolute Passage, NWT, Canada. *Mar. Ecol. Prog. Ser.* 111(1-2): 121-127.
- Maranger, R. and D. F. Bird (1995) Viral abundance of aquatic systems- A comparison between marine and fresh-waters. *Mar. Ecol. Prog. Ser.* 121(1-3): 217-226.
- Maranger, R. and D. F. Bird (1996) High concentrations of viruses in the sediments of Lac Gilbert, Quebec. *Microb. Ecol.* 31(2): 141-151.
- Magurran, A. E. (1988) *Ecological diversity and its measurement*. New Jersey, Princeton University Press.
- McManus, G. B. and J. A. Fuhrman (1988) Control of marine bacterioplankton populations: Measurement and significance of grazing. *Hydrobiologia* 159: 51-62.
- Metzler, P. M., P. M. Gilbert, S. A. Gaeta, and J. M. Ludlam (2000) Contrasting effects of substrate and grazer manipulations on picoplankton in oceanic and coastal waters off Brazil. *J. Plankton. Res.* 22(1): 77-90.
- Middleboe, M., N. O. G. Jørgensen, and N. Kroer (1996) Effects of viruses on nutrient turnover and growth efficiency of non-infected marine bacterioplankton. *Appl. Environ. Microbiol.* 62: 1991-1997.
- Middleboe, M., Å. Hagström, N. Blackburn, B. Sinn, U. Fischer, N. M. Borch, J. Pinhassi, K. Simu, and M. G. Lorenz (2001) Effects of bacteriophages on the population dynamics of four strains of pelagic bacteria. *Microb. Ecol.* 42(3): 395-406.
- Moeseneder, M. M., C. Winter, and G. J. Herndl (2001) Horizontal and vertical complexity of attached and free-living bacteria of the eastern Mediterranean Sea, determined by 16S rDNA and 16S rRNA fingerprints. *Limnol. Oceanogr.* 46(1): 95-107.

- MullerNiklas, G. and G. J. Herndl (1996) Dynamics of bacterioplankton during a phytoplankton bloom in the high Arctic waters of the Franz-Joseph Land archipelago. *Aquat. Microb. Ecol.* 11(2): 111-118.
- Murray, A. E. (1994) Community fingerprint analysis: a molecular method for studying marine bacterioplankton diversity. Thesis, Department of Biology. San Francisco State University.
- Murray, A. E., J. T. Hollibaugh and C. Orrego (1996) Phylogenetic compositions of bacterioplankton from two California estuaries compared by denaturing gradient gel electrophoresis of 16S rDNA fragments. *Appl. Environ. Microbiol.* 62(7): 2676-2680.
- Muyzer, G., E. C. de Waal, and A. G. Uitterlinden (1993) Profiling of complex microbial populations by denaturing gradient gel electrophoresis analysis of polymerase chain reaction-amplified genes coding for 16S rRNA. *Appl. Environ. Microbiol.* 59(3): 695-700.
- Muyzer, G., S. Hottentrager, A. Teske and C. Wawer (1996) Denaturing gradient gel electrophoresis of PCR-amplified 16S rDNA- a new molecular approach to analyze the genetic diversity of mixed microbial communities. Netherlands, Kluwer Academic Publishers.
- Myers, R.M., S.G. Fischer, L.S. Lerman, and T. Maniatis (1985) Nearly all single base substitutions in DNA fragments joined to a GC-clamp can be detected by denaturing gradient gel electrophoresis. *Nucleic Acids Res.* 13: 3131-3145.
- Myers, R. M., T. Maniatis and L. S. Lerman (1987) Detection and localization of single base changes by denaturing gradient gel electrophoresis. *Meth. Enz.* 155: 501-527.
- Noble, R. T., and J. A. Fuhrman (1998) Use of SYBR Green I for rapid epifluorescence counts of marine viruses and bacteria. *Aquat. Microb. Ecol.* 14: 113-118.
- Noble, R. T. and J. A. Fuhrman (1999) Breakdown and microbial uptake of marine viruses and other lysis products. *Aquat. Microb. Ecol.* 20(1): 1-11.
- Noble, R. T., M. Middleboe, and J. A. Fuhrman (1999) Effects of viral enrichment on the mortality and growth of heterotrophic bacterioplankton. *Aquat. Microb. Ecol.* 18(1): 1-13.
- Noble, R. T., and J. A. Fuhrman (2000) Rapid virus production and removal as Measured with fluorescently labeled viruses as tracers. *Appl. Environ. Microbiol.* 66(9): 3790-3797.

- Olsen, G. J., D. L. Lane, S. J. Giovannoni, N. R. Pace, and D. A. Stahl (1986) Microbial ecology and evolution: A ribosomal RNA approach. *Annu. Rev. Microbiol.* 40: 337-366.
- Paul, J. H., and B. Myers (1982) Fluorometric determination of DNA in aquatic microorganisms by use of Hoechst 33258. *Appl. Environ. Microbiol.* 43:1393-1399.
- Peduzzi, P., and M. G. Weinbauer (1993) The submicron size fraction of seawater containing high numbers of virus particles as bioactive agent in unicellular plankton community succession. *J. Plankton Res.* 15: 1375-1386.
- Pinhassi, J., U. L. Zweifel, and Å. Hagström (1997). Dominant marine bacterioplankton species found among colony-forming bacteria. *Appl. Environ. Microbiol.* 63: 3359-3366.
- Pomeroy, L. (1974). The ocean's food web, a changing paradigm. *BioScience* 24 (9): 499-504.
- Pomeroy, L. R. and D. Deibel (1986) Temperature regulation of bacterial activity during the spring bloom in Newfoundland coastal waters. *Science* 233: 359-361.
- Pomeroy, L. R., S. A. Macko, P. H. Ostrom and J. Dunphy (1990) The microbial food web in Arctic seawater: concentration of dissolved free amino acids and bacterial abundance and activity in the Arctic Ocean and in Resolute Passage. *Mar. Ecol. Prog. Ser.* 61: 31-40.
- Pomeroy, L. R., W. J. Weibe, D. Deibel, R. J. Thompson, G. T. Rowe and J. D. Pakulski (1991) Bacterial responses to temperature and substrate concentration during the Newfoundland spring bloom. *Mar. Ecol. Prog. Ser.* 75: 143-159.
- Poremba, K., U. Tillmann, and K. J. Hesse (1999) Distribution of bacterioplankton and chlorophyll-a in the German Wadden Sea. *Helgoland Mar. Res.* 53(1): 28-35.
- Porter, K. G., and Y. S. Feig (1980) The use of DAPI for identifying and counting aquatic microflora. *Limnol. Oceanogr.* 25: 943-948.
- Proctor, L. M., and J. A. Fuhrman (1990) Viral mortality of marine bacteria and cyanobacteria. *Nature* 343: 60-62.
- Proctor, L. M., and J. A. Fuhrman (1991) Roles of viral infection in organic particle flux. *Mar. Ecol. Prog. Ser.* 69: 133-142.

- Proctor, L. M., and J. A. Fuhrman (1992) Mortality of marine-bacteria in response to enrichments of the virus size fraction from seawater. *Mar. Ecol. Prog. Ser.* 87(3): 283-293.
- Proctor, L. M., A. Okubo and J. A. Fuhrman (1993) Calibrating estimates of phage-induced mortality in marine-bacteria-ultrastructural studies of marine bacteriophages development from one-step growth experiments. *Microbiol. Ecol.* 25(2): 161-182.
- Rehnstam, A. S., S. Bäckman, D. C. Smith, F. Azam, and Å. Hagström (1993) Blooms of sequence-specific culturable bacteria in the sea. *FEMS Microbiol. Ecol.* 102: 161-166.
- Rich, J., M. Gosselin, E. Sherr, B. Sherr, and D. L. Kirchman (1998). High bacterial production, uptake and concentrations of dissolved organic matter in the Central Arctic Ocean. *Deep-Sea Res. II* 44: 1645-1663.
- Riemann, L., G. F. Steward, and F. Azam (2000) Dynamics of bacterial community composition and activity during a mesocosm experiment. *Appl. Environ. Microbiol.* 66(2): 578-587.
- Riemann, L., and A. Winding (2001) Community dynamics of free-living and particle-associated bacterial assemblages during a freshwater phytoplankton bloom. *Microbiol. Ecol.* 42(3): 274-285.
- Rivkin, R. B., and M. R. Anderson (1997) Inorganic nutrient limitation of oceanic bacterioplankton. *Limnol. Oceanogr.* 42(4): 730-740.
- Saiki, R. K., D. H. Gelfand, S. Stoffel, S. J. Scharf, R. Higuchi, G. T. Horn, K. B. Mullis, and H. A. Erlich (1988) Primer-directed enzymatic amplification of DNA with a thermostable DNA polymerase. *Science* 239: 487-491.
- Sherr, E. B., and B. F. Sherr (1994) Bacterivory and herbivory: Key roles of phagotrophic protists in pelagic food webs. *Microb. Ecol.* 28: 233-235.
- Sherr, E. B., Sherr, B. F., and Fessenden, L. (1997) Heterotrophic protists in the central Arctic Ocean. *Deep-Sea. Res. II* 44: 1665-1682.
- Schmidt, T. M., E. F. DeLong, and N. R. Pace (1991) Analysis of a marine picoplankton community by 16S rRNA gene cloning and sequencing. *J. Bacteriol.* 173: 4371-4378.
- Schut, F., R. A. Prins, and J. C. Gottschal (1997) Oligotrophy and pelagic marine bacteria: Facts and fiction. *Aquat. Microb. Ecol.* 12(2): 177-202.

- Schut, F., E. J. Vries, J. C. Gottschal, B. R. Robertson, W. Harder, R. A. Prins, and D. K. Button (1993) Isolation of typical marine bacteria by dilution culture: Growth, maintenance, and characteristics of isolates under laboratory conditions. *Appl. Environ. Microbiol.* 59: 2150-2161.
- Simek K, P. Kojecka, J. Nedoma, P. Hartman, J. VrbaJ, and J. R. Dolan (1999) Shifts in bacterial community composition associated with different microzooplankton size fractions in a eutrophic reservoir. *Limnol. Oceanogr.* 44 (7): 1634-1644.
- Simek, K., J. Pernthaler, M. G. Weinbauer, K. Hornak, J. R. Dolan, J. Nedoma, M. Masin, and R. Amann (2001) Changes in bacterial community composition and dynamics and viral mortality rates associated with enhanced flagellate grazing in a mesoeutrophic reservoir. *Appl. Environ. Microbiol.* 67(6): 2723-2733.
- Skoog, A. D. Thomas, R. Lara, and K. Richter (1997) Methodological investigations on DOC determinations by the HTCO method, *Marine Chemistry* 56, 39-44.
- Smith, W. O., Jr. and Nelson, D. M. (1985) Phytoplankton bloom produced by a receding ice edge in the Ross Sea: spatial coherence with the density field. *Science* 227: 163-166.
- Smith, W. O., Jr., and Sakshaug, E. (1990) Polar Phytoplankton. In *Polar Oceanography Part B: Chemistry, Biology, and Geology*, ed. W. O. Smith, Jr. Academic Press, Inc., San Diego.
- Sokal, R. R. and F. J. Rohlf (1995) *Biometry: the principles and practice of statistics in biological research* (3<sup>rd</sup> Ed.). W. H. Freeman and Co., New York.
- Solorzano, L. (1969) Determination of ammonia in natural waters by the phenylhypochlorite method. *Limnol. Oceanogr.* 14: 799-801.
- Steward, G. F., D. C. Smith, and F. Azam (1996) Abundance and production of bacteria and viruses in the Bering and Chukchi Seas. *Mar. Ecol. Prog. Ser.* 131: 287-300.
- Steward, G. F., J. L. Monteil, and F. Azam (2000) Genome size distributions indicate variability and similarities among viral assemblages from diverse environments. *Limnol. Oceanogr.* 45(8): 1697-1706.
- Strickland, J. D. H. and T. R. Parsons (1972) A practical handbook of seawater analysis. Fisheries Board of Canada: 49-52.
- Sullivan, C. W., McClain, C. R., Comiso, J. C., and Smith, W. O., Jr. (1988) Phytoplankton standing crops within an Antarctic ice edge assessed by satellite remote sensing. *J. Geophys. Res.* 93: 12487-12498.

- Sullivan, C. W., Cota, G. F., Krempin, D. W., and Smith, W. O., Jr. (1990) Distribution and activity of bacterioplankton in the marginal ice zone of the Weddell-Scotia Sea during austral spring. *Mar. Ecol. Prog. Ser.* 63: 239-252.
- Suttle, C. A. (1994) The significance of viruses to mortality in aquatic microbial communities. *Microb. Ecol.* 28(2): 237-243.
- Suttle, C. A., and C. Feng (1992) Mechanisms and rates of decay of marine viruses in seawater. *Appl. Environ. Microbiol.* 58(11): 3721-3729.
- Suzuki, M. T. (1999) Effect of protistan bacterivory on coastal bacterioplankton diversity. *Aquat. Microb. Ecol.* 20(3): 261-272.
- Sverdrup, H. U. (1953) On conditions for the vernal blooming of phytoplankton. *Journal du Conseil International pour l'Exploration de la Mer* 18: 287-295.
- Thingstad, T. F., and R. Lignell (1997) Theoretical models for the control of bacterial growth rate, abundance, diversity and carbon demand. *Aquat. Microb. Ecol.* 13(1): 19-27.
- Tuomi, P., K. M. Fagerbakke, G. Bratbak, and M. Heldal (1995) Nutritional enrichment of a microbial community: The effects of activity, elemental composition, community structure and virus production. *FEMS Microb. Ecol.* 16: 123-134.
- Tuomi, P., T. Torsvik, M. Heldal, and G. Bratbak (1997) Bacterial population dynamics in a meromictic lake. *Appl. Environ. Microbiol.* 63: 2181-2188.
- van Hannen, E. J., G. Zwart, M. P. Van Agterveld, H. J. Gons, J. Ebert, and H. J. Laanbroek (1999) Changes in bacterial and eukaryotic community structure after mass lysis of filamentous cyanobacteria associated with viruses. *Appl. Environ. Microbiol.* 65: 795-801.
- Vrede, K., T. Vrede, A. Isaksson, and A. Karlsson (1999) Effects of nutrients (phosphorus, nitrogen, and carbon) and zooplankton on bacterioplankton and phytoplankton—a seasonal study. *Limnol. Oceanogr.* 44(7): 1616-1624.
- Waterbury, J. B., and F. W. Valois (1993) Resistance to co-occurring phages enables marine *Synechococcus* communities to coexist with cyanophages abundant in seawater. *Appl. Environ. Microbiol.* 59: 3393-3399.
- Watson, S. W., T. J. Novitsky, H. L. Quinby, and F. W. Valois (1977) Determination of bacterial number and biomass in the marine environment. *Appl. Environ. Microbiol.* 33: 940-946.

- Weinbauer, M. G., and P. Peduzzi (1995) Significance of viruses versus heterotrophic nanoflagellates for controlling bacterial abundance in the northern Adriatic Sea. *J. Plankton Res.* 17(9): 1851-1856.
- Weinbauer, M. G., D. Fuks, S. Puskaric, and P. Peduzzi (1995) Diel, seasonal, and depth-related variability of viruses and dissolved DNA in the Northern Adriatic Sea. *Microb. Ecol.* 30: 25-41.
- Weinbauer, M. G., and C. A. Suttle (1999) Lysogeny and prophage induction in coastal and offshore bacterial communities. *Aquat. Microb. Ecol.* 18(3): 217-225.
- Wheeler, P. A., Gosselin, M., Sherr, E., Thibault, D., Kirchman, D. L., Benner, R. and Whittedge, T. E. (1996) Active cycling of organic carbon in the central Arctic Ocean. *Nature* 380: 697-699.
- Wiggins, B. A., and M. Alexander (1985) Minimum bacterial density for bacteriophages replication: implications for significance of bacteriophages in natural ecosystems. *Appl. Environ. Microbiol.* 49: 19-23.
- Wilcox, R. M., and J. A. Fuhrman (1994) Bacterial viruses in coastal seawater: Lytic rather than Lysogenic production. *Mar. Ecol. Prog. Ser.* 114: 35-45.
- Williams, P. le B. (1981) Incorporation of microheterotrophic processes into the classical paradigm of the planktonic food web. *Keiler Meeresforsch.* 5: 1-28.
- Wommack, K. E. and R. R. Colwell (2000) Virioplankton: Viruses in aquatic environments. *Microbiol. Molecular Biol. Reviews* 64(1): 69-114.
- Wommack, K. E., R. T. Hill, M. Kessel, E. Russek-Cohen and R. R. Colwell (1992) Distribution of viruses in the Chesapeake Bay. *Appl. Environ. Microbiol.* 58(9): 2965-2970.
- Wommack, K. E., J. Ravel, R. T. Hill, and R. R. Colwell (1999) Population dynamics of Chesapeake Bay virioplankton: total community analysis using pulsed field gel electrophoresis. *Appl. Environ. Microbiol.* 65: 231-240.
- Yager, P. L. (1996) The microbial fate of carbon in high latitude seas: impact of the microbial loop on oceanic uptake of CO<sub>2</sub>. Thesis, University of Washington.
- Yager, P. L., T. L. Connelly, B. Mortazavi, K. E. Wommack, N. Bano, J. E. Bauer, S. Opsahl, and J. T. Hollibaugh (2001) Dynamic bacterial and viral response to an algal bloom at subzero temperatures. *Limnol. Oceanogr.* 46(4): 790-801.

Zehr, J. P., J. B. Waterbury, P. J. Turner, J. P. Montoya, E. Omoregie, G. F. Steward, A. Hansen, and D. M. Karl (2001) Unicellular cyanobacteria fix N<sub>2</sub> in the subtropical North Pacific Ocean. *Nature* 412 (6847): 635-638.

**Appendix.** AWS00 bacterial isolate BIOLOG data. Substrate utilization scores range from 0-3 according to color darkness (0=negative/no substrate utilization, 3=darkest/highest substrate utilization).

STATION	ISOLATE	water	$\alpha$ -cyclodextrin	dextrin	glycogen	tween 40	tween 80	N-acetylD - galactosamine	N-acetylD - glucosamine	adonitol	L-arabinose	D-amaditol	cellobiose
1	AW S001-A1	0	3	3	3	2	2	0	3	3	0	3	0
	AW S001-A1'	0	3	3	3	2	2	0	3	3	0	0	3
	AW S001-A2	0	2	3	3	1	1	0	3	3	0	3	3
	AW S001-A2'	0	2	3	3	1	1	0	3	3	0	3	3
	AW S001-B1	0	1	2	0	1	1	0	2	0	0	0	0
	AW S001-B1'	0	1	2	0	1	1	0	3	0	0	0	0
	AW S001-B2	0	3	3	3	2	3	0	3	3	0	3	3
	AW S001-B2'	0	3	3	3	2	2	0	3	3	0	3	0
	AW S001-C1	0	3	3	0	2	2	0	3	0	0	0	1
	AW S001-C1'	0	3	3	0	2	2	0	3	0	0	0	2
	AW S001-C2	0	3	3	0	2	3	0	3	0	0	0	0
	AW S001-C2'	0	3	3	0	2	2	0	3	0	0	0	0
STATION													
2	AW S002-A1	0	0	0	0	2	2	0	3	2	0	3	3
	AW S002-A1'	0	2	0	0	3	3	0	3	3	0	3	3
	AW S002-A2	0	0	0	0	3	3	0	3	3	0	3	3
	AW S002-A2'	0	0	0	0	3	3	0	3	3	0	3	3
	AW S002-B1	0	0	0	0	2	2	0	3	0	0	0	3
	AW S002-B1'	0	0	0	0	2	2	0	3	0	0	0	3
	AW S002-B2	0	0	0	0	3	3	0	3	3	0	3	3
	AW S002-B2'	0	0	0	0	2	2	0	3	3	0	3	3
	AW S002-C1	0	0	0	0	3	3	0	3	3	0	3	3
	AW S002-C1'	0	0	0	0	3	3	0	3	3	0	3	3
	AW S002-C2	0	3	3	3	3	3	0	3	3	0	3	3
	AW S002-C2'	0	3	3	3	3	3	0	3	3	0	3	3
STATION													
3	AW S003-A1	0	0	3	2	2	2	0	3	0	0	0	0
	AW S003-A1'	0	0	3	2	2	3	0	3	0	0	0	0
	AW S003-A2	0	0	2	1	0.5	0.5	0	2	0	0	0	2
	AW S003-A2'	0	0	2	1	1	1	0	2	0	0	0	2
	AW S003-B1	0	0	0	0	0	0	0	0	0	0	0	0
	AW S003-B1'	0	0	0	0	3	0	0	0	0	0	0	0
	AW S003-B2	0	3	3	2	1	0	0	2	0	0	0	3
	AW S003-B2'	0	3	3	3	1	1	2	2	0	0	0	3
	AW S003-C1	0	3	3	3	3	3	0	3	0	0	0	3
	AW S003-C1'	0	3	3	3	3	3	2	2	0	0	2	3
	AW S003-C2	0	3	3	2	0	0	3	3	0	0	0	3
	AW S003-C2'	0	3	3	3	2	1	0	3	0	0	0	3
STATION													
4	AW S004-A1	0	0	3	3	3	2	0	0	0	0	0	3
	AW S004-A1'	0	0	3	3	3	2	0	0	0	0	0	3
	AW S004-A2	0	3	3	3	3	3	0	3	0	0	0	3
	AW S004-A2'	0	3	3	3	3	3	0	0	0	0	0	3
	AW S004-B1	0	2	3	3	3	3	0	3	0	0	0	3
	AW S004-B1'	0	3	3	3	3	3	0	3	0	0	0	3
	AW S004-B2	0	3	3	3	3	3	0	3	0	0	0	3
	AW S004-B2'	0	3	3	3	3	3	0	3	0	0	0	3
	AW S004-C1	0	3	3	3	3	3	0	3	0	0	0	3
	AW S004-C1'	0	3	3	3	3	3	0	3	0	0	0	3
	AW S004-C2	0	3	3	3	3	3	0	3	0	0	0	3
	AW S004-C2'	0	3	3	3	3	3	0	3	0	0	0	3

Appendix (cont.).

STATION	ISOLATE	erythritol	D-fructose	L-fucose	D-galactose	gentiobiose	$\alpha$ -D-glucose	m-inositol	$\alpha$ -D-lactose	lactulose	maltose	D-mannitol	D-mannose
1	AW S001-A1	2	3	3	3	0	3	0	3	0	3	3	3
	AW S001-A1'	3	3	3	3	0	3	3	3	0	3	0	3
	AW S001-A2	3	3	0	0	0	3	3	3	0	3	3	3
	AW S001-A2'	3	3	3	3	0	3	3	3	0	3	0	3
	AW S001-B1	0	0	0	0	0	3	0	0	0	3	0	0
	AW S001-B1'	0	0	0	0	0	3	0	0	0	3	0	0
	AW S001-B2	3	3	3	3	0	3	3	3	0	3	3	3
	AW S001-B2'	3	3	3	3	0	3	3	3	0	3	3	3
	AW S001-C1	0	0	0	0	0	3	0	0	0	3	0	0
	AW S001-C1'	0	0	0	0	0	3	0	0	0	3	0	0
	AW S001-C2	0	0	0	0	0	3	0	0	0	3	0	0
	AW S001-C2'	3	0	0	0	0	3	0	0	0	3	0	0
STATION													
2	AW S002-A1	0	3	0	2	0	3	3	0	0	3	3	3
	AW S002-A1'	0	3	0	3	0	3	3	0	0	3	3	3
	AW S002-A2	0	2	0	2	0	3	0	0	0	3	0	3
	AW S002-A2'	0	2	0	2	0	3	0	0	0	3	0	3
	AW S002-B1	0	0	0	0	3	2	0	0	0	0	0	0
	AW S002-B1'	0	0	0	0	3	3	0	0	0	0	0	0
	AW S002-B2	0	2	0	3	0	3	2	0	0	3	3	0
	AW S002-B2'	0	2	0	0	0	3	0	0	0	3	3	3
	AW S002-C1	0	3	0	3	0	3	0	0	0	3	3	3
	AW S002-C1'	0	2	0	2	0	3	1	0	0	3	3	3
	AW S002-C2	3	3	3	3	0	3	3	0	0	3	3	3
	AW S002-C2'	3	3	3	3	0	3	3	3	0	3	3	3
STATION													
3	AW S003-A1	0	3	0	3	0	3	0	3	0	3	3	0
	AW S003-A1'	0	3	0	3	0	3	0	3	0	3	3	0
	AW S003-A2	0	0	0	0	0	2	0	0	0	2	0	0
	AW S003-A2'	0	0	0	0	0	2	0	0	0	2	0	0
	AW S003-B1	0	0.5	0	0	0	2	0	0	0	0	0	0
	AW S003-B1'	0	0.5	0	1	0	2	0	0	0	1	0	0
	AW S003-B2	0	3	0	3	3	3	0	3	3	3	3	3
	AW S003-B2'	0	3	0	3	3	3	0	3	3	3	3	2
	AW S003-C1	3	3	3	3	3	3	0	3	0	3	3	3
	AW S003-C1'	0	3	0	3	3	3	0	3	0	3	3	0
	AW S003-C2	0	3	0	3	3	3	0	3	0	3	3	0
	AW S003-C2'	3	3	3	3	3	3	1	3	0	3	3	0
STATION													
4	AW S004-A1	0	3	0	3	3	0	0	3	3	3	3	3
	AW S004-A1'	0	3	0	3	3	2	0	3	3	3	3	3
	AW S004-A2	0	3	0	3	3	3	0	3	0	3	3	0
	AW S004-A2'	0	3	0	3	3	3	0	2	0	3	3	0
	AW S004-B1	2	3	0	3	3	3	0	3	0	3	3	0
	AW S004-B1'	0	3	0	3	3	3	0	3	0	3	3	0
	AW S004-B2	0	3	0	3	3	3	0	3	0	3	3	0
	AW S004-B2'	3	3	0	3	3	3	0	0	0	3	3	0
	AW S004-C1	0	3	0	3	3	3	0	3	0	3	3	0
	AW S004-C1'	3	3	0	3	3	3	0	3	0	3	3	0
	AW S004-C2	0	3	3	3	3	3	0	0	0	3	3	0
	AW S004-C2'	0	3	0	3	3	3	3	3	0	3	3	0

Appendix (cont.).

STATION	ISOLATE	D-melibiose	$\beta$ -methyl-D-galactoside	D-psicose	D-raffinose	L-rhamnose	D-sorbitol	sucrose	D-trehalose	turanose	xylitol	methyl pyruvate	mono-methyl succinate
1	AW S001-A 1	3	0	0	0	0	3	0	3	0	0	0	0
	AW S001-A 1'	3	0	0	0	0	3	0	3	0	0	0	0
	AW S001-A 2	3	0	0	0	0	3	0	3	0	0	0	0
	AW S001-A 2'	3	0	0	0	0	3	0	3	0	0	0	0
	AW S001-B 1	0	0	0	0	0	0	0	0	0	0	0	0
	AW S001-B 1'	0	0	0	0	0	0	0	0	0	0	0	0
	AW S001-B 2	0	0	0	0	0	3	0	3	0	0	3	0
	AW S001-B 2'	3	0	0	0	0	3	3	0	0	0	0	0
	AW S001-C 1	0	0	0	0	0	0	0	0	0	0	0	0
	AW S001-C 1'	0	0	0	0	0	0	0	0	0	0	0	0
	AW S001-C 2	0	0	0	0	0	0	0	0	0	0	0	0
	AW S001-C 2'	0	0	0	0	0	0	0	0	0	0	0	0
STATION													
2	AW S002-A 1	2	0	0	0	0	3	0	3	0	0	1	0
	AW S002-A 1'	3	0	0	0	0	3	0	3	0	0	1	0
	AW S002-A 2	0	0	0	0	0	3	0	3	0	0	0	0
	AW S002-A 2'	0	0	0	0	0	0	0	3	0	0	0	0
	AW S002-B 1	0	0	0	0	0	0	0	0	0	0	0	0
	AW S002-B 1'	0	0	0	0	0	0	0	0	0	0	0	0
	AW S002-B 2	1	0	0	0	0	3	0	0	0	0	0	0
	AW S002-B 2'	0	0	0	0	0	3	0	3	0	0	0	0
	AW S002-C 1	0	0	0	0	0	3	0	3	0	0	0	0
	AW S002-C 1'	0	0	0	0	0	3	0	3	0	0	0	0
	AW S002-C 2	3	0	0	0	0	3	3	3	0	0	3	0
	AW S002-C 2'	3	0	0	0	0	3	0	3	0	0	3	0
STATION													
3	AW S003-A 1	0	0	0	0	0	0	0	3	0	0	0	0
	AW S003-A 1'	0	0	0	0	0	0	0	3	0	0	0	0
	AW S003-A 2	0	0	0	0	0	0	0	2	0	0	0	0
	AW S003-A 2'	0	0	0	0	0	0	0	2	0	0	0	0
	AW S003-B 1	0	0	0	0	0	0	0	2	0	0	0	0
	AW S003-B 1'	0	0	0	0	0	0	0	0	0	0	0	0
	AW S003-B 2	3	0	0	3	0	0	3	3	0	0	1	0
	AW S003-B 2'	3	0	0	3	0	0	3	3	0	0	2	0
	AW S003-C 1	3	0	0	0	0	3	3	3	0	0	3	0
	AW S003-C 1'	3	0	0	0	0	3	3	3	0	0	3	0
	AW S003-C 2	3	0	0	2	0	0	3	3	0	0	2	0
	AW S003-C 2'	3	0	0	3	0	0	3	3	0	0	2	0
STATION													
4	AW S004-A 1	3	0	0	3	0	0	3	3	0	0	3	0.5
	AW S004-A 1'	3	0	0	3	0	0	3	3	0	0	3	0.5
	AW S004-A 2	3	0	0	0	0	0	3	3	0	0	3	0
	AW S004-A 2'	3	0	0	0	0	0	3	3	0	0	3	0
	AW S004-B 1	3	0	0	0	0	0	3	3	0	0	3	0
	AW S004-B 1'	3	0	0	0	0	0	3	3	0	0	3	0
	AW S004-B 2	3	0	0	0	0	0	3	3	0	0	3	0
	AW S004-B 2'	3	0	0	0	0	0	3	3	0	0	3	0
	AW S004-C 1	3	0	0	0	0	0	3	3	0	0	3	0
	AW S004-C 1'	3	0	0	0	0	0	3	3	0	0	3	0
	AW S004-C 2	3	0	0	0	0	0	3	3	0	0	3	0
	AW S004-C 2'	3	0	0	3	0	0	3	3	0	0	3	0

Appendix (cont.).

STAT DN	ISOLATE	acetic acH	cis-aconitic acH	citric acH	fomic acH	D-galactonic acH	D-galacturonic acH	D-gluconic acH	D-glucosaminic acH	D-glucuronic acH	α-hydroxybutyric acH	γ-hydroxybutyric acH	β-hydroxybutyric acH
1	AW S001-A1	0.5	0	1	0	0	0	3	0	0	0	1	0
	AW S001-A1'	1	0	1	0	0	0	3	0	0	0	1	0
	AW S001-A2	0	0	0	0	0	0	3	0	0	0	1	0
	AW S001-A2'	0	0	1	0	0	0	3	0	0	0	1	0
	AW S001-B1	0	0	0	0	0	0	2	0	0	0	0	0
	AW S001-B1'	0	0	0	0	0	0	3	0	0	0	0	0
	AW S001-B2	0	0	2	0	0	0	3	0	0	0	2	0
	AW S001-B2'	0	0	2	0	0	0	3	0	0	0	1	0
	AW S001-C1	1	0	0	0	0	0	3	0	0	0	0	0
	AW S001-C1'	0	0	0	0	0	0	3	0	0	0	0	0
STAT DN	AW S001-C2	0	0	0	0	0	0	3	0	0	0	0	0
	AW S001-C2'	0	0	0	0	0	0	3	0	0	0	0	0
	2	AW S002-A1	0	2	2	0	0	3	0	0	0	1	0
	AW S002-A1'	0	2	2	0	0	0	3	0	0	0	1	0
	AW S002-A2	0	2	2	0	0	0	3	0	0	0	1	0
	AW S002-A2'	0	1	2	0	0	0	3	0	0	0	1	0
	AW S002-B1	0	0	0	0	0	0	3	0	0	0	0	0
	AW S002-B1'	0	0	0	0	0	0	3	0	0	0	0	0
	AW S002-B2	0	2	2	0	0	0	3	0	0	0	2	0
	AW S002-B2'	0	2	2	0	0	0	3	0	0	0	2	0
STAT DN	AW S002-C1	0	1	1	0	0	0	3	0	0	0	1	0
	AW S002-C1'	0.5	0.5	2	0	0	0	3	0	0	0	1	0
	AW S002-C2	0	1	1	0	0	0	3	0	0	0	1	0
	AW S002-C2'	0	1	1	0	0	0	3	0	0	0	1	0
	3	AW S003-A1	1	0	3	0	0	3	0	0	0	0	0
	AW S003-A1'	0	0	3	0	0	0	3	0	0	0	0	0
	AW S003-A2	0.5	0	0	0	0	0	0	0	0	0	2	0
	AW S003-A2'	0.5	0	0	0	0	0	0	0	0	0	2	0
	AW S003-B1	0	0	0	0	0	0	0	0	0	0	0	0
	AW S003-B1'	0	0	0	0	0	0	0	0	0	0	0	0
AW S003-B2	0	0	2	0	0	0	3	0	0	0	0	0	
STAT DN	AW S003-B2'	0	0	2	0	0	0	3	0	0	0	0	0
	AW S003-C1	0	0	2	0	0	0	3	0	0	0	3	0
	AW S003-C1'	0	0	2	0	0	0	2	0	0	0	2	0
	AW S003-C2	0	0	2	0	0	0	3	0	0	0	0	0
	AW S003-C2'	0	0	2	0	0	0	3	0	0	0	0	0
	4	AW S004-A1	0.5	2	3	0	0	3	0	0	0	0	0
	AW S004-A1'	1	1	3	0	0	0	3	0	0	0	0	0
	AW S004-A2	0	0	2	0	0	0	3	0	0	0	1	0
	AW S004-A2'	0	0	2	0	0	0	3	0	0	0	0	0
	AW S004-B1	0	0	2	0	0	0	3	0	0	0	2	0
AW S004-B1'	0	0	2	0	0	0	3	0	0	0	1	0	
AW S004-B2	0	0	2	0	0	0	3	0	0	0	1	0	
AW S004-B2'	0	0	1	0	0	0	3	0	0	0	1	0	
AW S004-C1	1	0	2	0	0	0	3	0	0	0	2	0	
AW S004-C1'	1	0	2	0	0	0	3	0	0	0	1	0	
STAT DN	AW S004-C2	0.5	0	2	0	0	0	3	0	0	0	2	0
	AW S004-C2'	1	0	2	0	0	0	3	0	0	0	1	0

Appendix (cont.).

STATDN	ISOLATE	p-hydroxy phenylacetic acid	itaconic acid	α-keto butyric acid	α-keto glutaric acid	α-keto valeric acid	D, L-lactic acid	malonic acid	pyruvic acid	quinic acid	D-saccharic acid	sebacic acid	succinic acid	
1	AW S001-A1	0	0	0	1	0	3	0	0	2	0	0	0	
	AW S001-A1'	0	0	0	1	0	3	0	0	3	0	0	1	
	AW S001-A2	0	0	0	1	0	3	0	2	2	0	0	1	
	AW S001-A2'	0	0	0	1	0	3	0	2	2	0	0	1	
	AW S001-B1	0	0	0	2	0	3	0	2	0	0	0	0	
	AW S001-B1'	0	0	0	3	0	3	0	1	0	0	0	0	
	AW S001-B2	0	0	0	2	0	3	0	2	2	0	0	1	
	AW S001-B2'	0	0	0	2	0	3	0	2	2	0	0	1	
	AW S001-C1	0	0	0	3	0	3	0	2	0	0	0	0	
	AW S001-C1'	0	0	0	2	0	3	0	3	0	0	0	2	
	AW S001-C2	0	0	0	2	0	3	0	2	0	0	0	1	
	AW S001-C2'	0	0	0	3	0	3	0	2	0	0	0	0	
	STATDN													
	2	AW S002-A1	0	0	0	2	0	2	0	0	0	0	0	1
AW S002-A1'		0	0	0	2	0	2	0	2	0	0	0	1	
AW S002-A2		0	0	0	2	0	2	0	0	0	0	0	1	
AW S002-A2'		0	0	0	2	0	2	0	0	0	0	0	2	
AW S002-B1		0	0	0	3	0	0	0	0	0	0	0	2	
AW S002-B1'		0	0	0	3	0	0	0	0	0	0	0	2	
AW S002-B2		0	0	0	2	0	2	0	0	0	0	0	2	
AW S002-B2'		0	0	0	3	0	3	0	0	0	0	0	2	
AW S002-C1		0	0	0	2	0	3	0	0	0	0	0	1	
AW S002-C1'		0	0	0	2	0	3	0	0	0	0	0	1	
AW S002-C2		0	0	0	1	0	3	0	1	2	0	0	1	
AW S002-C2'		0	0	0	1	0	3	0	1	2	0	0	1	
STATDN														
3		AW S003-A1	0	0	0	3	0	3	0	2	0	0	0	1
	AW S003-A1'	0	0	0	3	0	3	0	2	0	0	0	2	
	AW S003-A2	0	0	0	0	0	1	0	2	0	0	0	1	
	AW S003-A2'	0	0	0	0	0	2	0	2	0	0	0	1	
	AW S003-B1	0	0	0	0	0	2	0	0	0	0	0	0	
	AW S003-B1'	0	0	0	0	0	3	0	2	0	0	0	0	
	AW S003-B2	0	0	0	0	0	0	0	1	0	0	0	2	
	AW S003-B2'	0	0	0	0	0	0	0	1	0	0	0	2	
	AW S003-C1	0	0	0	2	0	3	0	2	0	0	0	1	
	AW S003-C1'	0	0	0	2	0	3	0	1	0	0	0	2	
	AW S003-C2	0	0	0	2	0	3	0	1	0	0	0	1	
	AW S003-C2'	0	0	0	2	0	3	0	2	0	0	0	2	
	STATDN													
	4	AW S004-A1	0	0	0.5	0.5	0	0	0	0.5	0	0	0	2
AW S004-A1'		0	0	0	0.5	0	0	0	0.5	0	0	0	3	
AW S004-A2		0	0	0	2	0	2	0	2	0	0	0	2	
AW S004-A2'		0	0	0	2	0	3	0	1	0	0	0	2	
AW S004-B1		0	0	0	2	0	0	0	1	0	0	0	2	
AW S004-B1'		0	0	0	0	0	3	0	1	0	0	0	2	
AW S004-B2		0	0	0	2	0	3	0	2	0	0	0	2	
AW S004-B2'		0	0	0	0	0	1	0	2	0	0	0	2	
AW S004-C1		0	0	0	2	0	0	0	2	0	0	0	2	
AW S004-C1'		0	0	0	2	0	0	0	2	0	0	0	2	
AW S004-C2		0	0	0	2	0	0	0	3	0	0	0	2	
AW S004-C2'		0	0	0	2	0	0	0	1	0	0	0	2	

Appendix (cont.).

STATDN	ISO LATE	homo succinic acid	succinic acid	glucosaminic acid	alanine	D-alanine	L-alanine	L-alanyl-glycine	L-asparagine	L-aspartic acid	L-glutamic acid	glycyl-L-aspartic acid	glycyl-L-glutamic acid	
1	AW S001-A1	0	0	0	0	3	3	3	0	0	3	0	2	
	AW S001-A1'	0	0	0	0	2	3	3	0	0	3	0	2	
	AW S001-A2	0	0	0	0	2	3	3	0	0	3	1	2	
	AW S001-A2'	0	0	0	0	2	3	3	0	0	3	0	1	
	AW S001-B1	0	0	0	0	0	3	2	0	0	0	2	1	
	AW S001-B1'	0	0	0	0	0	3	2	0	0	0	2	1	
	AW S001-B2	0	0	0	0	2	3	3	0	0	3	2	2	
	AW S001-B2'	0	0	0	0	2	0	0	0	0	0	1	2	
	AW S001-C1	0	0	0	0	0	3	3	0	0.5	3	3	2	
	AW S001-C1'	0	0	0	0	0	3	3	0	1	3	3	2	
	AW S001-C2	0	0	0	0	0	3	1	0	0	2	2	1	
	AW S001-C2'	0	0	0	0	0	3	3	0	0	1	2	1	
	STATDN													
	2	AW S002-A1	0	0	0	0	0	3	3	0	0	3	1	3
AW S002-A1'		0	0	0	0	0	3	3	0	0	3	3	3	
AW S002-A2		0	0	0	0	0	3	3	0	0	3	3	3	
AW S002-A2'		0	0	0	0	0	3	3	0	0	3	3	3	
AW S002-B1		0	0	0	0	0	3	3	0	0	3	3	3	
AW S002-B1'		0	0	0	0	0	3	3	0	0	3	3	3	
AW S002-B2		0	0	0	0	0	3	3	0	0	3	2	3	
AW S002-B2'		0	0	0	0	0	3	3	0	0	3	3	3	
AW S002-C1		0	0	0	0	0	3	3	0	0	3	3	2	
AW S002-C1'		0	0	0	0	0	3	3	0	0	3	3	3	
AW S002-C2		0	0	0	0	2	3	3	0	0	3	2	2	
AW S002-C2'		0	0	0	0	2	3	3	0.5	0.5	3	1	2	
STATDN														
3		AW S003-A1	0	0	0	0	3	3	3	0	1	3	3	3
	AW S003-A1'	0	0	0	0	3	3	3	0	2	3	0	3	
	AW S003-A2	0	0	0	0	2	3	3	0	0	0	2	2	
	AW S003-A2'	0	0	0	0	3	3	3	0	0	0	2	2	
	AW S003-B1	0	0	0	0	0	3	3	0	0	0	0	0	
	AW S003-B1'	0	0	0	0	0	3	3	0	0	0	0	0	
	AW S003-B2	0	0	0	0	0	3	3	0	0	3	0	2	
	AW S003-B2'	0	0	0	0	0	3	3	0	0	3	0	3	
	AW S003-C1	0	0	0	0	0	3	3	0	0	3	2	2	
	AW S003-C1'	0	0	0	0	0	3	3	0	0	0	3	3	
	AW S003-C2	0	0	0	0	0	3	3	0	0	3	0	2	
	AW S003-C2'	0	0	0	0	0	3	3	0	0	3	0	3	
	STATDN													
	4	AW S004-A1	0	0	0	0	0	2	2	0.5	0	2	2	2
AW S004-A1'		0	0	0	0	0	2	2	1	1	2	1	2	
AW S004-A2		0	0	0	0	0	3	3	0	0	3	0	3	
AW S004-A2'		0	0	0	0	0	3	2	0	0	2	0	2	
AW S004-B1		0	0	0	0	0	3	3	0	0	3	0	3	
AW S004-B1'		0	0	0	0	0	3	3	0	0	2	0	2	
AW S004-B2		0	0	0	0	0	3	3	0	0	0	0.5	2	
AW S004-B2'		0	0	0	0	0	3	3	0	0	2	0	2	
AW S004-C1		0	0	0	0	0	3	3	0	0	1	0	2	
AW S004-C1'		0	0	0	0	0	3	3	0	0	3	0.5	2	
AW S004-C2		0	0	0	0	0	3	3	0	0	3	0	3	
AW S004-C2'		0	0	0	0	0	3	3	0	0	1	0	2	

Appendix (cont.).

STATDN	ISOLATE	L-histidine	hydroxy L-proline	L-leucine	L-ornithine	L-phenylalanine	L-proline	L-pyroglytam acid	D-serine	L-serine	L-threonine	D,L-carnitine	γ-amino butyric acid	
1	AW S001-A1	3	3	1	2	0	3	3	0	3	3	0	2	
	AW S001-A1'	1	3	1	2	0	3	2	0	3	3	0	2	
	AW S001-A2	3	3	1	2	0	3	2	0	3	3	0	2	
	AW S001-A2'	3	3	2	2	0	3	3	0	3	2	0	2	
	AW S001-B1	0	0	2	0	0	0	0	0	2	0	0	0	
	AW S001-B1'	0	0	2	0	0	0	0	0	2	0	0	0	
	AW S001-B2	3	3	3	3	0	3	3	0	3	3	0	2	
	AW S001-B2'	3	3	3	3	0	3	3	0	3	3	0	2	
	AW S001-C1	0	0	3	0	0	1	0	0	3	0	0	0	
	AW S001-C1'	0	0	3	0	0	1	0	0	3	0	0	0	
	AW S001-C2	0	0	2	0	0	1	0	0	3	0	0	0	
	AW S001-C2'	0	0	3	0	0	1	0	0	3	0	0	0	
	STATDN													
	2	AW S002-A1	3	3	0	2	0	3	3	0	3	3	0	3
AW S002-A1'		3	3	3	3	0	3	3	0	3	3	0	3	
AW S002-A2		0	3	0	0	0	3	1	0	3	3	0	3	
AW S002-A2'		0	0	2	0	0	3	3	2	3	3	0	2	
AW S002-B1		0	0	0	0	0	2	0	0	2	2	0	0	
AW S002-B1'		0	0	0	0	0	2	0	0	3	1	0	0	
AW S002-B2		3	2	0	0.5	0	3	3	0	3	3	0	3	
AW S002-B2'		3	3	0	0	0	3	3	0	3	3	0	3	
AW S002-C1		1	1	1	2	0	3	3	0	3	3	0	2	
AW S002-C1'		3	2	2	0.5	0	3	3	0	3	3	0	3	
AW S002-C2		3	2	2	2	0	3	3	0	3	3	0	2	
AW S002-C2'		1	2	2	2	0	3	3	1	3	3	0	2	
STATDN														
3		AW S003-A1	2	0	0	0	0	3	0	0	3	3	0	0
	AW S003-A1'	2	0	0	0	0	3	0	0	3	3	0	0	
	AW S003-A2	0	3	0	0	3	3	0	0	3	3	0	0	
	AW S003-A2'	0	2	0	0	3	3	0	0	3	3	0	0	
	AW S003-B1	0	0	0	0	0	0	0	0	2	2	0	0	
	AW S003-B1'	0	0	0	0	0	0	0	0	3	1	0	0	
	AW S003-B2	0	0	0	0	2	3	0	0	2	3	0	0	
	AW S003-B2'	0	0	0	0	3	3	0	0	3	3	0	0	
	AW S003-C1	3	0	2	2	2	3	3	0	3	3	0	0	
	AW S003-C1'	0	3	3	0	3	3	3	0	3	3	0	0	
	AW S003-C2	0	2	2	2	2	3	0	0	3	0	0	2	
	AW S003-C2'	0	2	2	0	2	3	0	0	3	3	0	0	
	STATDN													
	4	AW S004-A1	0	0	0.5	0	1	2	0	0	0	0.5	0	0
AW S004-A1'		0	0	1	0	0.5	2	0	0	0	0	0	0	
AW S004-A2		0	0	3	0	0	3	0	0	3	0	0	0	
AW S004-A2'		0	0	3	0	0	3	0	0	3	0.5	0	0	
AW S004-B1		0	0	3	0	0	3	0	0	3	0.5	0	3	
AW S004-B1'		0	0	3	0	1	3	0	0	0	0	0	0	
AW S004-B2		0	0	3	0	0	3	0	0	3	0	0	0	
AW S004-B2'		0	0	3	0	0	3	0	0	3	0	0	0	
AW S004-C1		0	3	3	0	0	3	0	0	3	0	0	0	
AW S004-C1'		3	0	2	0	0	3	0	0	3	0	0	0	
AW S004-C2		0	0	3	0	0	3	0	0	3	0	0	0	
AW S004-C2'		0	0	3	0	0	3	1	0	2	0.5	0	0	

Appendix (cont.).

STATION	ISOLATE	urocanic acid	inosine	uridine	thymidine	phenylethylamine	putrescine	2-aminoethanol	2,3-butanediol	glycerol	D, L-α-glycerol phosphate	glucose-1-phosphate	glucose-6-phosphate
1	AW S001-A1	0	3	0	0	0	1	1	0	3	0	0	1
	AW S001-A1'	0	3	0	0	0	1	0.5	0	3	0	0	2
	AW S001-A2	0	2	0	0	0	1	0.5	0	3	0	0	1
	AW S001-A2'	0	2	0	0	0	1	0.5	0	0	0	0	1
	AW S001-B1	0	1	0	0	0	0	0	0	0	0	0	0
	AW S001-B1'	0	2	0	0	0	0	0	0	0	0	0	0
	AW S001-B2	0	3	0	0	0	2	2	0	3	0	0	1
	AW S001-B2'	0	2	0	0	0	2	0	0	2	0	0	1
	AW S001-C1	0	2	2	0	0	1	0	0	3	0	0	0
	AW S001-C1'	0.5	3	2	0	0	1	0	0	3	0	0	0
	AW S001-C2	0.5	2	1	0	0	1	0	0	3	0	0	0
	AW S001-C2'	0	2	0	0	0	1	0	0	3	0	0	0
STATION													
2	AW S002-A1	0	3	0	0	0	1	0	0	3	0	0	0
	AW S002-A1'	0	3	0	0	0	0	0	0	3	0	0	0
	AW S002-A2	0	3	0	0	0	0	0	0	3	0	0	0
	AW S002-A2'	0	3	0	0	0	0	0	0	3	0	0	0
	AW S002-B1	0	3	0	0	0	0	0	0	3	0	0	0
	AW S002-B1'	0	3	0	0	0	0	0	0	3	0	0	0
	AW S002-B2	0	3	0	0	0	0	0	0	3	0	0	0
	AW S002-B2'	0	3	0	0	0	0	0	0	3	0	0	0
	AW S002-C1	0	3	0	0	0	0	0	0	3	0	0	0
	AW S002-C1'	0	3	0	0	0	0	0	0	3	0	0	0
	AW S002-C2	0	3	0	0	0	2	2	0	3	0	0	2
	AW S002-C2'	0	3	0	0	0	2	0.5	0	3	0	0	1
STATION													
3	AW S003-A1	0	3	3	2	0	0	0	0	3	0	0	0
	AW S003-A1'	0	2	2	2	0	0	0	0	3	0	0	0
	AW S003-A2	0	3	2	2	0	0.5	0	0	0	0	0	0
	AW S003-A2'	0	0	3	2	0	2	0	0	0	0	0	0
	AW S003-B1	0	0	2	0	0	0	0	0	0	0	0	0
	AW S003-B1'	0	0	2	0	0	0	0	0	3	0	0	0
	AW S003-B2	0	0	0	0	0	0	0	0	3	0	0	0
	AW S003-B2'	0	0	0	0	0	0	2	0	3	0	0	0
	AW S003-C1	0	3	3	0	0	2	0	0	0	0	0	0
	AW S003-C1'	0	3	3	2	0	2	0	0	3	0	0	1
	AW S003-C2	0	3	0	0	0	2	0	0	3	0	0	1
	AW S003-C2'	0	3	0	0	0	2	0	0	3	0	0	0
STATION													
4	AW S004-A1	0	0	3	0	0	0	0	0	0	0.5	0.5	0
	AW S004-A1'	0	0	2	0	0	0	0	0	3	0	0	0
	AW S004-A2	0	3	0	0	0	1	0.5	0	3	0	0	0
	AW S004-A2'	0	3	0	0	0	1	0	0	3	0	0	0
	AW S004-B1	0	3	0	0	0	1	0	0	3	0	0	0
	AW S004-B1'	0	3	0	0	0	1	0	0	2	0	0	0
	AW S004-B2	0	1	0	0	0	1	0	0	3	0	0	0
	AW S004-B2'	0	3	0	0	0	1	0	0	3	0	0	1
	AW S004-C1	0	3	0	0	0	1	0	0	3	0	0	0
	AW S004-C1'	0	3	0	0	0	1	0	0	3	0	0	0
	AW S004-C2	0	3	0	0	0	0.5	0	0	3	0	0	0
	AW S004-C2'	0	3	0	0	0	1	2	0	3	0	0	0